Mineral Res. Expl. Bull., 141, 1-25, 2010

GEOLOGY OF THE EARLY MIOCENE ALAÇAMDAĐ (DURSUNBEY-BALIKESÝR) MAGMATIC COMPLEX AND IMPLICATIONS FOR THE WESTERN ANATOLIAN EXTENSIONAL TECTONICS

Fuat ERKÜL* and Sibel TATAR ERKÜL**

ABSTRACT.- Extensional regime in western Anatolia caused development of metamorphic core complexes, NE- and E-W-trending basins and emplacement of magmatic rocks since Late Oligocene and Early Miocene. The Alaçamdað magmatic complex, which is located to the west of the Simav metamorphic core complex, includes significant data that highlight the style of extensional regime in western Turkey. It consists of Early Miocene granitic intrusions and volcanic rocks with variable compositions ranging from basalt to rhyolite. The granitic intrusions that were emplaced into the basement rocks of the Menderes Massive and Ýzmir-Ankara Zone are divided into two facies based on their lithological and textural characteristics: Musalar and Alaçam granites. The Musalar granite has typical holocystalline equigranular texture, while the Alaçam granite is characterised by its porphyritic texture defined by abundant K-feldspar megacrysts. Both granite units were locally transformed into mylonites along shear zones. Volcanic rocks consist of Saðýrlar volcanic unit and felsic volcanic rocks. Saðýrlar volcanic unit is made up of andesitic/dacitic intrusions, domes, lava flows, dykes and volcanogenic sedimentary rocks. The felsic volcanic rocks, which unconformably overlies the Saðýrlar volcanic unit, consist of ignimbrite, dacite and rhyolite. These rocks have transitional contacts with alluvial/lacustrine sedimentary deposits. Ductile deformation on the granitic rocks, intra-basinal unconformities and syn-sedimentary deformational structures within the deposits are closely associated with the development of extensional regime during Early Miocene in western Turkey.

Key words: Stratigraphy, ductile deformation, extensional tectonics, volcano-sedimentary successions, north-western Anatolia.

INTRODUCTION

As one of the region experienced by extensional tectonics, the Aegean region has been subjected to crustal thickening related to the closure of the northern Neotethys, which continued from Early Cretaceous to Eocene times and led to the juxtaposition of various tectonic units in western Turkey (Þengör et al., 1984; Whitney and Bozkurt, 2002; Rimmele et al., 2003*a, b*; Bozkurt, 2004; Erdoðan and Güngör, 2004) (Figure 1a). Magmatic rocks with variable compositions were extensive over these tectonic units following the closure of the northern branch of the Neotethys. They extend along an E-W-trending zone of about 600 km long and 250 km wide (Figure 1a) (Borsi et al., 1972; Krushensky, 1976; Bingöl et al., 1982; Savaþçýn and Güleç, 1990; Seyitoðlu and Scott, 1992; Seyitoðlu et al., 1997; Genç, 1998; Karacýk and Yýlmaz, 1998; Delaloye and Bingöl, 2000; Yýlmaz et al., 2001). Recent research revealed that the extensional regime in western Turkey occurred since Late Oligocene-Early Miocene following the collisional events. However, some researchers suggest that the compressional period lasted until the end of Middle Miocene (Altunkaynak ve Yýlmaz, 1998; Karacýk ve Yýlmaz, 1998; Westaway, 2006; Hasözbek et al., 2009, in press). Extensional tectonic regime caused the development of metamorphic core complexes, fault-controlled NE- and E-W-trending basins and emplacement of the magmatic rocks in western Turkey (Savaþçýn and Güleç 1990; Seyitoðlu and Scott, 1992;

* Akdeniz Üniversitesi, Teknik Bilimler Meslek Yüksekokulu, Dumlupýnar Bulvarý, Kampüs - Antalya
** Akdeniz Üniversitesi, Mühendislik Fakültesi, Jeoloji Mühendisliði Bölümü, Dumlupýnar Bulvarý, Kampüs - Antalya

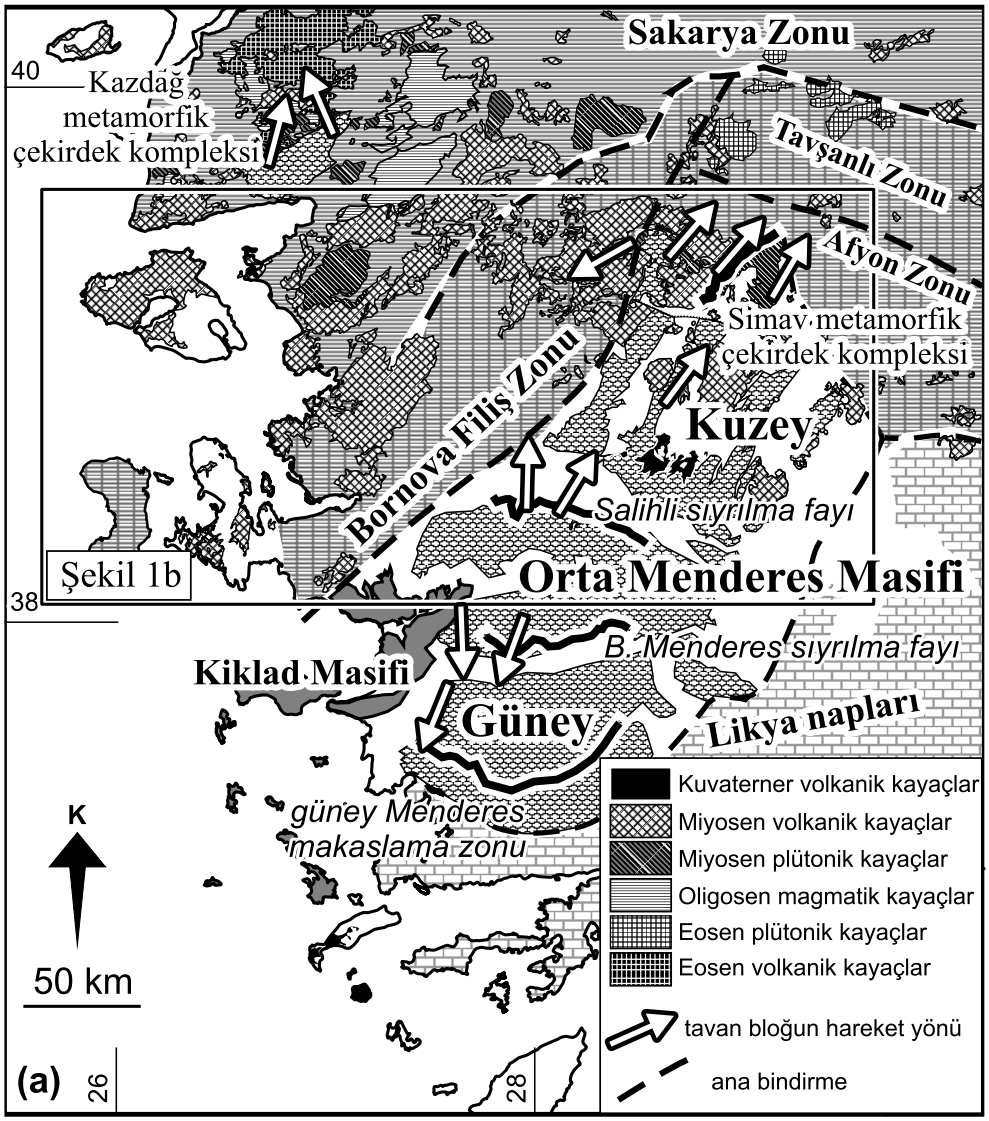

Figure 1a- A geological map showing major tectonic elements of the Aegean region (compiled from Hetzel et al., 1995*a,b*; Okay and Tüysüz, 1999; Ring et al., 1999; Ring and Collins, 2005; Okay and Satýr, 2000).

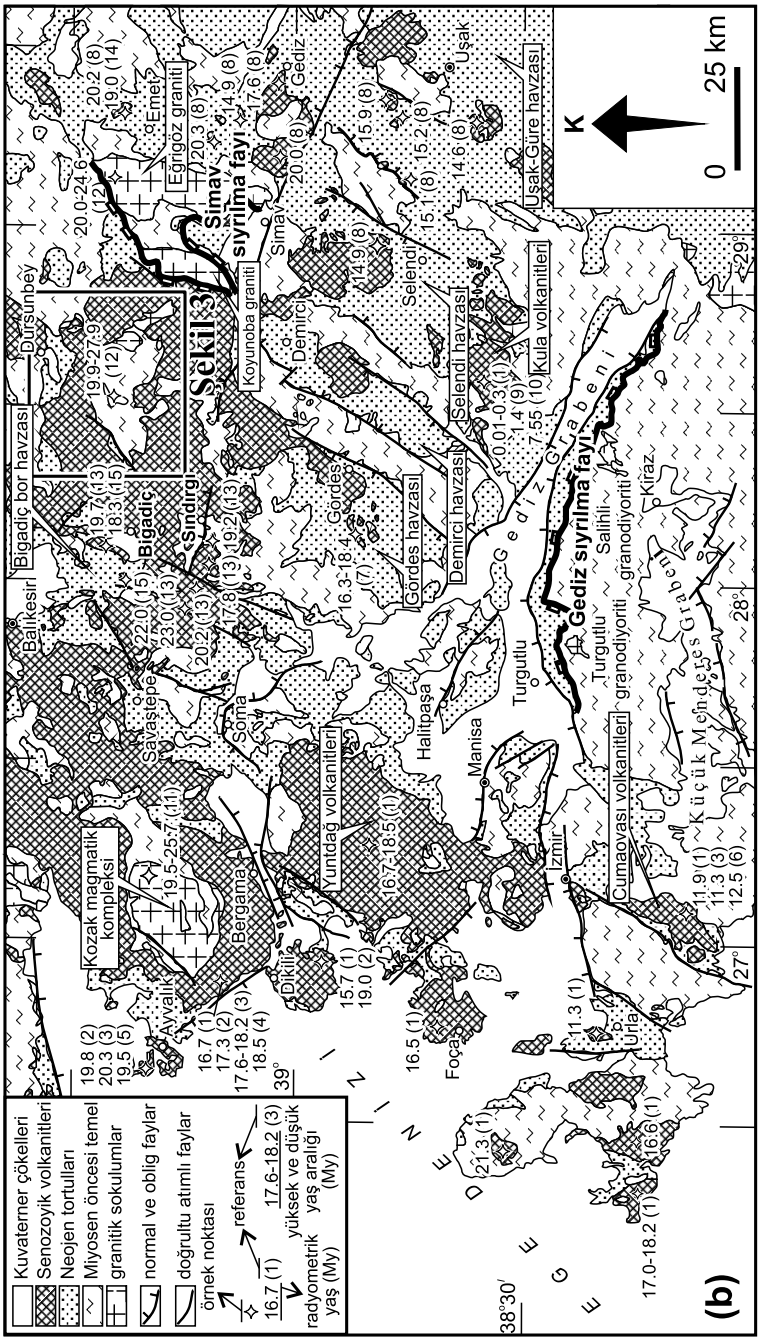

Figure 2b- Generalised geological map showing the distribution of Neogene to recent rocks, major tectonic lines and compiled radiometric age data (Bozkurt, 2000, 2001a,*b*, 2003; Yılmaz et al., 2000; Erkül et al., 2005a). Radiometric age data: (1) Borsi et al. (1972), (2) Ercan (1979), (3) Ercan et al. (1985), (4) Akyürek and Soysal (1982), (5) Krushensky (1976), (6) Innocenti and Mazzouli (1972), (7) Seyitoğlu and Scott (1992), (8) Seyitoğlu et al. (1997), (9) Ercan (1982), (10) Ercan and Öztunalý(1983), (11) Delaloye and Bingöl (2000), Ar-Ar data (12) Bingöl et al. (1982), (13) Erkül et al. (2005 a,*b*), (14) Helvacýand Alonso (2000), (15) Helvacý(1995).

Seyitoðlu et al., 1997; Altunkaynak and Yýlmaz, 1998; Genç, 1998; Aldanmaz, 2000; Delaloye and Bingöl, 2000; Pe-Piper and Piper, 1989, 2001; Yýlmaz et al., 2001; Iþýk et al., 2004; Altunkaynak and Dilek, 2006; Dilek and Altunkaynak, 2007).

Radiometric dating of syn-tectonic granitoids and detachment-related fault rocks indicate that the central Menderes, Kazdað and Simav metamorphic core complexes occurred during Early and Middle Miocene (Hetzel et al., 1995*a,b*; Bozkurt and Park, 1997*a,b*; Okay and Satýr, 2000; Ring et al., 2003; Iþýk et al., 2004; Ring and Collins, 2005; Glodny and Hetzel, 2007). Studies on the Koyunoba and Eðrigöz plutons which are located in the east of the Alaçamdað magmatic complex indicate that the plutonism in the region is closely associated with detachment faulting (Iþýk and Tekeli, 2001; Iþýk et al., 2003, 2004; Ring and Collins, 2005). Ar-Ar cooling ages from the detachment-related fault rocks and syn-extensional plutons range between 23 and 20 Ma (Iþýk et al., 2004).

Exhumation of the Menderes Massif along extensional detachment faults was accompanied by the emplacement of numerous volcano-sedimentary basins in western Turkey (Figure 1b) (Bozkurt and Park, 1994; Koçyiðit et al., 1999; Yýlmaz et al., 2000; Bozkurt, 2000, 2001*a,b*, 2003; Sözbilir, 2001, 2002*a,b*; Seyitoðlu et al., 2002; Bozkurt and Sözbilir, 2004; Iþýk et al., 2003, 2004; Purvis and Robertson, 2004). The NE - trending basins, Soma, Bigadiç, Demirci, Gördes and Selendi basins, were formed during the extensional period around the Alaçamdað region (Figure 2). These basins, which rest on the pre-Miocene basement, are characterized by lacustrine/fluvial sedimentary deposits, interbedded lavas and volcaniclastic rocks that were extruded along the NE-trending volcanic edifices. Radiometric dating of the basaltic to rhyolitic volcanic rocks indicates that the NE-trending basins were formed during Early-Middle Miocene. These volcano-sedimentary successions commonly include intra-basinal unconformities.

The Alaçamdað region, which is located on the various tectonic units, is one of the least studied regions in western Turkey (Akdeniz and Konak, 1979; Erkül et al., 2009*a,b*; Hasözbek et al., in press). Recent structural and geochronological studies provide a convincing evidence for the syn-extensional ductile deformation of the Alaçamdað granites (Erkül, 2010). However, role of ductile deformation in the volcanism and co-eval basins remains unclear. In this paper, we aimed to described geology of the magmatic rocks in the Alaçamdað region and to discuss structural data from the deformed granites in the framework of western Anatolian extensional province.

STRATIGRAPHY

The Alaçamdað region is underlain by the Miocene-Quaternary magmatic and sedimentary rocks that rest on the basement rocks of the Menderes Massif and the Ýzmir-Ankara Zone (Figure 3). Rock units are, from bottom to top, Menderes Massif, Ýzmir-Ankara Zone, Alaçamdað granites, Saðýrlar volcanic unit, fluvial/lacustrine sedimentary deposits, felsic volcanic rocks, continental deposits, alluvium and scree deposits (Figure 4).

Menderes Massif

Menderes Massif is formed by a NE-trending, dome-shaped outcrop with length of 250 km and width of 150 km. It consists of orthogneiss, schist, phyllite, quartzite amphibolite and marbles (Akdeniz and Konak, 1979; Bozkurt and Oberhänslý, 2001; Gessner et al., 2001; Iþýk et al., 2004), which is widely exposed in the west of the Alaçam village (Figure 3). Phyllites are defined by typical cream and grey colours and distinct cleavage seams. Mica schists are mainly composed of biotite, muscovite and quartz. Quartzite bands are up to 1-meter-thick structures within the mica schists. Menderes Massif is tectonically overlain by the Ýzmir-Ankara Zone (Erdoðan 1990*a,b*). Metamorphic rocks of the

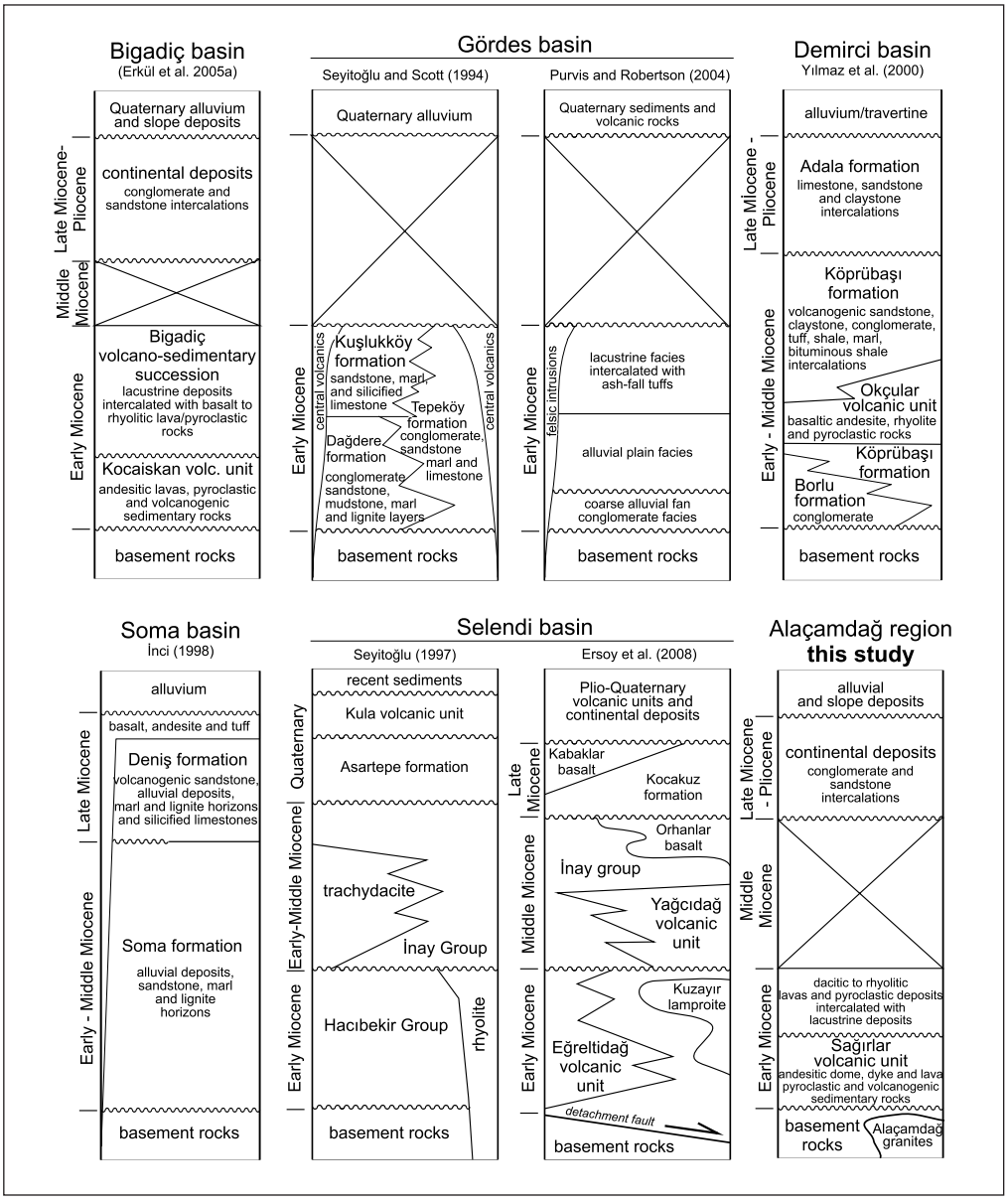

Figure 2- Stratigraphic correlation of the NE-trending Neogene basins located around the Alaçamdağ region.

Menderes Massif are juxtaposed with the re-crystallized limestone and flysch-type sediments of the Ýzmir-Ankara Zone along a steeply dipping contact that is distingusihed as a ductile shear zone in the west of the Alaçamdağ region.

Ýzmir-Ankara Zone

The Ýzmir-Ankara Zone is a NE-trending melange zone between Menderes Massif and the Sakarya Zone. It consists of olistostomes and ophiolite slices within a sheared matrix of flysch-

type sediments (Erdoðan, 1990*a,b*; Okay ve Siyako, 1993). The Ýzmir-Ankara Zone is divided into the NE-trending Bornova Flysch Zone and the E-W-trending Afyon Zone in the Alaçamdað region. These zones have similar lithological features to each other in the western part of the Alaçamdað region. The Bornova Flysch Zone consists of greyish recrystallized limestone olistoliths and serpentinite (formerly gabbro) slices surrounded by a sheared, claret red to greyish matrix of sandstone and shale intercalations. The matrix locally includes limestone lenses. The Afyon Zone is located in the north of the Alaçamdað region and characterized by detrital sedimentary rocks, olistrostromal limestones and ophiolitic slices with local low-grade metamorphic overprints.

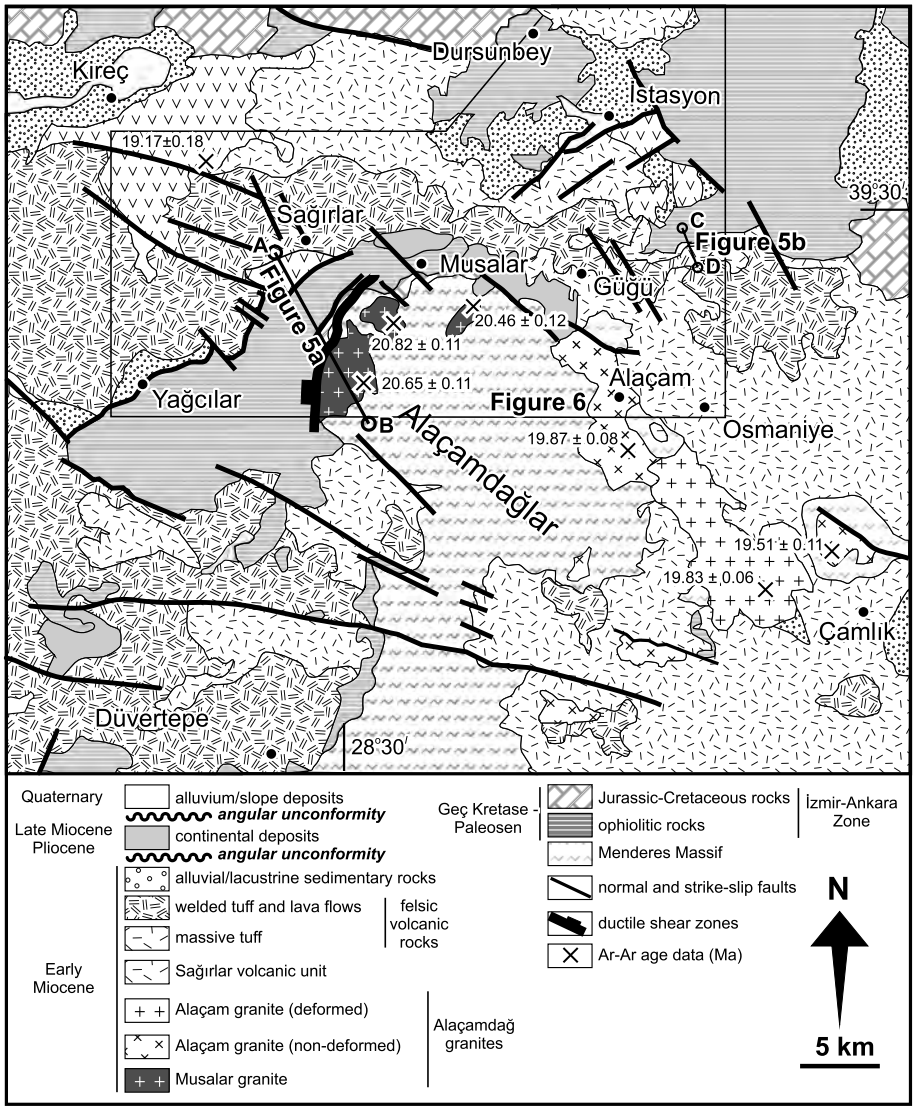

Figure 3- Geological map of the Alaçamdað region (lithological boundaries were modified from Akdeniz and Konak (1979) and Ar-Ar ages of granites are from).

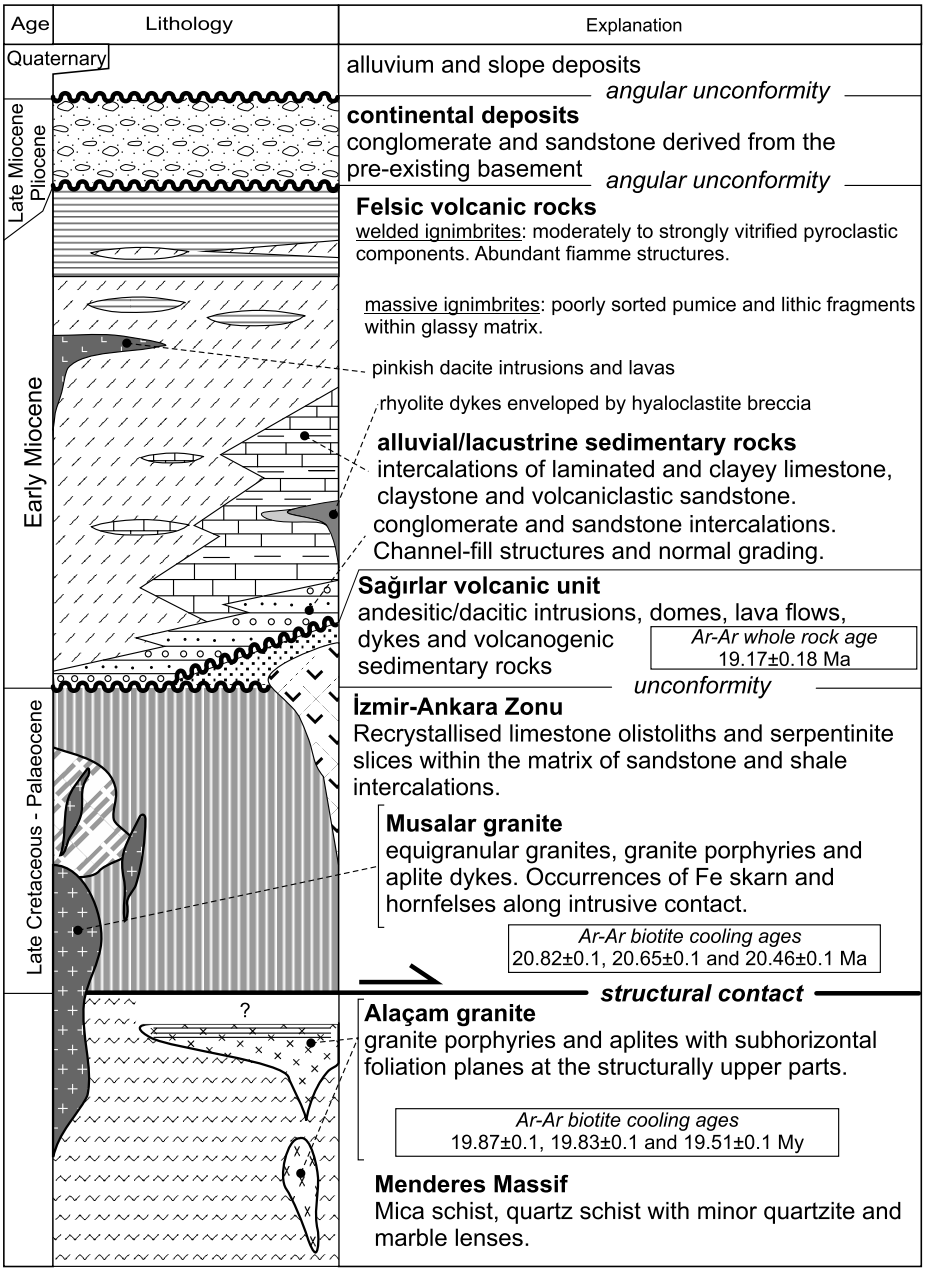

Figure 4- Generalised stratigraphic columnar section of the Alaçamdað region.

Alaçamdað granites

The Alaçamdað granites crop out in an area of 30 km^2 within an arc-shaped zone (Figure 3). Granitic rocks of the Alaçamdað magmatic complex are divided into two facies: Musalar and Alaçam granites (Table 1).

Musalar granite.- Musalar granite is exposed in an area of about 16 km^2 around Aþaðýmusalar

Table 1- General characteristics of the Musalar and Alaçam granites

Unit	Musalar granite	Alaçam granite
Texture	equigranular	porphyritic
Megacryst	minor K-feldspar megacrysts	relatively abundant K-feldspar megacrysts
Mafic microgranular enclaves (MME)	present	present
Hypabyssal equivalents	granite porphyries and aplites	aplites
Name of rock	granite	granite
Major mineralogical constituents	quartz, plagioclase, orthoclase, biotite and hornblende	quartz, plagioclase, orthoclase, biotite and hornblende
Deformation	a high-angle ductile shear zone along the western margin of the Musalar granite.	a shear zone formed by subhorizontal foliation surfaces within the southern part of the largest, NW-trending stock.
Ductile deformation structures within the granites	ultramylonites are common • dynamic recrystallisation of quartz • ondulatory extinction in quartz and biotite • Asymmetrical quartz porphyroclasts • Microfaults cutting the pre-existing foliation planes	protomylonites are common. • C' shear bands • Syn-tectonic deformation of aplitic dykes • Dynamic recrystallisation of quartz • asymmetrical mica-fish structure • ondulatory extinction in K-feldspars

and Yukarýmusalar villages. Each granite stock, which covers an area up to 11 km^2, has commonly elliptical, rhomb-shaped and circular plan views. Elliptical and rhomb-shaped stocks extends NE-SW and N-S in direction. Musalar granites are characterized by equigranular granites, granite porphyries and aplitic dykes. Equigranular granites are distinguished by their typical spherical wheathering in the field. Foliation planes also occur within the Musalar granites that are locally affected by ductile deformation along their margins. Equigranular Musalar granite is composed of orthoclase, quartz, plagioclase, biotite and hornblende. It also contain centimeter to decimeter-sized mafic microgranular enclaves, indicating magma mingling processes. Granite porphyries are usually known as having relatively small megacrysts of orthoclase within the fine-grained matrix of rock-forming minerals. They are greyish coloured in the field, have a dyke morphology, extending in a NE direction and include minor amount of mafic minerals. Aplitic dykes are recognized by their microcrystalline texture. They are composed of quartz, plagioclase, orthoclase and minor biotite. Musalar granite intrudes the Menderes Massif and the Bornova Flysch Zone to the west of the Alaçamdað region (Figure 5a). The intrusive contact of the Musalar granite with the Bornova Flysch Zone is characterized by an iron skarn zone between recrystallized limestone and N-S-trending granite stock. This relationship is well exposed around the Geyiktepe vicinity (Figure 5a). A skarn zone is made up a few meters around it which consists of garnet, diopside, epidote, actinolite, tremolite, chlorite and

pyrite. It is also recognized by iron disseminations within the recrystallized limestones. The intrusive contact of the Musalar granite with the Menderes Massif is defined by hornfelsic rocks within mica schists and quartzites. Hornfelsic rocks are a few meters wide and are recognized by their gray-green clours. Clastic sedimentary rocks and recrystallized limestones are intruded by a few meter wide granite porphyry dykes (Figure 5a). Aplitic dykes cut the recrystallized limestone, metamorphic rocks and Musalar granite. The Musalar granite has cooling ages between 20.17 and 20.82 Ma while U-Pb zircon crystallization age is 20.3 Ma (Table 2).

Alaçam granite.- Alaçam granite crop out in an area of about 65 km^2 around the Alaçam and Çamlýk districts and has NW-SE- and NE-SW-trending exposures. Largest granite outcrop is about 19 km long and 3 km wide. Alaçam granite consists of porphyritic granites and aplitic dykes. Porphyritic granites are defined by large megacrysts of orthoclase surrounded by plagioclase, quartz, biotite and hornblende. Length of the individual megacryst reaches up to 5 cm. The Alaçam granite contains mafic microgranular enclaves and xenoliths near the contact zone. The enclaves, up to a decimeter long, are dioritic composition. Aplitic dykes are usually a few to locally 50 centimeter wide, which intrude marginal parts of the granites and metamorphic host rock. The Alaçam granite cuts mica schists of the Menderes Massif and includes metamorphic xenoliths around contact zone. Intrusive contact relationships are well exposed around Alaçam village. The intrusive contact of the granite with mica schists is sharp and is characterized by the aplitic dykes that occurs in a 100 metres wide zone. The aplitic dykes also cross-cut the mica-schist foliation within the zone. Alaçam granite is also unconformably overlain by Early Miocene ignimbrites that have crude stratification and poorly sorted pumice clasts. No deformational features are exposed within the ignimbrites. Cooling ages of the Alaçam granites range between 20.01 and 19.51 Ma while their U-Pb crystallization age is 20 Ma (Table 2).

Saðýrlar volcanic unit

Saðýrlar volcanic unit consists of andesitic/dacitic intrusions, domes, lava flows, dykes and volcanogenic sedimentary rocks. The unit is exposed in an area of about a few tens of km^2 in the south of Saðýrlar and southeast of Dursunbey (Figure 6). Intrusions are located in the east of Yaðcýlar and south of Deðirmenciler. They have circular plan views and their diametre is up to 300 metre. Andesitic/dacitic intrusions are massive and locally display radial cooling joints. In a hand specimen, andesites and dacites are made up of feldspar, biotite and minor quartz phenocrysts within pink and grey coloured matrix. Intrusions cut the clastic sediments of the Izmir-Ankara Zone. Domes consist of grey and pink coloured dacite and andesite. They are exposed in the west of Saðýrlar and south of Beyel. Domes around Saðýrlar are distinguished by their massive appearence. Domes are usually surrounded by andesite/dacite breccia and cut by late-stage faults. They display similar lithologies to those exposed in the south of Beyel. The dome, up to 200 metre high, contains radial cooling joints and is surronded by monomictic breccia (Figure 7a). Andesitic/dacitic lavas are typically distinguished by their pink colours and porphyritic textures that are defined by plagioclase, biotite, hornblende and minor quartz phenocrysts within the hyalopilitic matrix. They include flow foliation and minor vesicles. Dykes of the Saðýrlar volcanic unit are only exposed around Kürsü district. They are a few tens of metres long and are up to 10 metres wide. Dip of dykes is nearly vertical and strike is N10-40°E. Andesitic dykes intrude the polymictic andesite breccia (Figure 7b). Andesitic dykes are distinguished with their brown and dark pink colours and include a few cm thick flow bands that have oriented phenocrysts. Volcanogenic sedimentary rocks consist of volcanic sandstone, breccia and conglomerates. Main components of the volcanogenic sedimentary rocks are polymictic, poorly sorted, angular and subrounded andesite and dacite clasts within a sand-size matrix

Table 2- Geochronological data from the magmatic rocks of the Alaçamdağ area

Location			Methods	Rock dated	Mineral dated	Age (Ma)	Reference
Alaçamdağ granites (undifferentiated)			K-Ar	Granite	biotite	20.3±0.6	Bingöl et al. (1982)
					potassium feldspar	20.0±0.8 19.9±0.7 20.6±0.8 20.9±0.5	
			Ar-Ar		biotite	20.6±0.8 20.9±0.5	Delaloye and Bingöl (2000)
			U-Pb		zircon	20.7±1.1	Hasözbek et al. (2009)
Alaçamdağ granites - west			U-Pb		zircon	20.3 ± 3.3	Hasözbek et al. (in press)
Alaçamdağ granites - east						20.0 ± 1.4	
Alaçamdağ granites - west			Rb-Sr		biotite	20.17 ± 0.2	
Alaçamdağ granites - east						20.01 ± 0.2	
Musalar granite	UTM coordinates (zone 35; longitude/latitude)						Erkül (2010)
	630390	4364466	Ar-Ar	Granite-equigranular	biotite	20.65±0.11	
	631542	4367877				20.82±0.11	
	636084	4368640				20.46±0.12	
Alaçam granite							
	644773	4360962	Ar-Ar	Porphyritic granite	biotite	19.87±0.08	
	651000	4353500		Granite-protomylonitic		19.83±0.06	
	655413	4355019		Granite-porphyritic		19.51±0.11	
Sağırlar volcanic unit							
	620822	4375278	Ar-Ar	andesite	whole rock	19.17±0.18	this study

(Figure 7c). Clasts may occur clast- or matrix-supported and are locally stained by iron oxides.

Intrusive rocks of the Saðýrlar volcanic unit cut the clastic sediments of the Ýzmir-Ankara Zone. Lava flows and volcanogenic sedimentary rocks are interfingered unconformably overlie the rocks of the Ýzmir-Ankara Zone (Figure 7d). The Saðýrlar volcanic unit is unconformably overlain by the alluvial/lacustrine sedimentary deposits and felsic volcanic rocks in Kürsü and south of Dursunbey. Ar-Ar cooling age measured from the andesite lava of the Saðýrlar volcanic unit is 19.17±0.18 Ma (Table 2).

Alluvial/lacustrine sedimentary rocks

Alluvial/lacustrine sedimentary rocks are located in Yaðcýlar, Kürsü and south of Dursunbey. They consist of conglomerate, sandstone, claystone, volcanic sandstone and laminated/clayey limestone intercalations. Largest exposures are located in the south of Dursunbey, covering an area of about 40 km^2. Conglomerates consist of basement-derived, subrounded to rounded clasts of andesite, recrystallized limestone, sandstone and shale within a sand-size matrix at the basal part of the succession. Proximity of the basement rocks defines abundance

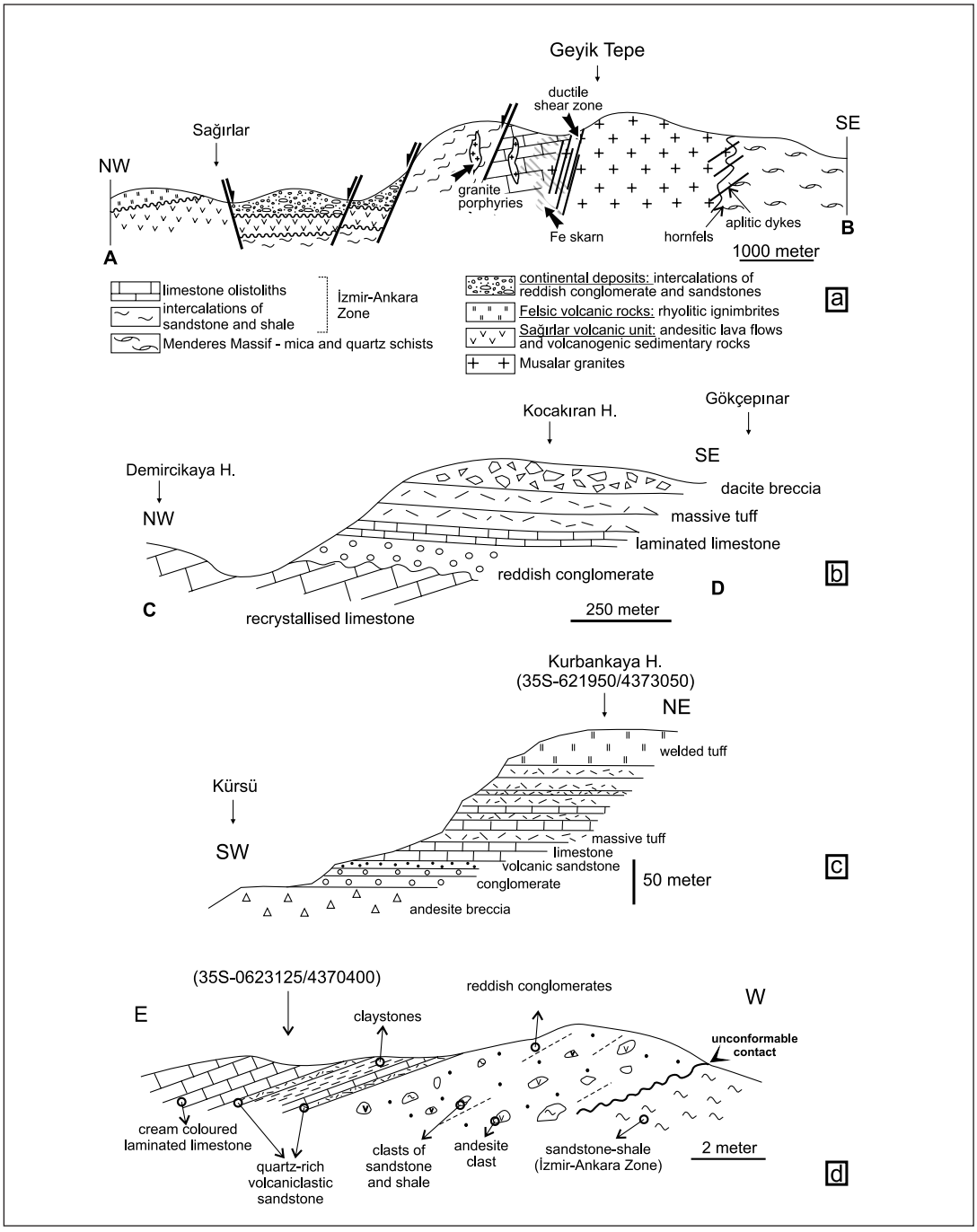

Figure 5- (a) Geological cross section along Saðýrlar and Geyiktepe districts. (b) Geological cross-section along Gökçepýnar. (c) Geological cross-section displaying lithologies and contact relationship of the alluvial/lacustrine sedimentary deposits on the volcanic breccia of the Saðýrlar volcanic unit. (d) Unconformable contact relationship between the alluvial/ lacustrine sedimentary rocks and the Ýzmir-Ankara Zone in the west of the Saðýrlar district. Location of figures 5a and 5b is shown in figure 3.

of clast type in the unit. Sandstones display limited extent above conglomerates as lenses. Thickness of sandstone and conglomerate intercalations may locally reach up to 80 meter. Volcanic sandstones are recognized by their grey to cream colours and include quartz, feldspar and biotite crystals. Thickness of the volcanic sandstones may reach up to a few metres. Uppermost part of the unit consists of laminated, well stratified and clayey limestones; they are distinguished by typical yellow to cream colours.

Alluvial/lacustrine sedimentary rocks are unconformably overlies the Ýzmir-Ankara Zone, while they are conformably overlain by volcaniclastic rocks of the felsic volcanic unit. Unconformable contacts are well exposed around Deðirmenciler, Kürsü, Saðýrlar and Saçayak districts. In the Deðirmencikaya district, recrystallized limestones are overlain by 20 meter thick reddish conglomerates. Conglomerates are overlain by laminated limestone, massive ignimbrites and dacite breccia from lower to upper parts of succession (Figure 5b). Andesite breccia is overlain by the basement-derived, well rounded and oxide stained conglomerates, volcanic sandstones, felsic tuffs and cream limestone. These rocks are conformably overlain by welded ignimbrites (Figure 5c). In the Saðýrlar area, a 5-6-meter thick conglomerate overlies the sandstone and shale intercalations of the Ýzmir-Ankara Zone. Conglomerate comprises well-rounded andesite and sandstone/shale intercalation. Conglomerate is conformably overlain by quartz-rich volcanic sandstone, claystone and cream coloured, laminated lacustrine limestones (Figure 5d). In the Saçayak district, lava flows of the Saðýrlar volcanic unit is covered by bedded sandstones (Figure 8). Bedded sandstones commonly have cross-stratification. They are overlain by massive conglomerates that occur as channel-fill deposits at the basal parts. Massive conglomerates also display clast imbrication and cross stratification. They gradually pass upward into the bedded sandstones that include channel-fills and lenses of conglomerates. This sequence is covered by chaotic claystone layers that have syn-sedimentary deformational patterns and conglomerate/clayey limestone lenses. The chaotic layers are covered by pebbly sandstones that have channel-fill structures and clayey limestone intercalations. They pass upward into the conglomerates with an erosinal basal contact and comprise andesite boulders up to 1 meter long within a matrix of pebbly sandstones. Intrabasinal unconformities are very common within the alluvial/lacustrine sedimentary deposits (Figure 9). Layers with dips about 35°, which consist of claystone, sandstone and clayey limestone intercalations, are overlain by nearly flat-lying beds of sandstone and conglomerate along an erosive contact. Clayey limestones transgressively overlie the Ýzmir-Ankara Zone at some localities.

Alluvial/lacustrine sedimentary deposits occur as lenses within the welded ignimbrites of felsic volcanic rocks around Çatalçam district. Age of these deposits are accepted Early Miocene owing to correlation and radiometric dating of felsic volcanic rocks in the surrounding regions.

Felsic volcanic rocks

Felsic volcanic rocks around Alaçamdað region cover hundreds of km^2 from Bigadiç to Simav and from Dursunbey to Düvertepe districts (Figures 3 and 6). They consist of dacites, rhyolites and ignimbrites. Ignimbrites are the most voluminous deposits in the Alaçamdað region and their thickness may reach up to 350-400 meters. They are recognized by pumice and lithic fragments together with basement-derived accidental clasts enclosed by an ash-size matrix. Columnar joints are common within ignimbrites. Ignimbrites are usually grey and brown coloured, but locally greenish owing to alteration of pumice fragments (Figure 10a). Textural characteriztics are usually defined by the degree of welding in ignimbrites. Flattened and virtrified pumice clasts, which form a typical fiammes, were locally transformed into volcanic glass (Figure 10b).

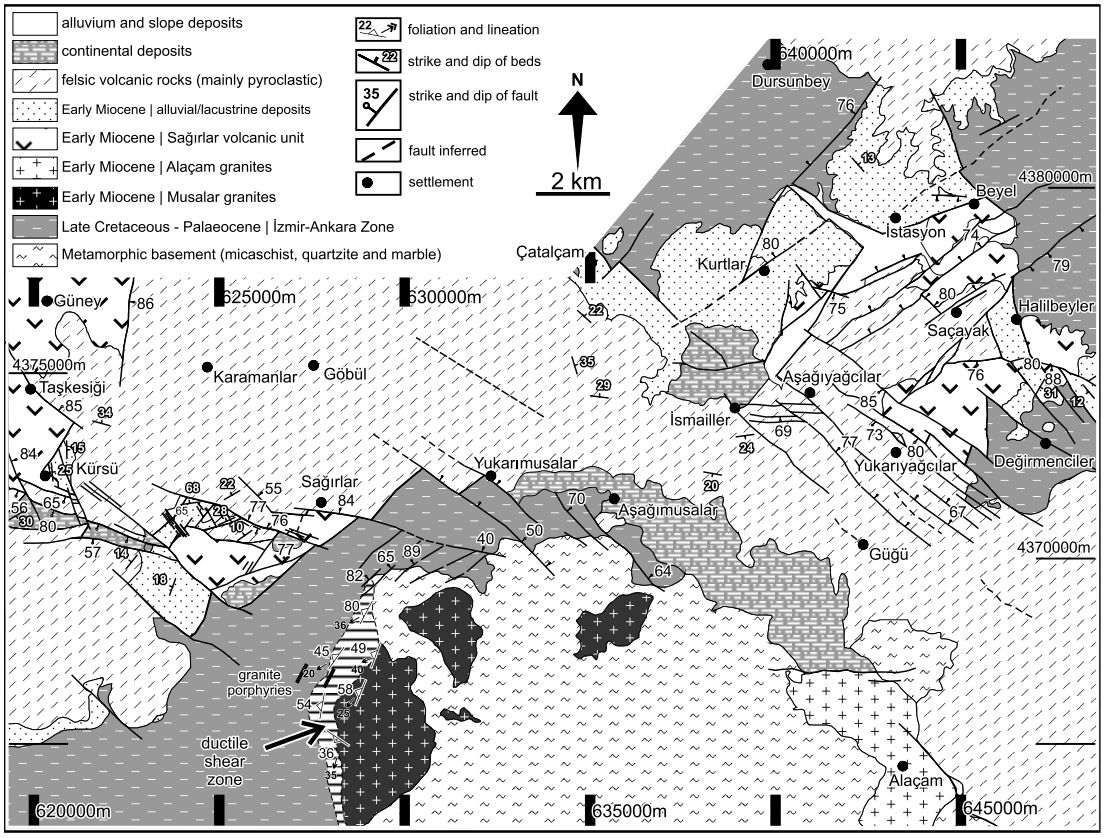

Figure 6- Geological map of the Alaçamdað region. Map coordinates: UTM - zone 35.

Dacites crop out in the Güðü area and are recognized by phenocrysts of quartz, plagioclase, biotite and hornblende within a grey and pink coloured matrix.

Rhyolites, which cover an area up to a few km^2, are characterized by typical flow foliations and quartz phenocrysts within a cream coloured matrix in a hand specimen. They are associated with hyaloclastite breccias in the north of Kürsü, suggesting a subaqueous emplacement. Hyaloclastite breccias surround rhyolitic dykes that are defined by subvertical distinct flow foliations. Dykes are up to about 10 metres wide and 100 metres long. Hyaloclastite breccias are recognized by its perlitic clasts that display a typical jig-saw fit texture (Figure 10c). Rhyolite dykes intrude alluvial/lacustrine sedimentary deposits.

Felsic volcanic rocks rest on the Menderes Massif, Ýzmir-Ankara Zone, Alaçam granite and Saðýrlar volcanic unit. They have vertically and horizontally transitional contacts with alluvial/lacustrine sedimentary deposits (Figure 10d). Ignimbrites unconformably overlies the Menderes Massif and Alaçam granite. Foliated granites are covered with pumice-rich massive ignimbrites along a sharp contact. Lithic-rich ignimbrites unconformably overlies the Ýzmir-Ankara Zone in the south of Dursunbey and southeast of Yukarýyaðcýlar areas (Figure 10e). Massive and welded ignimbrites, which are transitional to alluvial/lacustrine sedimentary deposits, unconformably overlie the andesite breccia of the Saðýrlar volcanic unit around Saðýrlar and Kürsü. Massive ignimbrites rest directly on the andesitic

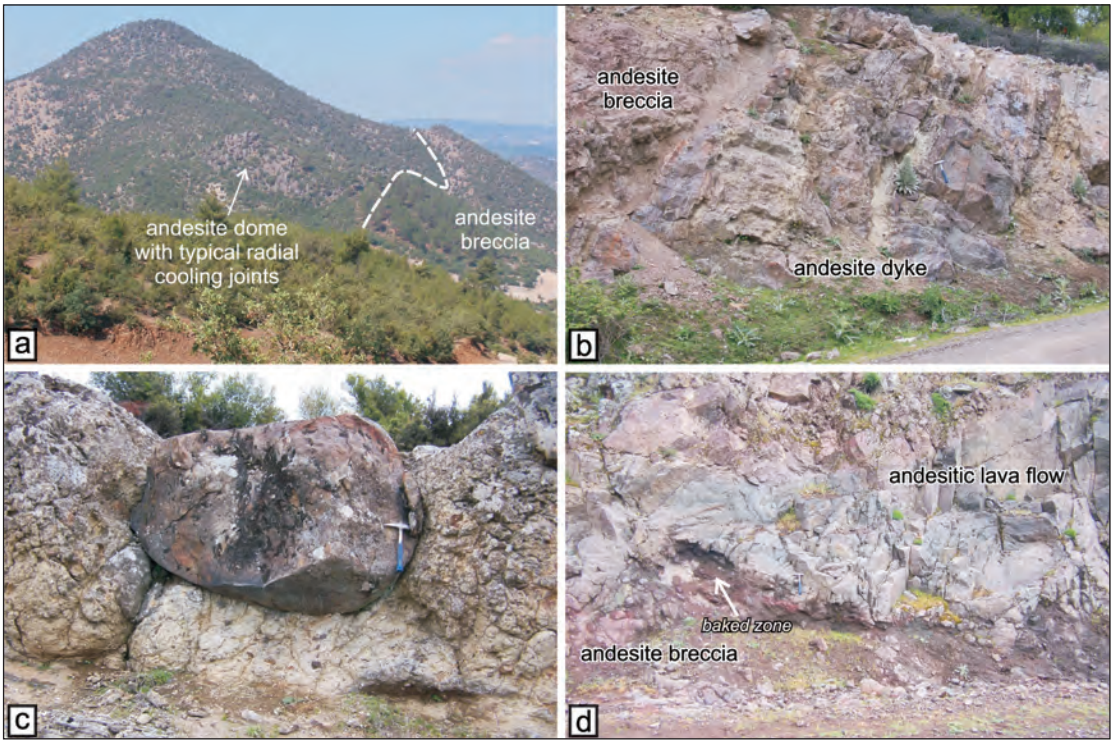

Figure 7- (a) An andesite dome surrounded by andesite breccia in the south of Beyel, Dedetepe. Field of view is about 800 metres wide. (b) an andesite dyke that intrudes the polymictic andesite breccia. The dyke trends in N10°E. Width of view is about 10 metres (35S-620385/4371955). (c) A large, rounded andesite clast within the lacustrine deposits (35S-620700/4371800). (d) basal conformable contact of the lava flows overlying the polymictic andesite breccias (35S-620262/4373555).

lava flows of the Saðýrlar volcanic unit around Saðýrlar area. The contact zone between these lithologies is represented by oxidation zone and a-few-decimetre-thick palaeosoil occurrences (Figure 10f). Felsic volcanic rocks radiometrically dated in the Bigadiç borate basin can be correlated with Early Miocene felsic volcanic units (Erkül et al., 2005*b*).

Continental deposits

Continental deposits crop out in an area of about 40 km^2 in the north of Alaçamdað region. They have variable clast types defined by basement source. Components are recognized by cream, brown and red colours in the south of Kürsü, Aþaðýmusalar, Yukarýmusalar and Ýsmailler areas (Figure 6).

In the Kürsü area, continental deposits are up to 200 metres thick and consist of subrounded welded ignimbrite boulders and cobbles within a loose matrix of sand and gravel. They display crude stratification and overlie the welded ignimbrites. In the Yukarýmusalar area, continental deposits are composed of well rounded and poorly sorted clasts of granites and rocks of the Ýzmir-Ankara Zone. In the Aþaðýmusalar area, they reach at their maximum thickness which is around 300 metres.

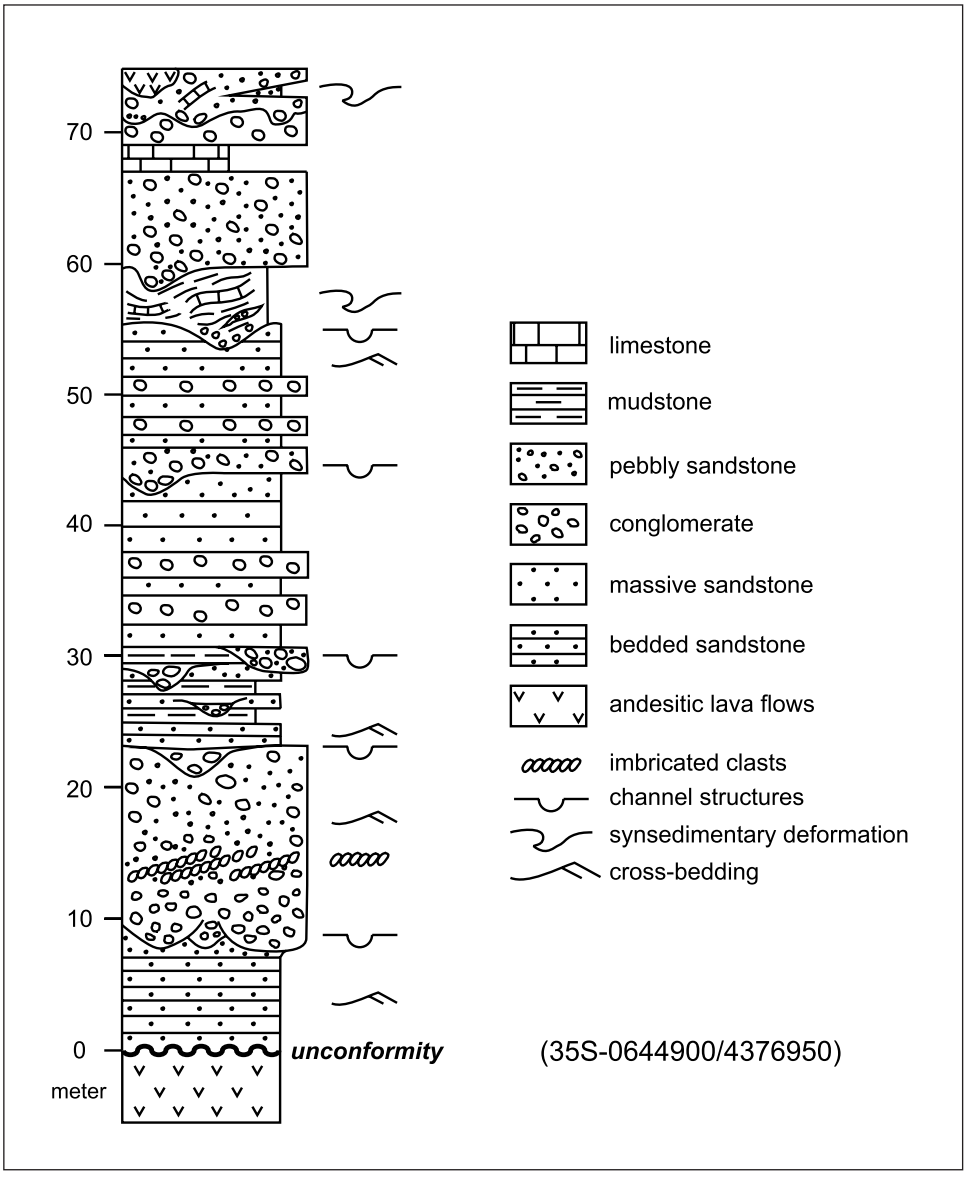

Figure 8- Measured stratigraphic log showing the contact zone between the Saðýrlar volcanic unit and the overlying alluvial/lacustrine sedimentary deposits.

Alluvium and scree deposits

Alluvial deposits are exposed in recent river beds and alluvial plains, which are commonly around Dursunbey area. Alluvial plains are generally surrounded by prominent topographic highs. Slope deposits are represented by unconsolidated and poorly sorted clasts, which were formed by rapid uplift and erosion processes.

GEOCHRONOLOGY

Granitic and volcanic rocks of the Alaçamdað magmatic complex were analysed by using Ar-Ar

Figure 9- Field appearance of an unconformity within the alluvial/lacustrine sedimentary deposits (Dursunbey - Gökçepýnar road-cut; 35S-0645855/4376435)

furnace step heating method in order to have cooling ages (Erkül, 2010). Analytical methods and ages of the Alaçamdað magmatic complex are summarized in table 2. In this study, Ar-Ar age of andesites of the Saðýrlar volcanic unit is presented.

The dated andesite sample consists of phenocrysts of plagioclase, biotite, hornblende and kersutite within a hyalopilitic matrix. Biotite and honblendes are commonly altered into opaque phases, forming pseudomorphs. Subhedral and anhedral phenocrysts of plagioclase contain tiny matrix inclusions.

Andesite sample of the Saðýrlar volcanic unit were run as conventional furnace step heating analyses. U-shaped age spectra are commonly associated with excess argon (the first few and final few steps often have lower radiogenic yields, thus apparent ages calculated for these steps are effected more by any excess argon present), and this is often verified by isochron analysis, which utilizes the analytical data generated during the step heating run, but makes no assumption regarding the composition of the non-radiogenic argon. Thus, isochrons can verify (or rule out) excess argon, and isochron ages are usually preferred if a statistically valid regression is obtained (as evidenced by an acceptably low MSWD value). If a sample yields no reliable isochron, the best estimate of the age is that the minimum on the age spectrum is a maximum age for the sample (it could be affected by excess argon, the extent depending on the radiogenic yield). $^{40}Ar/^{39}Ar$ total gas ages are equivalent to K/Ar ages. Plateau ages are sometimes found, these are simply a segment of the age spectrum which consists of 3 or more steps, comprising >50% of the total gas released. Such ages are preferred to total gas or maximum ages if obtained. However, in general an isochron age is the best estimate of the age of a sample, even if a plateau age is obtained.

The age spectrum for an andesite sample is very strongly U-shaped (Figure 11). Initial ages are very old, ranging up to ~429 Ma, in comparison to the minimum ages which are ~21 Ma. This is a very clear indication of excess argon and with no other information one would simply use the minimum age of ~21.3 Ma as a maximum age for the sample. The total gas age of 42.8 ± 0.2 Ma is very likely to be anomalously old. There was no plateau age defined for this sample. Isochron analysis reveals that 3 steps (6-8) define an age of 19.2 ± 0.2 Ma and suggest excess argon is present (initial $^{40}Ar/^{36}Ar$ = 338.0 ± 1.9). This isochron is defined by the minimum number of data points allowable (n = 3) and comprises 42% of the total gas released. In this case, the isochron indicates excess argon and this is also indicated by the U-shaped age spectrum. The isochron indicates an age less than the minimum on the age spectrum and this is what would be expected if excess argon is present. For these reasons, this particular isochron age of 19.2 ± 0.2 Ma can be accepted.

STRUCTURAL GEOLOGY

Ductile deformation in the Alaçamdað granites

Patterns of ductile deformation were observed in the Musalar and Alaçam granites. Ductile deformation within the Musalar granite is

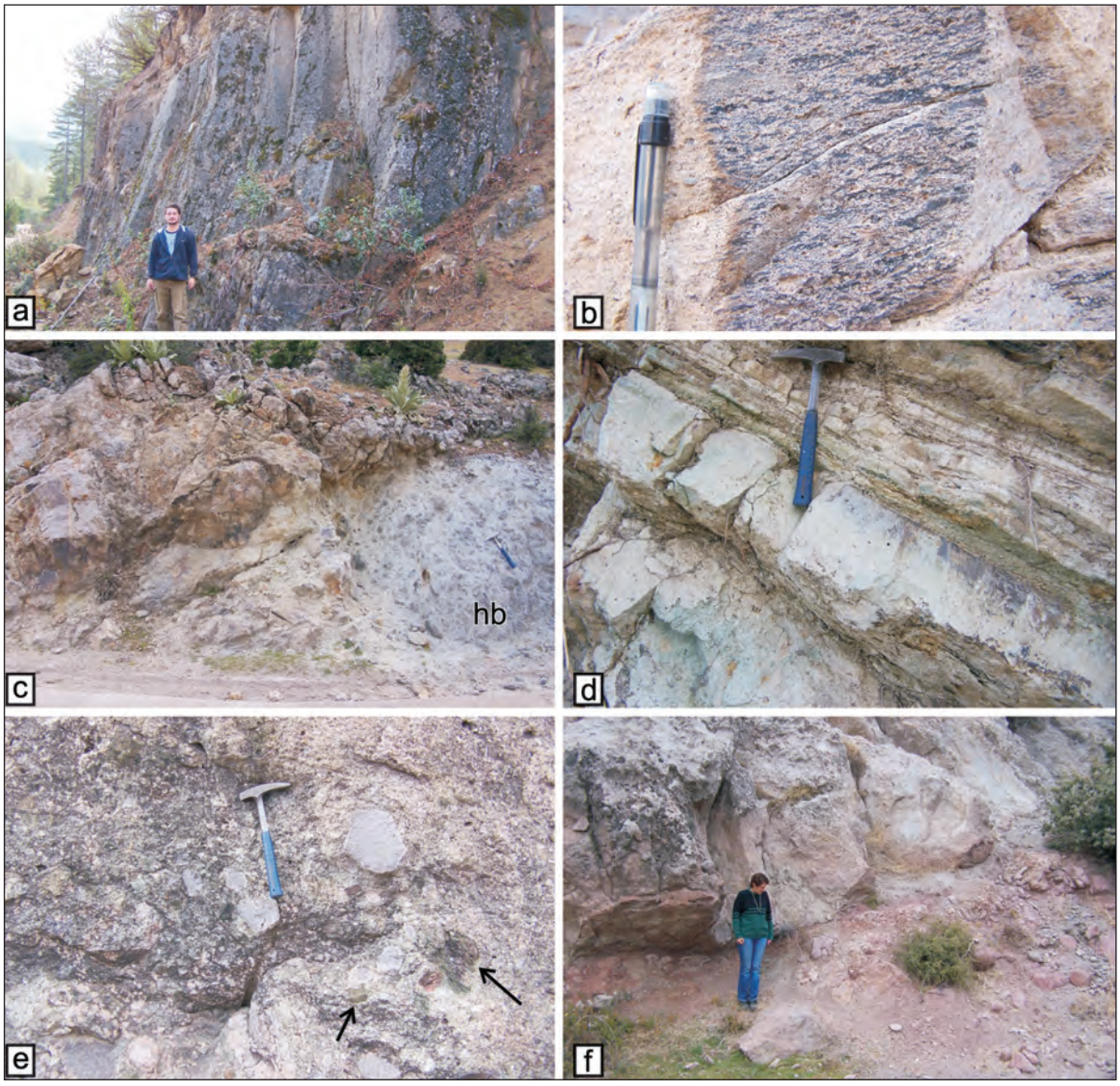

Figure 10- (a) Columnar-jointed ignimbrites on the clastic sediments of the Ýzmir-Ankara Zone is up to 400 metres thick. (b) welded ignimbrites on the massive ignimbrites. Pumice clasts were entirely transformed into fiamme (35S-0625325/4370650). (c) hyaloclastite breccias (hb) surrounding rhyolitic dykes in the Kürsü area (35S-0620580/4372100). (d) greenish massive ignimbrites intercalated with laminated limestones and claystones (35S-0618350/4366225). (e) lithic-rich ignimbrites on the Ýzmir-Ankara Zone. Volcanic clasts are angular and monomictic. Sandstone, shale and serpentinite clasts are shown by arrows (35S-0625200/4358000). (f) the contact relationship between breccias of the Saðýrlar volcanic unit and the overlying massive ignimbrites (south of Saðýrlar, 35S-0626398/4370750). The contact is represented by an up-to-50 cm-thick palaeosoil.

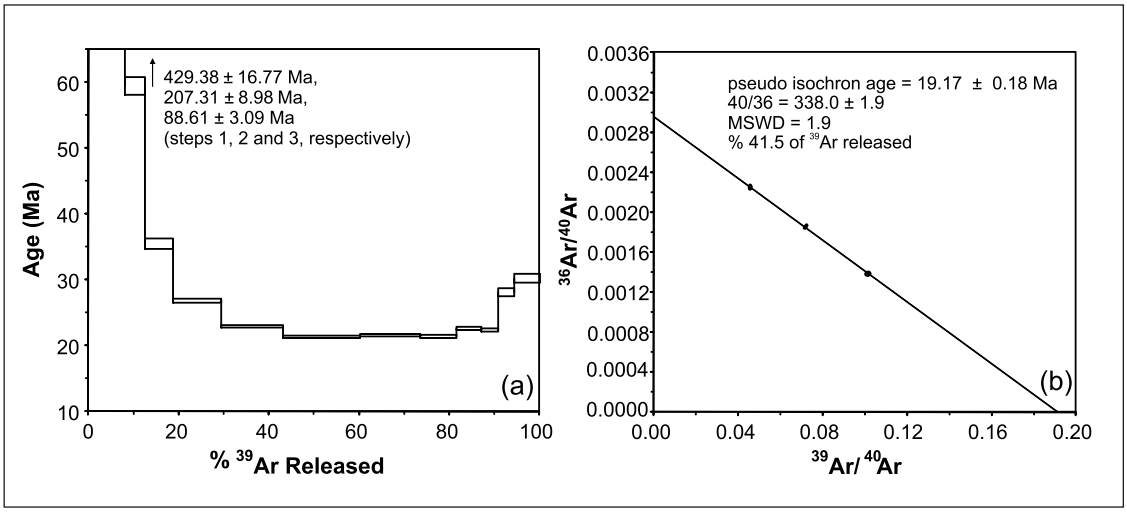

Figure 11- (a) apparent age spectrum and (b) isochron for andesite sample of the Saðýrlar volcanic unit.

located along a western margin of a rhomb-shaped stock (Figure 6). The contact between schists of the Menderes Massif and izmir-Ankara Zone is more or less vertical, defined by cm-thick foliation and lineation patterns. Undeformed granites have sharp contact with deformed, fo-liated granites (Figure 12a). Deformed granites display increasing deformation patterns and thinner foliation planes towards the marginal parts (Figure 12b). Deformation zone, the shear zone, usually consists of microcrystalline quartz, sericite and minor biotite crystals. Mafic minerals are less abundant in the shear zone with respect to those in the undeformed granites. Strike of foliation is variable, ranging between N45°E and N45°W. Dip of foliation is relatively low, ranging between 35 and 85 and plunging towards west. Lineation completely plunges towards the south-west with angles of between 2 and 56°.

Petrographic studies show that mylonitic rocks associated with Musalar granites consist of quartz, sericite, hornblende, biotite and minor potassium feldspar. These rocks are classified as ultramylonites based on abundance of matrix, which are by parallel microfaults (Figure 12c). These microfaults indicate a top-to-the-SW sense of shear. Quartz grains typically display oblique grain-shape foliation (Figure 12d) and occurs between foliation surfaces mainly defined by biotite crystals. Undulatory extinction and microfractures are common in large quartz grains. Sericites, which are after feldspars, become predominant towards the marginal parts of stocks.

Mylonitic foliation within the Alaçam granite is exposed in the southeastern and structurally upper parts of the NW-trending granite stock. In the northwestern part, porphyritic granites are completely undeformed (Figure 12e). Foliation planes are defined by lineation and quartzite bands formed by microcrystalline quartz grains (Figure 12f). Strike of foliation is variable and dip is relatively low angle ranging between 8 and 54°. Steeply dipping foliation is commonly exposed in the southern parts of the region. Lineation plunges toward NE and SW at an angle of 1-36°. Deformed Alaçam granites, which can be classified as protomylonites, are locally cut by C' shear bands. These shear bands indicate a top-to-the-NE sense of shear. At a mesoscopic scale, deformed granites are composed of quartz, plagioclase, potassium feldspar and biotite. They are also associated with aplites and mafic microgranular enclaves, which display

ductile deformation patterns such as sword-like intrusions of aplites and flattened enclaves.

Petrographic observations indicate the presence of some intense shear bands. Recrystallized quartz grains occur as clusters within asymmetrical shear bands (Figure 12g). Biotites within protomylonites display mica fish structures (Figure 12h). Potassium feldspars are subhedral to unhedral, brittlely fractures and display undulose extinction. Recrystallized quartz grains, shear bands, asymmetric potassium feldspar porphyroclasts and mica fish structures indicate a top-to-the NE displacement within the Alaçam granites.

DISCUSSION

Geological mapping studies in the Alaçamdağ region pointed out two volcanic episodes in the region. These episodes comprise Sağýrlar volcanic unit and felsic volcanic rocks, which are separated by an unconformity. Unconformable contact zones, which are characterized by palaeosoil occurrences and angular unconformities, indicate fast erosion and hiatus after emplacement of the Sağýrlar volcanic unit. Intrabasinal unconformities within the Early Miocene alluvial/lacustrine sedimentary/volcanic deposits together with extensive syn-sedimentary deformation suggest an active tectonic environment during sedimentation and volcanism in the Alaçamdağ region.

Ignimbrites, which have transitional contacts with alluvial/lacustrine sedimentary deposits, unconformably overlie mylonites of the Alaçam granites. Similar contact relationship was already described in the Koyunoba granites (Iþýk et al., 2004; Ring and Collins, 2005). Ductilely deformed Koyunoba granites are unconformably overlain by massive ignimbrites. Apatite fission track and U-Pb zircon ages from the Koyunoba ve Eðrigöz granites indicate that uplift of granites and their exhumation were associated with Simav detachment fault that was active during 25 to 19 Ma (Thomson and Ring, 2006; Ring and Collins, 2005; Hasözbek et al., 2009).

Thomson and Ring (2006) pointed out that erosional processes had a significant contribution to granite exhumation. Erkül (in press) provides convincing evidence for syn-extensional ductile deformation during emplacement of the Alaçam granite. The Alaçam granite includes a gently-dipping shear zone that is exposed in the structurally upper levels. Ar-Ar cooling ages of between 19.8 and 19.5 Ma were obtained from the deformed and undeformed granites, supporting the syn-tectonic emplacement of the Alaçam granite. These granites were probably exhumed by extensional shear zones that caused rapid uplift and erosion. Erosional processes operated after the emplacement of the Sağýrlar volcanic unit during 19.2 Ma.

Another important point is the time and space relationships between the Alaçamdağ granites and the overlying felsic volcanic rocks. This study demonstrates that the felsic volcanic rocks intercalated with alluvial/lacustrine deposits emplaced after the cooling of the Alaçamdağ granites. This suggests that the felsic volcanic rocks are not directly associated with exhumed Alaçamdağ granites and that younger and unexposed granite intrusions occurred following the exhumation processes in the Alaçamdağ region. Therefore, felsic volcanic rocks are not spatially and temporally associated with the Alaçamdağ granites.

Geological relationships among volcanism, plutonism and extensional tectonic patterns in the Alaçamdağ region strongly resemble to those of metamorphic core complexes exposed in the northwest Turkey. Early Miocene metamorphic core complexes were described in the northern Menderes and Kazdağ Massifs (Okay and Satýr, 2000; Iþýk and Tekeli 2001; Iþýk et al., 2004; Ring and Collins 2005). Evidence from these massifs indicate that extensional regime commenced during about 20 Ma. This age correspods to

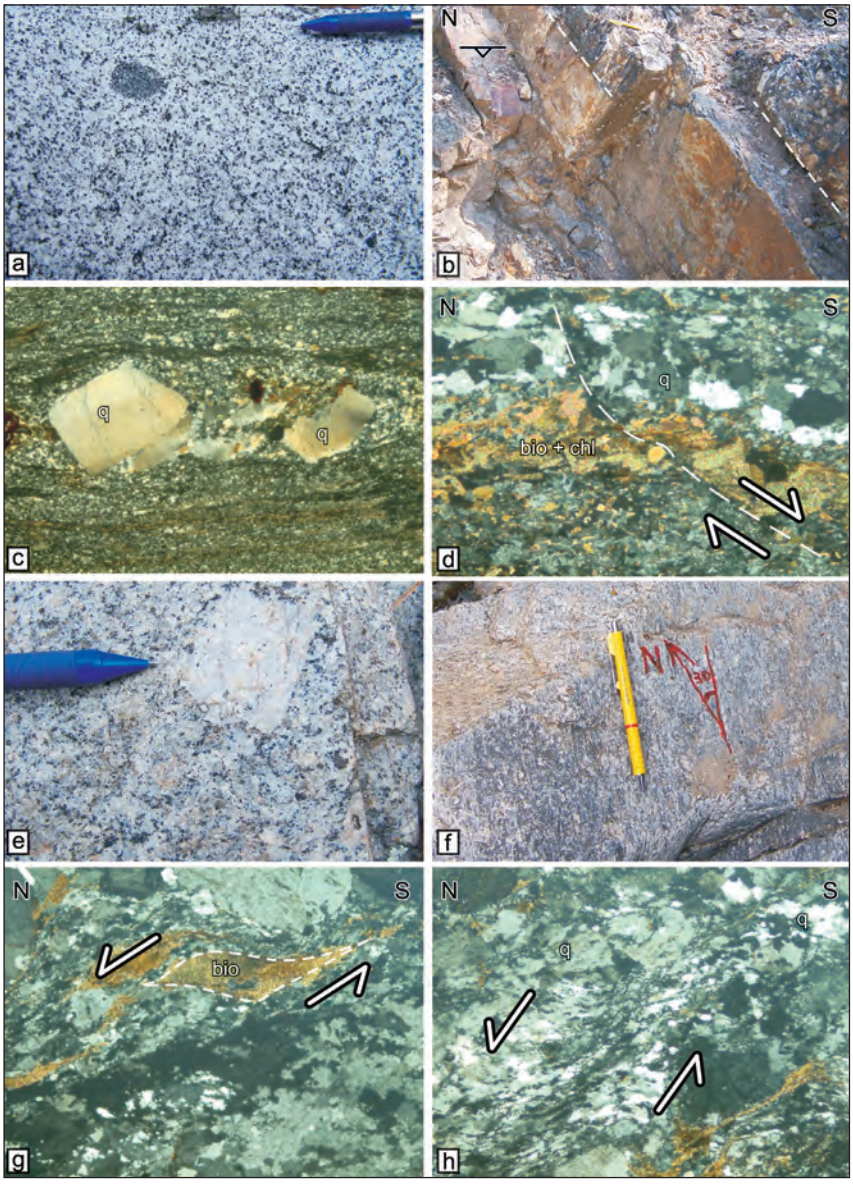

Figure 12 - Petrographic and structural characteristics of the Musalar (a-d) and Alaçam granites (e-h). (a) mafic microgranular enclaves within the equigranular Musalar granite. (b) mesoscopic appearance of shear-related foliation planes within the Musalar granite. Foliation dips towards southwest. (c) photomicrograph of domino-type structures in quartz grains within the sericite-rich ultramylonites. Dynamically recrystallised quartz grains display ondulatory extinction and microfractures. (d) photomicrograph of chlorite-filled microfaults cutting the quartz-rich ultramylonites Microfaults indicate a top-to-the southwest sense of shear. (e) orthoclase megacrysts in the porphyritic Alaçam granite. (f) mineral lineation on the protomylonitic granites. Pen is 15 cm long. (g) mica-fish structure within protomylonites. Kinematic data indicate a top-to-the northeast sense of shear. (h) shear bands formed by dynamically recrystallised quartz grains in the protomylonites. q: quartz, chl: chlorite, bio: biotite. Width of view in microphotographs is 3 millimetres.

emplacement and cooling ages of the Alaçamdað granites. Streching lineations from the ductile shear zones occurred in the Alaçamdað granites indicate that the hanging-wall rocks, the Ýzmir-Ankara Zone, displaced in different directions. Streching lineations within shear zones in the Alaçam granites show top-to-the-NE displacement of hanging-wall rocks, while shear zones within the Musalar granite indicate a top-to-the-SW displacement of the Bornova Flysch Zone. Ductile shear zones within the Musalar granite suggest the presence of a high-angle sinistral displacement between the juxtaposed rocks of the Menderes Massif to the west and the Bornova Flysch Zone to the east. Shear zones in the Alaçam granites are gently dipping and have streching lineations indicating top-to-the NE sense of shear. These kinematic indicators in the Alaçam granites are consistent with those measured in the Kazdað and Simav metamorphic core complexes. All kinematic data from the metamorphic core complexes suggest that northwestern Turkey experienced a NE-SW-directed extension during at least Early to Middle Miocene times.

Stratigraphy of the Alaçamdað region is similar to that of the NE-trending basins in western Turkey. Volcanism accompanied the deposition of alluvial and lucustrine sedimentary deposits in the NE-trending Bigadiç, Gördes, Demirci and Soma basins during Early Miocene. Unconformities observed in volcanic and sedimentary successions appear to be associated with the regional-scale detachment faults and extensional shear zones occurred in western Turkey.

CONLCUSION

The Alaçamdað region has been subjected to the rapid uplift and erosional processes owing to activity of steeply and gently dipping shear zones during Early Miocene. Evidence for operation of these processes were recorded in the Early Miocene volcano-sedimentary successions in the Alaçamdað region: (1) angular unconformities between the Saðýrlar volcanic unit and the overlying alluvial/lacustrine sedimentary and felsic volcanic rocks, (2) intrabasinal unconformities and syn-sedimentary deformation structures within the alluvial/lacustrine sedimentary deposits, and (4) felsic volcanic rocks overlying the mylonitised Alaçam granites.

Streching lineations and kinematic indicators associated with the Alaçam granites are consistent with shear sense recorded from other metamorphic core complexes in western Turkey. These data indicate that the western Anatolia experienced NE-SW-directed extension during Early Miocene.

ACKNOWLEDGEMENTS

This work was supported by a project of the Scientific and Technological Research Council of Turkey (TÜBÝTAK) (Project no: 104Y274). Pýnar Tatar is thanked for help with English.

Manuscript received June 29, 2009

REFERENCES

Akdeniz, N. and Konak, N. 1979. Menderes Masifi'nin Simav dolayýndaki kaya birimleri ve metabazik, metaultramafik kayalarýn konumu. Türkiye Jeoloji Kurumu Bülteni, 22, 175-183.

Akyürek, B. and Soysal, Y. 1982. Biga yarýmadasý güneyinin (Savaþtepe Kýrkaðaç-Bergama-Ayvalýk) temel jeoloji özellikleri. Maden Tetkik Arama Enstitüsü Dergisi, 95/96, 1-12.

Aldanmaz, E., Pearce J., Thirlwall, M. F, and Mitchell, J. G., 2000. Petrogenetic evolution of Late Cenozoic, post-collision volcanism in western Anatolia, Turkey. Journal of Volcanology and Geothermal Research, 102 1-2, 67-95.

Altunkaynak, Þ. and Yýlmaz, Y. 1998. The Mount Kozak Magmatic Complex, Western Anatolia. Journal of Volcanology and Geothermal Research, 85 1-4, 211-231.

Altunkaynak, Þ., and Dilek, Y., 2006. Timing and nature of postcollisional volcanism in western Anatolia and geodynamic implications. Geology Society of American Special Paper, 409, 321-351

Bingöl, E., Delaloye, M. and Ataman, G. 1982. Granitic intrusions in Western Anatolia: A contribution to the geodynamic study of this area. Eclogae Geologica Helvetica, 75, 437-446.

Borsi, J., Ferrara, G., Innocenti, F. and Mazzuoli, R. 1972. Geochronology and petrology of recent volcanics in the easthern Aegean Sea (West Anatolia and Lesvos Island). Bulletin of Volcanology, 36, 473-496.

Bozkurt, E. 2000. Timing of extension on the Büyük Menderes Graben, western Turkey, and its tectonic implications. Geological Society, London, Special Publications, 173 1, 385-403.

_____, 2001*a*. Late Alpine evolution of the central Menderes Massif, Western Anatolia, Turkey. International Journal of Earth Sciences, 89, 728-744.

_____, 2001*b*. Neotectonics of Turkey-a synthesis. Geodinamica Acta, 14 (1-3), 3-30.

_____, 2003. Origin of NE-trending basins in western Turkey. Geodinamica Acta, 16, 61-81.

_____, 2004. Granitoid rocks of the southern Menderes Massif (southwestern Turkey): field evidence for Tertiary magmatism in an extensional shear zone. International Journal of Earth Sciences 93 (1), 52-71.

_____ and Park, R.G. 1994. Southern Menderes Massif-an incipient metamorphic core complex in western Anatolia, Turkey. Journal of the Geological Society, 151, 213-216.

_____ and _____, 1997*a*. Microstructures of deformed grains in the augen gneisses of southern Menderes Massif (western Turkey) and their tectonic significance. Geologische Rundschau 86 (1), 103-119.

_____ and _____, 1997*b*. Evolution of a mid-Tertiary extensional shear zone in the southern Menderes massif, western Turkey. Bulletin De La Societe Geologique De France 168 1, 3-14.

Bozkurt, E. and Oberhänsli, R. 2001. Menderes Massif (Western Turkey): Structural, metamorphic and magmatic evolution-a synthesis. International Journal of Earth Sciences, 89, 679-708.

_____ and Sözbilir, H. 2004. Tectonic evolution of the Gediz Graben: field evidence for an episodic, two-stage extension in Western Turkey. Geological Magazine, 141 1, 63-79.

Delaloye, M. and Bingöl, E. 2000. Granitoids from Western and Northwestern Anatolia: Geochemistry and modeling of geodynamic evolution. International Geology Review, 42 3, 241-268.

Dilek, Y. and Altunkaynak, Þ., 2007. Cenozoic crustal evolution and mantle dynamics of post-collisional magmatism in western Anatolia. International Geology Review, 49, 431-453.

Ercan, T. 1979. Batý Anadolu, Trakya ve Ege adalarýndaki Senozoyik volkanizmasý. Jeoloji Mühendisliði Dergisi, 10, 23-46.

_____, 1982. Batý Anadolu Tersiyer volkanitleri ve Bodrum yarýmadasýndaki volkanizmanýn durumu. Ýstanbul Yerbilimleri Dergisi, 2, 263-281.

_____ and Öztunalý, Ö. 1983. Demirci-Selendi çevresinde Senozoyik yaþlý volkanitlerin petrolojisi ve kökensel yorumu. Yerbilimleri, 10, 1-15.

_____, Satýr, M., Kreuzer, H., Türkecan, A., Günay, E., Çevikbaþ, A., Ateþ, M. and Can, B. 1985. Batý Anadolu Senozoyik volkanitlerine ait yeni kimyasal, izotopik ve radyometrik verilerin yorumu. Türkiye Jeoloji Kurumu Bülteni, 28, 121-136.

Erdoðan, B. 1990*a*. Tectonic relations between Izmir-Ankara Zone and Karaburun Belt. Bulletin of the Mineral Research and Exploration Institute of Turkey, 110, 1-15.

_____, Altýner, D., Güngör, T., and Özer, S. 1990*b*. Stratigraphy of Karaburun Peninsula. Bulletin of the Mineral Research and Exploration Institute of Turkey, 111, 1-20.

Erdoðan, B. and Güngör, T. 2004. The problem of the core-cover boundary of the Menderes Massif and an emplacement mechanism for regionally extensive gneissic granites, western Anatolia (Turkey). Turkish Journal of Earth Sciences 13 1, 15-36.

Erkül, F., 2010. Tectonic significance of synextensional ductile shear zones within the Early Miocene Alaçamdað granites, northwestern Turkey. Geology Magazine, 1-27.

_____, Helvacý, C. and Sözbilir, H. 2005*a*. Evidence for two episodes of volcanism in the Bigadic borate basin and tectonic implications for western Turkey. Geological Journal 40, 545-570.

_____, _____ and _____, 2005*b*. Stratigraphy and geochronology of the Early Miocene volcanic units in the Bigadiç borate basin, Western Turkey. Turkish Journal of Earth Sciences, 14 3, 227-253.

_____, Tatar-Erkül, S., Bozkurt, E, Sözbilir, H., and Helvacý, C., 2009*a*. Tectonic significance of ductile shear zones within the syn-extensional Alaçamdag granite, northwestern Turkey. 62. Geological Kurultai of Turkey, Abstract, 178-179.

Erkül S.T., Erkül, F., Bozkurt, E., Sözbilir, H. and Helvacý, C., 2009*b*. Geodynamic setting of the early Miocene Alaçamdag volcano-plutonic complex based on petrologic, isotopic and geochronological data: northwestern Turkey. 62. Geological Kurultai of Turkey, Abstract, 180-181.

Ersoy, Y., Helvacý, C., Sözbilir, H., Erkül, F. and Bozkurt, E. 2008. A geochemical approach to Neogene-Quaternary volcanic activity of western Anatolia: An example of episodic bimodal volcanism within the Selendi Basin, Turkey. Chemical Geology, 255(1-2), 265-282.

Genç, C. Þ. 1998. Evolution of the Bayramiç Magmatic Complex, Northwestern Anatolia. Journal of Volcanology and Geothermal Research, 85, 233-249.

Gessner, K., Ring, U., Johnson, C., Hetzel, R., Passchier, C.W., and Güngör, T. 2001. An active bivergent rolling-hinge detachment system; central Menderes metamorphic core complex in western Turkey. Geology, 29, 611-614.

Glodny, J., and Hetzel, R. 2007. Precise U-Pb ages of syn-extensional Miocene intrusions in the central Menderes Massif, western Turkey. Geological Magazine 144 (2), 235-246.

Hasözbek, A., Satýr, M., Erdoðan, B., Akay, E., and Siebel, W. 2009. KB Anadolu'daki çarpýþmaya baðlý granitlerin U-Pb Jeokronolojisi, Sr-Nd izotop jeokimyasý ve Petrojenetik Evrimlerinin Karþýlaþtýrýlmasý. 62. Türkiye Jeoloji Kurultayý, 13-17 Nisan 2009, Maden Tetkik ve Arama Genel Müdürlüðü, Ankara.

_____, _____, _____, _____ and _____ (in press). Early Miocene post-collisional magmatism in NW Turkey: geochemical and geochronological constraints. International Geology Review.

Helvacý, C. 1995. Stratigraphy, mineralogy and genesis of the Bigadiç Borate deposits, Western Turkey. Economic Geology, 90, 1237-1260.

_____ and Alonso, R.N. 2000. Borate deposits of Turkey and Argentina: A summary and geological comparison. Turkish Journal of Earth Sciences, 24, 1-27.

Hetzel, R., Passchier, C.W., Ring, U., and Dora, O.O. 1995*a*. Bivergent Extension in Orogenic Belts: the Menderes Massif (Southwestern Turkey). Geology, 23 (5), 455-458.

_____, Ring, U., Akal, C., and Troesch, M. 1995*b*. Miocene NNE-directed extensional unroofing in the Menderes Massif, southwestern Turkey. Journal of the Geological Society London, 152, 639-654.

Innocenti, F. and Mazzuoli, R. 1972. Petrology of Ýzmir-Karaburun volcanics (west Turkey). Bulletin of Volcanology, 36, 1-22.

Iþýk, V and Tekeli, O., 2001. Late orogenic crustal extension in the northern Menderes massif (western Turkey): evidence for metamorphic

core complex formation. International Journal of Earth Sciences, 89 4, 757-765.

Iþýk, V., Seyitoðlu, G., and Çemen, Ý, 2003. Ductile-brittle transition along the Alasehir detachment fault and its structural relationship with the Simav detachment fault, Menderes massif, western Turkey. Tectonophysics, 374 1-2, 1-18.

_____, Tekeli, O., and Seyitoðlu, G., 2004. The Ar-40/Ar-39 age of extensional ductile deformation and granitoid intrusion in the northern Menderes core complex: implications for the initiation of extensional tectonics in western Turkey. Journal of Asian Earth Sciences, 23 4, 555-566.

Ýnci, U. 1998. Lignite and carbonate deposition in Middle Lignite succession of the Soma Formation, Soma coalfield, western Turkey. International Journal of Coal Geology, 37, 287-313.

Karacýk, Z. and Yýlmaz, Y., 1998. Geology of the ignimbrites and the associated volcano-plutonic complex of the Ezine area, northwestern Anatolia. Journal Vof Volcanology and Geothermal Research, 85 1-4, 251-264.

Koçyiðit, A., Yusufoðlu, H., and Bozkurt, E. 1999. Evidence from the Gediz graben for episodic two-stage extension in western Turkey. Journal of the Geological Society, 156, 605-616.

Krushensky, R.D. 1976. Volcanic rocks of Turkey. Bulletin of Geological Survey Japan, 26, 393.

Okay, A.Ý and Siyako, M. 1993. The revised location of the Ýzmir-Ankara Suture in the region between Balýkesir and Ýzmir (In Turkish). Tectonics and Hydrocarbon Potential of Anatolia and Surrounding Regions, 333-355.

_____ and Tüysüz, O. 1999. Tethyan Sutures of northern Turkey. In: B. Durand, L. Jolivet, F. Horvath ve M. Seranne (Eds.), Mediterranean Basins: Tertiary extension within the Alpine Orogen. Geological Society of London Special Publication, 475-515.

_____ and Satýr, M. 2000. Coeval plutonism and metamorphism in a latest Oligocene metamorphic core complex in northwest Turkey. Geological Magazine, 137/5, 495-516.

Pe-Piper, G. and Piper, D.J.W. 1989. Spatial and temporal variation in Late Cenozoic back-arc volcanic rocks, Aegean Sea region. Tectonophysics, 169, 113-134.

_____ and _____, 2001. Late Cenozoic, postcollisional Aegean igneous rocks: Nd, Pb and Sr isotopic constraints on petrogenetic and tectonic models. Geological Magazine, 138 6, 653-668.

Purvis, M. and Robertson, A. 2004. A pulsed extension model for the Neogene-Recent E-W-trending Alasehir Graben and the NE-SW-trending Selendi and Gordes Basins, western Turkey. Tectonophysics, 391 1-4, 171-201.

Rimmele, G., Jolivet, L., Oberhänsli, R., and Goffe, B. 2003*a*. Deformation history of the high-pressure Lycian Nappes and implications for tectonic evolution of SW Turkey. Tectonics 22 2, 1-21.

_____, Oberhänsli, R., Goffe, B., Jolivet, L., Candan, O., and Çetinkaplan, M. 2003*b*. First evidence of high-pressure metamorphism in the "Cover Series" of the southern Menderes Massif. Tectonic and metamorphic implications for the evolution of SW Turkey. Lithos 71 1, 19-46.

Ring, U., Laws, S., and Bernet, M. 1999. Structural analysis of a complex nappe seqýuence and late orogenic basins from the Aegean Island of Samos, Greece. Journal of Structural Geology, 21 11, 1575-1601.

_____, Johnson, C., Hetzel, R., and Gessner, K. 2003. Tectonic denudation of a Late Cretaceous-Tertiary collisional belt: regionally symmetric cooling patterns and their relation to extensional faults in the Anatolide belt of western Turkey. Geological Magazine, 140 4, 421-441.

_____ and Collins, A.S. 2005. U-Pb SIMS dating of synkinematic granites: Timing of core-complex formation in the northern Anatolide belt of western Turkey. Journal of the Geological Society, 162, 289-298.

Savaþçýn, M. Y. and Güleç, N. 1990. Relationship between magmatic and tectonic activities in western Turkey. In: M.Y. Savaþçýn and A.H. Eronat (Eds.), International Earth Science Colloquum on the Aegean Region (IESCA) Proceedings, 300-313.

Seyitoðlu, G. 1997. Late Cenozoic tectono-sedimentary development of the Selendi and Usak-Gure basins: a contribution to the discussion on the development of east-west and north trending basins in western Turkey. Geological Magazine, 134, 163-175.

_____ and Scott, B. 1992. Late Cenozoic volcanic evolution of the northeastern Aegean region. Journal of Volcanology and Geothermal Research, 54, 157-176.

_____, Anderson, D., Nowell, G., and Scott, B. 1997. The evolution from Miocene potassic to Quaternary sodic magmatism in western Turkey: implications for enrichment processes in the lithospheric mantle. Journal of Volcanology and Geothermal Research, 76, 127-147.

_____, Tekeli, O., Çemen, Ý, Þen, S., and Iþýk, V. 2002. The role of the flexural rotation/rolling hinge model in the tectonic evolution of the Alaþehir graben, western Turkey. Geological Magazine, 139 1, 15-26.

Sözbilir, H. 2001. Extensional tectonics and the geometry of related macroscopic structures with their relations to the extensional tectonics: Field evidence from the Gediz detachment, western Turkey. Turkish Journal of Earth Sciences, 10, 51-67.

_____, 2002*a*. Geometry and origin of folding in the Neogene sediments of the Gediz Graben, western Anatolia, Turkey. Geodinamica Acta, 15 5-6, 277-288.

Sözbilir, H. 2002*b*. Revised stratigraphy and facies analysis of Palaeocene - Eocene supra-allochthonous sediments (Denizli, SW Turkey) and their tectonic significance. Turkish Journal of Earth Sciences, 11, 87-112.

Þengör, A. M. C. 1984. Timing of tectonic events in the Menderes massif, Western Turkey: implications for tectonic evolution and evidence for Pan-African basement in Turkey. Tectonics, 3 7, 693-707.

Thomson, S.N. and Ring, U. 2006. Thermochronologic evaluation of postcollision extension in the Anatolide orogen, western Turkey. Tectonics, 25 3.

Westaway, R. 2006. Cenozoic cooling histories in the Menderes Massif western Turkey, may be caused by erosion and flat subduction, not low-angle normal faulting. Tectonophysics, 412 1-2, 1-25.

Whitney, D. L. and Bozkurt, E. 2002. Metamorphic history of the southern Menderes massif, western Turkey. Geological Society of America Bulletin 114 7, 829-838.

Yýlmaz, Y., Genç, S.C., Gürer, F., Bozcu, M., Yýlmaz, K., Karacýk, Z., Altunkaynak, Þ. and Elmas, A. 2000. When did the western Anatolian grabens begin to develop? In: E. Bozkurt, J.A. Winchester ve J.D.A. Piper (Eds.), Tectonics and Magmatism in Turkey and the Surrounding Area. Geological Society, London, Special Publications, 353-384.

_____, _____, Karacýk, Z. and Altunkaynak, Þ. 2001. Two contrasting magmatic associations of NW Anatolia and their tectonic significance. Journal of Geodynamics, 31, 243-271.

Mineral Res. Expl. Bull., 141, 27-52, 2010

APATITE-BEARING MAGNETITE DEPOSIT OF PINARBAÞI (ADIYAMAN); GEOLOGICAL, GEOCHEMICAL PROPERTIES AND ECONOMICAL POTENTIAL

Hüseyin ÇELEBÝ*, Cahit HELVACI** and Ali UÇURUM***

ABSTRACT.- In the near vicinity of the apatitebearing magnetite deposit of Pýnarbaþý Permianaged Malatya Metamorphites consisting of, from bottom to top, chlorite schists, cericite schists, calcschists and recrystallized limestones cover large areas. These folded and faulted metamorphic rocks, which thrust over the Eoceneaged Maden Complex, underwent one regional metamorphism and one subsequent retrograde metamorphism in the greenschist facies. Mineralizations associated with chloritesericite schists are in the form of magnetitebearing apatite lenses. The ore horizons, which reach a thickness of 15 m and have a northsouth strike, dip approximately 30 degrees to the west. In the field, massive, banded and disseminated ore types are distinguished. The most important ore mineral is magnetite. It is followed by hematite, siderite, goethite and specularite. The proportion of the fluorapatite, the most valuable gangue mineral, reaches up to 30% in some places. Quartz, calcite, chlorite and sericite are other common gangue minerals. Rarely, rutile, zircon, monazite and xenotime are also observed. There is a significant positive correlation between Fe, P_2O_5 and depth. The variograms reveal holeeffects which reflect orerock alternations. Frequency distributions of the elements are logarithmic. Magnetite reserves with an iron content of over 20% Fe are approximately 78 Mt. The average P_2O_5 concentration of these reserves having an average Fe tenor of 35% is 1.57%. The F concentration of 3.46% in apatite is significant. However, rare earth element (REE) concentration of apatite (900 ppm) and V concentration of magnetite (800 ppm) are low. This deposit defined as classic Kirunatype sedimentary apatitebearing magnetite deposit, is not considered to be economically mined.

Key words: Pýnarbaþý, magnetite, apatite, geochemistry and metamorphism.

INTRODUCTION

Iron deposits are considerably miscellaneous in nature with regard to both origin and structure. Apatite-bearing magnetite deposits constitute an important mineralization type of iron, which can form any kind of deposits. Deposits of this type, like Pýnarbaþý Apatite-bearing Magnetite Deposit have great economical importance, which constitute the most important source of the Swedish steel industry, and are termed as "Kiruna-type iron deposits" in the literature (Wright, 1986). Other important apatite-bearing magnetite deposits are Cerro de Mercado (Mexico), El Laco (Chile) and Bafq (Iran) (Mücke and Younessi, 1994; Förster and Jafarzadeh, 1994). Examples of these deposits in Turkey are Avnik (Bingöl) and Ünaldý (Bitlis) apatite-bearing magnetite deposits.

Pýnarbaþý apatite-bearing magnetite deposit is located approximately 6 km to the west of Çelikhan County of Adýyaman Province. The study area is easily accessible by an asphalt road of 30 km from Sürgü Subdistrict, located on Malatya-Gaziantep Highway (Figure 1).

PREVIOUS WORKS

There are numerous researches regarding various disciplines of geology on the deposit area and the near vicinity. The pioneer researchers are Tolun (1955) and Koþal (1967).

* Mersin Üniversitesi, Mühendislik Fakültesi, Jeoloji Mühendislið Bölümü, 33343 Çiftlikköy, Mersin
** Dokuz Eylül Üniversitesi, Mühendislik Fakültesi, Jeoloji Mühendisliði Bölümü, 35100 Bornova/Ýzmir
*** Cumhuriyet Üniversitesi, Mühendislik Fakültesi, Jeoloji Mühendisliði Bölümü, 58140 Sivas

They are followed by Perinçek (1979), Gözübol and Önal (1986), Önal et al. (1986), Yazgan and Chessex (1991) and Önal and Gözübol (1992). Iron and phosphorous contents, reserves and mineability subjects were studied by Öztürk (1982), Akar (1983), Büyükkýdýk and Aras (1984) and Güneþ (1994). Subsequent studies were performed by Önal et al. (2002) on the mineralogical nature and geochemical composition of the mineralization. Lastly, mineralogical and geochemical properties of the deposit were examined, radiometric age determination was performed and its economic potential was discussed by Çelebi et al. (2005).

The cuts and trenches observed in the study area prove that the widely outcropping Pýnarbaþý apatite-bearing magnetite deposit has long been known and worked. Recent mining activities such as drilling works and ore heaps confirm that this area has been attracting interest since the middle of the 20th century. However some experimental works were performed in 1930s and 1990s, the high phosphorous content of the ores was not carried on (Çelebi et al., 2005).

Modern investigation studies were started in 1970 by MTA (General Directorate of Mineral Research and Exploration). During mapping, drilling and enrichment works, which were intermittently continued up to 1984, 9 drill holes, 385 m^3 trenches, 347 cores and 145 point samples have been examined, the reserve of the deposit was calculated and the extension of the ore was partly determined (Büyükkýdýk and Aras, 1984). As a result of these works a magnetite reserve of 69.2 million tons with 28.56 % Fe and 2.01 % P_2O_5 grade was calculated. Güneþ (1994)

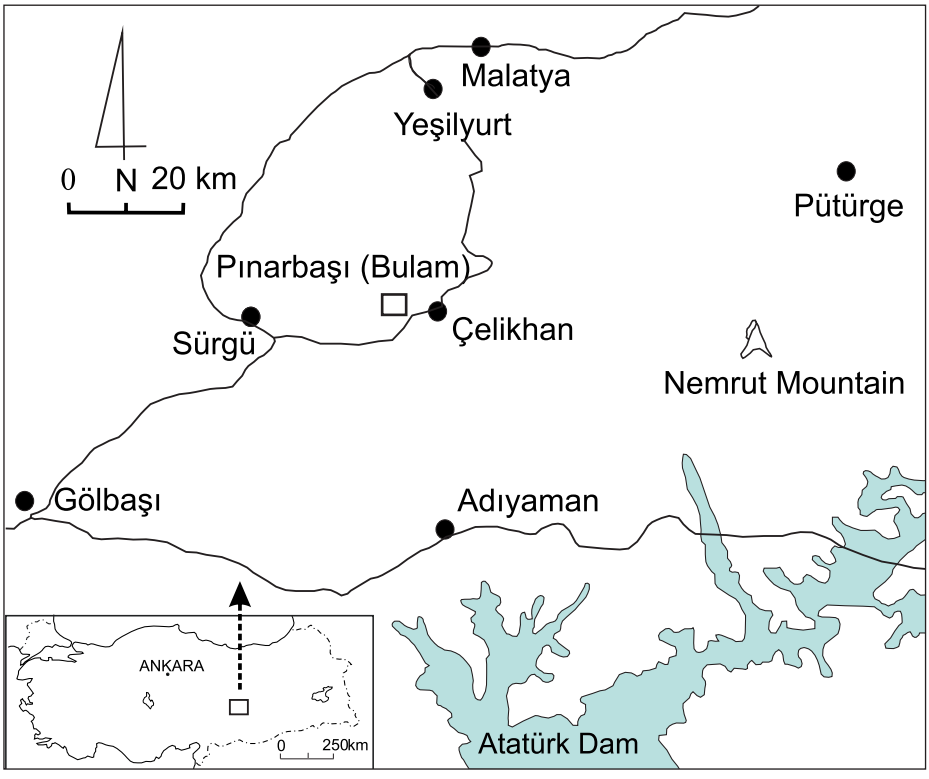

Figure 1 - Geographical location of the study area

declares 66.2 Mt (36.04 % Fe and 2.07 % P_2O_5) and Sývacý et al. (2003) give 78 Mt (35.07 % Fe and 1.57 % P_2O_5).

SCOPE AND WORKING METHODS

The scope of this study is to investigate the geological structure and mineralogical properties of the Pýnarbaþý deposit, macro and micro compositions of the ore and the wall rock, and to determine the economical significance of the deposit. For this purpose, the geology of the deposit and its near vicinity has been studied, and the nature, composition and potential of the mineralization were determined. In addition, fluorite and heavy element contents, which carry great importance for the production of vanadium and fluoric acid used especially in steel and battery production were analyzed, and the conditions of formation were interpreted by examining inter-elemental relationships and proportions.

GEOLOGICAL STRUCTURE

In the near vicinity of the Pýnarbaþý apatite-bearing magnetite deposit, there are rock units of various age and origin. These are rock units of Paleozoic, Mesozoic, Tertiary and Quaternary ages (Figure 2) in which, the most important ones are: Paleozoic (Permo-Carboniferous) Pütürge and Malatya Metamorphites having wide distribution in the north of the collisional belt of Anatolian and Arabian Plates (Tolun, 1955; Perinçek, 1979), Eocene Maden Complex (Perinçek, 1979), and Quaternary alluviums.

STRATIGRAPHY

Pütürge Metamorphites constitute the lowermost unit of the area. Maden Complex, composed of volcano-sedimentary rocks, overlies this unit with an angular unconformity. Malatya Metamorphites, composed of schists and recrystallized limestones, thrust over this complex (Figure 2). At the top, Pliocene conglomerates and Quaternary alluvial sediments cover all these units with an unconformity.

Pütürge metamorphites

Pütürge Metamorphites are not observed in the deposit area and in its near vicinity. They are mainly exposed in the Pütürge district, the region which they were named. This unit, which is a product of regional metamorphism, presents greenschist facies conditions. From bottom to top, it is composed of gneiss, amphibolite schist, mica schist and recrystallized limestones. Pütürge Metamorphites is considered as the part of Bitlis Massif (Brinkman, 1971; Yýlmaz and Yiðitbaþ, 1990) and gained their present form in Eocene time. According to Önal et al. (1986), while the lower contact of the unit is not observed, the upper contact is angularly unconformable with Eocene Maden Complex composing of andesitic, spilitic tuffs, red mudstones and limestones (Figure 2).

Malatya Metamorphites

This unit is also called as "Kilkaya Limestone" and "Amanos Formation" by Gözübol and Önal (1986). Perinçek (1979) named it "Malatya Metamorphites" for its distinctive appearance in the south of Malatya and divided it into Lower and Upper Metamorphites. While took the unit into hand as Lower and Upper Units Gözübol and Önal (1986) examined this metamorphics by dividing into four units, from bottom to top, Pýnarbaþý Formation, Koltik Limestone, Düzaðaç Formation and Kalecik Limestones (Figure 2).

The Pýnarbaþý apatite-bearing magnetite deposit takes place in the Malatya Metamorphites (Figure 3 and 5). Malatya Metamorphites thrust over Maden Complex and Pütürge Metamorphites. Gündüzbey Group of Upper Cretaceous which is represented by schists and recrystallized limestones as the products of intermediate and low-grade regional metamorphism (Önal and Gözübol, 1992), overlies this unit with an angular unconformity (Önal et al., 1986).

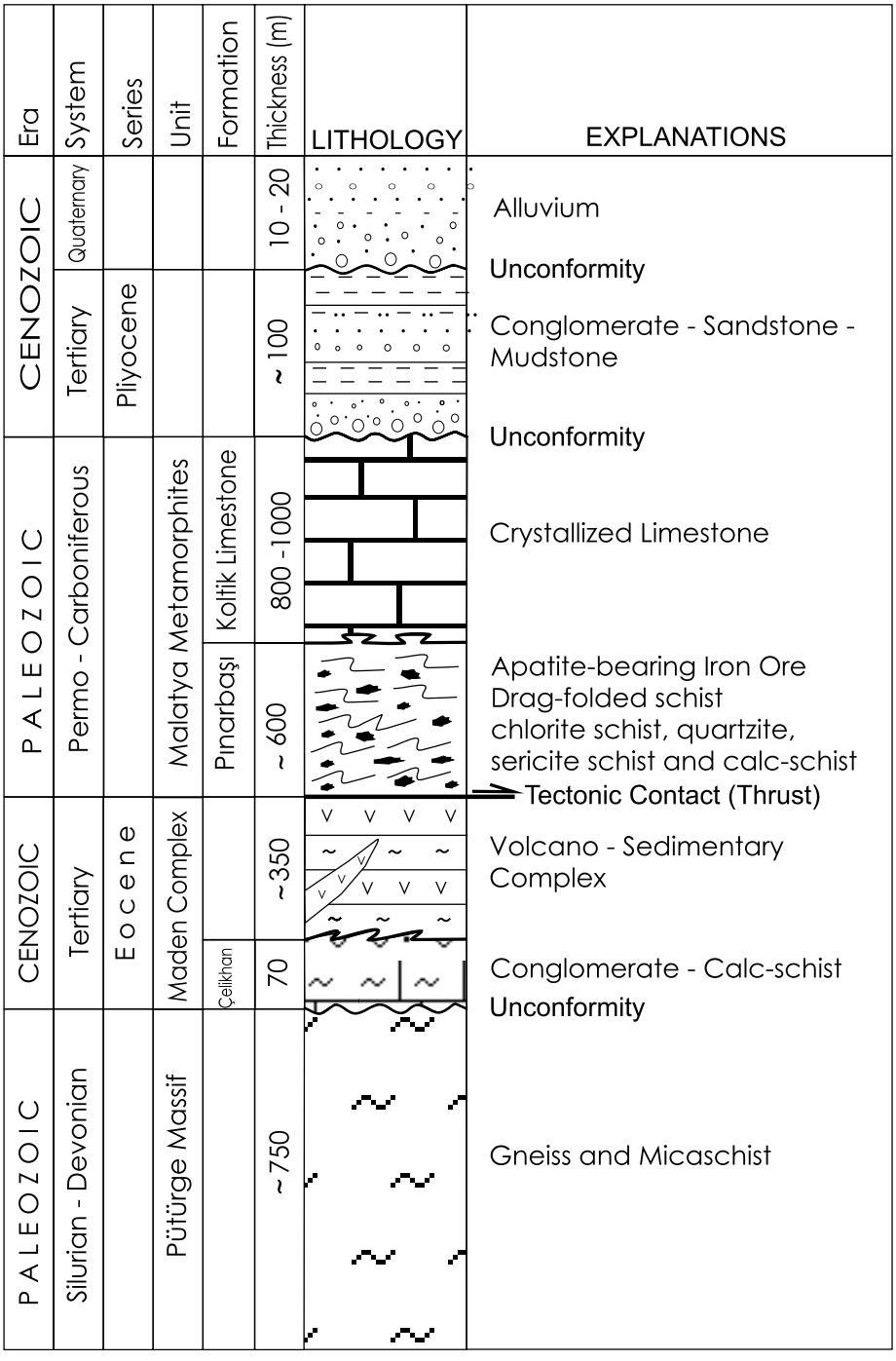

Figure 2- Generalized stratigraphic columnar section of Çelikhan District (Modified after Gözübol and Önal, 1986).

Figure 3 - Malatya Metamorphites observed in the north of Pýnarbaþý Deposit. Ore-bearing schists of Pýnarbaþý Formation (middle, dark), Koltik Limestones (up, light) and alluviums of Çelikhan Plain (front)

Pýnarbaþý Formation is widespread in the north of the deposit. From bottom to top, the unit is composed of chlorite schists, sericite schists and calc-schists. Schistosity is well-developed in the unit. Abundant quartz veins in various thicknesses cross-cut the formation. Rarely, sulfites are also observed within these veins. Calc-schists, which are presented around the chlorite schists, are bituminous and dolomitic in places. Dolomitic parts are thick-bedded and fine-grained. Pýnarbaþý mineralizations are mainly located in this unit (Figure 4).

Pýnarbaþý Formation gradationally passes into Koltik Limestone. The thickness of this unit reaches up to 1000 m, and is widespread in the eastern part of the deposit. The lower parts of the unit are bedded and their color is dark gray and

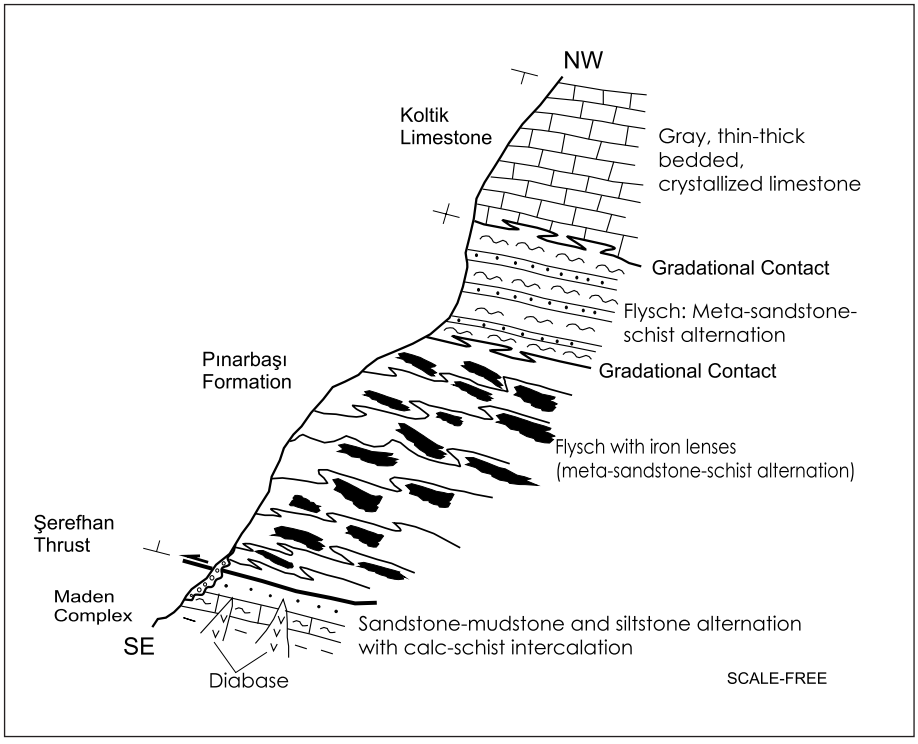

Figure 4 - Cross-section of Malatya Metamorphites at Çelikhan Hill, it explains Maden Complex and its relation with thrust line.

white. This recrystallized unit contains epidote, chlorite and quartz. Fractured limestones here are named Düzaðaç Formation, and dolomitic limestones are named Kalecik Limestones by Önal and Gözübüyük (1992) and the age is given as Permo-Carboniferous according to their fossils. This unit does not exist in the deposit area.

MADEN COMPLEX

Maden Complex mainly consists of various colors limestones, sandstones, conglomerates and claystones. The unit includes andesites, diabases and spilitic basalts in the northeast of the district. This unit was named 'Maden' Complex by Perinçek (1979) because of it is observed best in the vicinity of 'Maden' County of Elazýð Province. The thickness of this unit reaches up to 350 m.

Maden Complex overlies Pütürge Metamorphites with an angular unconformity at the base (Önal et al., 1986). In the upper contact the unit is thrusted by Malatya Metamorphites. According to Gözübol and Önal (1986) it is probably of Lower Eocene age and was formed within an intracontinental basin.

INTRUSIVE ROCKS

Granitic and dacitic intrusions of various ages and compositions are observed in the region. The most important of these is a granitic intrusion observed in the south of Çelikhan. It formed a marked alteration zone around itself (Büyükkýdýk and Aras, 1984). In addition, there are smaller intrusions formed on the thrust line, related to faulting. The ore minerals such as pyrite, malachite, azurite and chalcopyrite are observed within these intrusions.

QUATERNARY SEDIMENTS

In the valleys northeast and east of the study area, terraces and talus deposits are widely observed. The mineralizations in the deposit are largely covered by these talus deposits, the thickness of which reaches up to several meters (Figure 5).

TECTONICS

The most important structural elements of the study area are thrusts and folds. As the area is situated in the collision zone of the Taurides and the Arabian Platform, it was considerably affected by tectonic movements.

According to the field observations the most common tectonic element of the study area is Þerefhan thrust line which passes from the south of the Pýnarbaþý Deposit. As a result of the collision of the Tauride Tectonic Belt with the Arabian Platform along this zone, Malatya Metamorphites moving westward, thrust over Maden Complex southward. As a result of this thrust, secondary thrusts and rock cleavages developed within the rock units.

Although in the north of the ore deposit a great number of folds, faults and dislocations are observed, they are not encountered in the south. Owing to north-south compression, folds and faults with north-south and east-west strikes developed. In the north of the area small-scale foldings developed within schists with anticline axis dipping to the south. As a result of these movements large recrystallized limestone blocks were driven into the schists (Figure 5) and thus caused foldings and faulting Önenç ve Yýlmaz, 1981. Crystallized limestones are preserved in the west section of the anticline, whereas they are eroded in the east section. Tectonic structures consist of local folding, faulting and vertical faults. The ore is highly folded together with the schists, which indicates that the mineralization is older than the deformation.

METAMORPHISM

The rock units of the Pýnarbaþý apatite-bearing magnetite deposit and its near vicinity under-

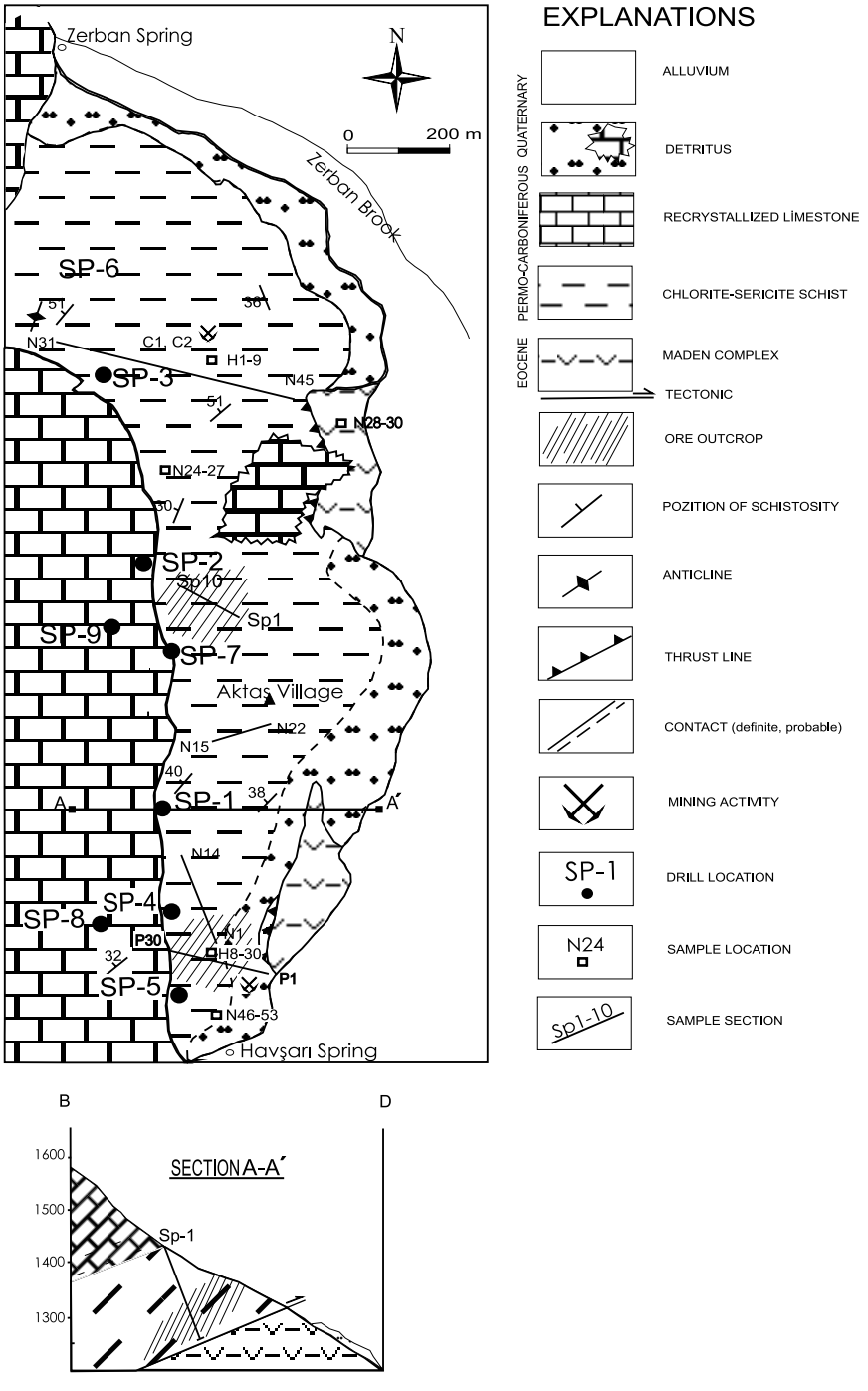

Figure 5 - Geological map of Pýnarbaþý Deposit (Modified after Büyükkýdýk and Aras, 1984).

went at least one regional metamorphism in the greenschist facies. According to microscopic examinations and diffractometric analysis, notable mineral association composed of chlorites (chlorite, chloritoid and sericite), micas (biotite and muscovite) and feldspars (albite) with epidote resulted from the grade of metamorphism has been determined (Çelebi and al., 2005). According to Winkler (1976) this mineral association corresponds to the quartz-albite-muscovite-chlorite subfacies of the greenschist facies of regional metamorphism. Index minerals determined here are shown in table 1 (Çelebi and al., 2005).

Rarely encountered biotite, epidote and garnet indicate that the mineralization in Pýnarbaþý was able to reach, at most, the beginning of the quartz - albite - epidote - biotite subfacies. Brownlow (1996) states that this typical mineral association can only be the metamorphic product of the sediments of pelitic origin in the greenschist facies. The values obtained from ^{18}O isotope analyses showed that the formation temperature of the deposit ranges from 282 °C to 372 °C (Çelebi et al., 2005). This temperature corresponds to greenschist facies temperature of the metamorphism. Hydrogen isotope analysis give sedimentary rock values and support geochemical findings (Çelebi et al., 2005).

Radiometric age determination gave 66 and 48 Ma. Of these, the older (66Ma) reflects the metamorphism age realized by ophiolite development (Campanian) (Çelebi et al., 2005). And 48 Ma expresses the age of the second metamorphism, retrograde metamorphism or tectonic movements (Eocene) (Yazgan and Chessex, 1991; Aktaþ and Robertson, 1984). According to these findings, the metamorphism in Pýnarbaþý can be defined as weak regional metamorphism referring to the Winkler classification (1976), during which pressure was effective. The formation conditions of such a metamorphism approximately correspond to 400 °C temperature and 400 MPa pressure.

MINERALIZATION

Form of mineralization

The principal ore mineral of Pýnarbaþý apatite-bearing magnetite deposit is magnetite. Apatite is present essentially as a gangue mineral together with quartz (Çelebi et al., 2005). According to field observations and drilling data, ore horizons which lie horizontally and consist of chlorite-sericite schist, magnetite and apatite alternation get deeper towards the south (Figure 6). These ore horizons, which concentrate in chlorite schists in the upper parts of the deposit, at various depths exist in the form of lenses or in tabular form. The mineralizations perpendicular to the north-south thrust direction dip to the west with an angle reaching partly to 70° (Figure 5, cross section A-A,) and grade laterally and

Table 1- Index minerals.

Facies	Subfacies	Index minerals
Greenschist facies	*Qu+Ab+Mu+Chl*	Chloritoid/chlorite, Muscovite
	Qu+Ab+Ep+Bi	Biotite, Epidote
	Qu+Ab+Ep+Alm	Almandine

Qu: Quartz, **Ab**: Albite, **Mu**: Muscovite, **Chl**: Chlorite, **Ep**: Epidote, **Bi**: Biotite and **Alm**: Almandine

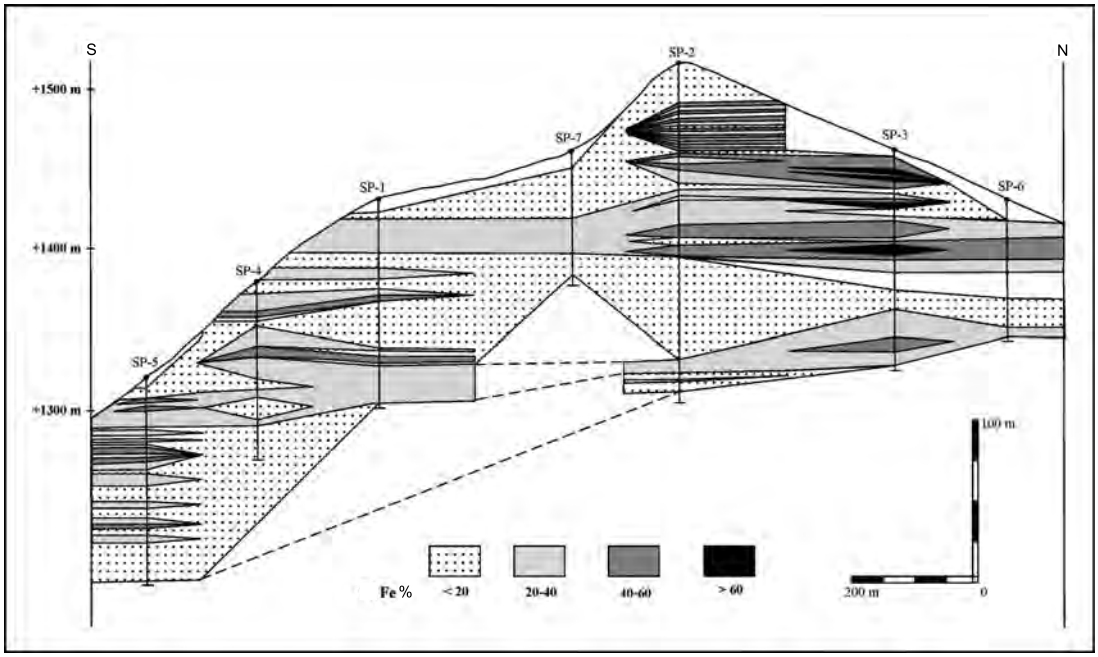

Figure 6 - Horizonal position of the ore zone in N-S direction, ore horizons go deeper southward (Çelebi et al, 2005; figure 5).

vertically into marbles (Büyükkýdýk and Aras, 1984). The thicknesses of the ore lenses reach up to 15 m, and their lateral extension reaches up to several hundred meters (Figure 5 and 6). The total thickness of the ore zone reaches up to 100 m (for example, in drill hole SP-3). According to the data obtained from SP-8 and SP-9, the ore continues eastward below the recrystallized limestones and it can be traced up to a depth of 200 m alternating with the wall rock (Çelebi et al., 2005). At the surface, limonitization is observed.

Magnetite, which is found in massive, banded and disseminated form in Pýnarbaþý apatite-bearing magnetite deposit, exhibits ore types of different structure and quality depending on the ratio of concentration. The most common ore mineral is magnetite. It is followed by hematite, goethite and very little amount of siderite.

Massive mineralization formed by the diminution of the wall rock in favor of the apatite and magnetite in the bulk volume remaining behind pure magnetite and apatite. The 'massive' concept here comprises ores with an iron content of over 50%. It is prevalent in the middle (drill hole SP-2) and northern (drill hole SP-3) parts of the deposit. It is denser in the upper horizons compared to the deeper ones. And this causes the iron content decrease with depth, as observed in SP-2 and SP-4. The thickness of the massive ore can reach 10 m as observed for example in SP-3 (Figure 6). Its lateral extent can be many times greater than its thickness.

Massive magnetite contains apatite and silicate only as bands and fine particles of mm dimensions. It displays conspicuous orientation. According to MTA's core and channel sample analyses, it is the ore type with the highest P_2O_5 content. This condition is best observed in drill hole SP-2. This determination reveals the existence of a positive correlation between apatite and magnetite.

Banded mineralization consists of the alternation of well-oriented magnetite, apatite and chlorite schist (Figure 7). This ore type, which is more conspicuously observed in the southern part of the deposit, can be of various depths and thicknesses. Most probably, during metamorphism, orientation occurred as a result of pressure. This is observed in all types of ore. The thickness of the bands can reach up to several cm varying with the grain size of the ore and gangue minerals. Banding is parallel to the schistosity. Laterally it passes into disseminated ores. In the magnetite content of this ore type large idiomorphic magnetite crystals are dominant, which the ratio is around 50%.

Figure 7- Banded magnetite (dark) alternating with chlorite schists (light).

Disseminated mineralization is the most common ore type. It is observed all over the deposit in various concentrations and dimensions. This mineralization type is always associated with banded and massive mineralizations. However, the normative magnetite content of this ore, composed of magnetite and apatite crystals of millimetric size, often irregular and fine-grained, in parts idiomorphic and oriented parallel to the schistosity, does not exceed 30% (Figure 8). Consequently the recovery of this ore type during an operation is only possible if they were together with the massive and banded ores.

MINERALOGICAL EXAMINATIONS

Microscopic examinations reveal that the mineralogy of the Pýnarbaþý deposit is quite simple. As mineral groups oxides (magnetite, hematite), silicates (mica and chlorites) and phosphates (apatite) are considerably prevalent (Çelebi et al., 2005). But this shows that the parent rocks of the deposit were not rich in all elements or the metamorphism did not reach the grade to constitute various mineral paragenesis. The existence of a marked orientation as a result of metamorphism is observed in ore and wall rocks. According to the results of the chemical analyses and optical and electron microscope observations, the wall rock consists of greenish-gray chlorite (chamosite, Fe-chlorite: $(Fe^{+2}, Mg, Fe^{+3})_5 Al(Si_3Al)O_{10} (OH,O)_8$) and gray (muscovite) and brown (biotite) mica minerals (Çelebi et al.,2005). By means of their fibrous structure, easily recognizable chlorites and flaky mica minerals are followed by quartz of various grain sizes. These three mineral groups are always associated with magnetite and apatite and often, as a result of the orientational forces of metamorphism, they are well-oriented or interrupted. Within the chlorite-schist texture composed of chlorite, sericite and quartz, a well-oriented, amorphous old magnetite and an idiomorphic secondary magnetite coexist (Figure 8). It is observed that the oriented, old magnetite is associated only with the chlorite schists and alternate with the wall rocks. Idiomorphic magnetites are not affected by deformation as they formed, most probably, after metamorphism, for example during retrograde metamorphism.

Recrystallized limestones, which overlie chlorite - sericite unit with normal contact, are moderately stratified and oriented parallel to the schistosity. Recrystallized limestones, which are microscopically composed of calcite, in places show dolomitic composition. Idiomorphic calcite grains show granoblastic texture and twinning lamellas. Chlorite, mica, epidote and opaque minerals are rarely encountered associated with calcite.

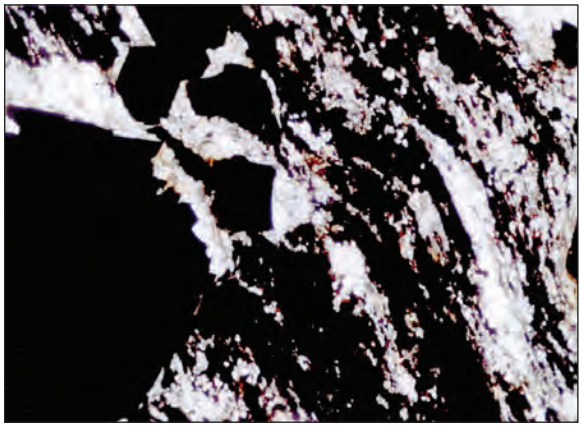

Figure 8 - Within well-oriented chlorite-sericite schist, alternating with quartz (white) and apatite old, amorphous and young, idiomorhic magnetite generations (black) are present together. Red parts are hematite.

According to ore microscopy examinations, magnetite exists in various forms in Pýnarbaþý apatite-bearing magnetite deposit. Magnetite grains, which can reach only a grain size of less than 0.5 mm in rich or massive ore zones, can display a grain size reaching several mm in diameter in disseminated ores. Idiomorphic magnetite crystals are encountered especially in poorly oriented disseminated ores.

Microscopically, magnetite is of dark gray color, coarse-grained, mostly idiomorphic and present a martitization developed in two directions along crystal edges. Thus, the octahedral surfaces of the crystal grains can be clearly observed (Figure 9). It is observed that the martitization is more advanced in fractures and fissures. It is also seen that free magnetite grains are transformed partially or completely into hematite. This can be interpreted at the same time as a replacement. It is possible to see that this is advanced up to goetite in the magnetite grains at the surface. Magnetite can rarely accommodate minerals such as hematite, pyrite and gangue minerals such as apatite and chlorite as inclusions.

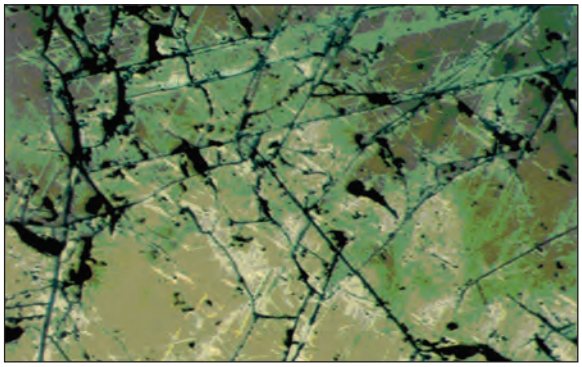

Figure 9 - Martitization, developed in two directions in magnetite crystal (idiomorphic and fractured). Brown indicates titanium, fractures indicate tectonics.

Hematite formed, most probably, totally as a secondary mineral from magnetite. Under microscope, it is distinguished by its light gray color. It is also rarely observed as inclusions in magnetite. It is not possible to distinguish original hematites from the ones which are the derivatives of magnetite. It is also possible to see that the magnetite, transformed into hematite at the surface, is transformed into goetite by decomposition. Together with iron oxide minerals, very small amount of rutile and some sulfite minerals such as pyrite and chalcopyrite in disseminated form are also observed.

In Pýnarbaþý apatite-bearing magnetite deposit, along with magnetite and hematite, the most important mineral of economic importance is fluorapatite. In the field, with the naked eye, it can be distinguished from quartz by its grayish color, prismatic crystal form and brittle nature. Apatite generally occurs in disseminated or banded forms. Its color is gray and pink, and it is generally fine-grained (< 1mm). Apatite, identified by its gray rods with fractures and threads under the microscope, is primarily associated with chlorite, quartz and magnetite (Figure 10). Its proportion in the ore ranges between 3% and 5%. However, horizons containing over 25% apatite are encountered in rare cases. It is observed that it was affected by tectonism and-

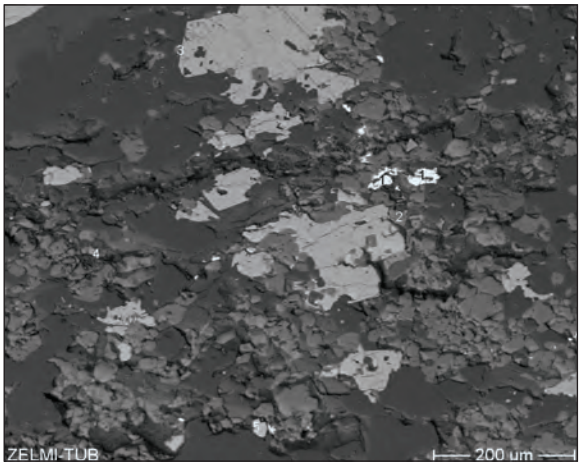

Figure 10- Magnetite with large crystals (light gray), monazite (1), rutile (2, 3, 4) and zircon (5) in a matrix composed of apatite (gray) and quartz (dark gray).

shows orientation with the wall rock. As a result of electron microscope examinations, rarely, some minerals such as hydroxylapatite, monazite, xenotime, and zircon were determined along with fluorapatite. Pink fluorescence color, low radioactivity (8-10 cps) and low content of trace elements (< % 1) are other important characteristics of Pýnarbaþý apatites.

GEOCHEMISTRY

In Pýnarbaþý apatite-bearing magnetite deposit, the method of taking representative samples was adopted. According to this method, as to form approximately perpendicular sections to the strike and dip of the ore, 154 pieces of representative samples weighing around 1 kg were taken (Figure 59). These samples consist of 107 ore samples and 47 wall-rock (Fe_2O_3<%20) samples taken from various parts of the deposit. When the study area was taken into consideration, approximately 80 samples were considered sufficient for a research of this range. Samples were taken from as fresh as possible ore or from the wall rock, and after being halved, they were ground (<100 µm) in chrome-carbide vessels. And then they were prepared for analysis.

Elemental analyses of the samples were carried out in the laboratory of Berlin Technical University, using rontgen fluorescence analysis apparatus (RFA). Percentages of the analyzed elements are given in Table 2. Ag, As, Bi, Br, Cl, Cu, Cs, Hg, Mo, Sb, Se, Sn, Tl, and W were not detected during the analyses. Cd, Cu, Ga, Sn and U are not in reliable concentrations. In parallel to these, analyses of gold, silver and platinum group elements (PGE) together with some important trace elements were performed by neutron activation method on 30 other samples (Çelebi et al., 2005). In these samples, Ag and PGEs were not detected. But, Au concentration reaching 1 ppm was detected. In addition, the values of MTA's approximately 287 drill core analyses were also examined for geostatistical evaluation.

Analyzed apatite-bearing magnetite samples of Pýnarbaþý Deposit seem to be poor in minor and trace elements. The most marked characteristic of the analyses is that the samples contain high P_2O_5 (phosphate) along with moderate Fe_2O_3. On the other hand, their Alkali (Na and K) and S contents are low. It is seen that many trace elements, for example, Ba, Mn, Ni, Sr, V, Zn and Zr, have high concentrations (Table 2). Compared with Clarke value, the most enriched element is P (12-fold). It is followed by Fe (7-fold), V (3-fold) and F (3-fold). Although some siderophile minor and trace elements, such as Co, Mn, Ni and Ti maintained their Clarke level; some alkaline earth elements such as Ba and Sr became diluted.

The main components of the analyzed samples are: Fe (47.18% Fe_2O_3) coming from magnetite and Si (27.45 SiO_2) coming from quartz and silicates (chlorite and mica). The average content of P_2O, considered as a valuable raw material, is 3.01%. This percentage is as high as to negatively influence the exploitability of the iron (maximum 500 ppm P= 0.14% P_2O_5 is demanded for steel production). However, it is known that it is possible to separate it

Table 2- Analysis values of representative ore samples of Pýnarbaþý (Bulam) Deposit and some important parameters

Line No	sample	SiO_2 %	TiO_2	Al_2O_3	Fe_2O_3[1]	MgO	CaO	Na_2O	K_2O	MnO	P_2O_5	F^2	SO_3	Ba ppm	Co	Cr	Ni	Pb	Rb	Sr	Th	V	Zn	Zr	H_2O^3	CO_2[3]	Total
1	SP-2	21,10	0,29	7,18	53,82	0,66	1,37	0,60	0,34	0,23	1,69		0,03	100		131	162	84		215	4	524	221	277			87,31
2	SP-3	22,05	0,32	8,82	56,06	1,84	1,67	0,46	0,24	0,26	1,91			61	2	111	136	53		165	10	664	270	316	0,16	4,04	97,83
3	SP-4	22,26	0,31	10,18	56,86	1,10	2,83	1,12	0,21	0,19	2,99		0,02	66		168	186	90		320	4	741	238	347			98,07
4	SP-5	35,90	0,53	7,66	40,62	0,78	4,46	0,47	0,17	0,18	4,32	0,34		125	40	27	76	62	9	241	2	189	178	299	0,13	2,99	98,55
5	SP-6	20,73	0,26	7,75	51,58	0,28	8,60	0,41	1,29	0,06	7,69	0,16	0,10	381		91	49	24	43	387	13	699	33	185			98,91
6	SP-7	20,98	0,45	11,34	51,38	0,85	2,17	0,08	0,02	0,50	2,37	0,31	0,03	76	24	46	82	76		67		564	206	153	0,35	6,57	97,40
7	SP-8	16,42	0,23	9,04	52,03	0,29	8,89	0,51	1,24	0,01	8,22	0,01		136		161	50	67	30	414	5	903	45	201			96,89
8	SP-9	20,12	0,28	10,01	55,28	0,38	6,93	0,57	1,66	0,02	6,64			159		136	56	67	47	330	5	904	43	211		0,24	102,13
9	SP-11	38,66	0,38	13,96	30,99	2,50	4,95	0,33	3,44	0,28	0,22	0,17	0,07	682	16		32	12	111	233	8	154	120	76			95,95
10	SP-12	41,55	0,35	12,66	31,38	2,74	4,36	1,82	2,03	0,21	0,21	0,12	0,04	566	16	9	36		65	260	7	106	84	95			97,47
11	N-1	58,46	0,61	12,86	17,89	0,43	0,85	0,10	0,06	0,05	0,79	0,15	0,05	30	13	136	34		10	20	11	117	58	404	0,18	3,78	96,26
12	N-2	10,40	0,40	8,68	66,56	0,74	3,86	0,10	0,20	0,93	3,43	0,01	0,48	248	101	144	205		23	437	10	934	329	436	0,14	3,18	99,13
13	N-3	56,02	0,98	19,24	14,38	0,32	0,40	0,26	2,40	0,07	0,31	0,13	0,05	337	15	160	28	40	54	26	20	92	124	713	0,06	2,57	97,19
14	N-4	26,95	0,52	8,87	48,76	0,62	3,69	0,10	0,04	0,71	2,93	0,20	0,08	81	43	125	66	26	10	164	21	384	158	185	0,28	4,80	98,55
15	N-6	49,37	1,10	24,95	15,24	0,49	0,13	1,20	3,02	0,05	0,10	0,01	0,05	355	10	521	110	92	108	271	14	159	116	226	0,05	4,24	100,00
16	N-8	17,08	0,32	9,73	61,37	0,30	4,00	0,27	1,53	0,18	2,87	0,01	0,12	352	17	116	90	27	67	469	18	503	110	232	0,12	1,20	99,10
17	N-9	14,73	0,40	8,90	65,53	0,30	3,24	0,10	0,67	0,41	2,42	0,01	0,13	401	66	149	153	15	39	345	22	480	164	308	0,16	2,69	99,68
18	N-15	17,44	0,45	9,65	61,25	0,30	4,77	0,40	1,34	0,10	3,18	0,01	0,08	197	15	107	65	30	59	437	25	441	88	262	0,07	0,05	99,10
19	N-17	31,87	0,49	14,67	39,22	0,35	1,17	0,17	2,20	0,11	0,90	0,24	0,06	279	28	151	77		79	28	16	339	121	607	0,12	6,63	98,20
20	N-21	13,89	0,24	11,92	64,00	0,30	2,35	0,77	1,38	0,15	1,86	0,08	0,24	434	10	68	36		94	166	10	799	106	176	0,06	1,44	98,68
21	N-22	17,04	0,67	11,31	61,37	0,30	2,95	0,10	0,06	0,25	2,42	0,17	0,06	55	32	173	74			46	13	344	126	157	0,07	2,59	99,36
22	N-24	15,75	0,47	10,00	61,03	1,60	2,90	0,10	0,07	0,32	2,07	0,20	0,08	102	29	115	95	19		69	19	495	169	164	0,16	4,21	98,96
23	N-27	48,55	0,71	15,35	27,45	0,56	0,75	0,10	0,06	0,10	0,77	0,19	0,05	30	46	200	81			44	10	143	172	326	0,13	4,68	99,45
24	N-32	23,56	0,58	12,04	47,16	0,30	3,71	0,10	0,48	0,34	2,89	0,35	0,06	101	25	195	70		17	59	11	413	161	285	0,13	6,91	98,62
25	N-39	26,22	0,25	8,94	49,07	0,30	5,52	0,27	0,95	0,14	5,03	0,18	0,09	207	10	112	29		43	386		386	40	148	0,13	1,77	98,86
26	N-40	46,77	0,41	8,59	34,70	0,33	1,59	0,10	0,15	0,06	1,34	0,22	0,05	109	24	155	54		10	105		217	60	212	0,17	4,22	98,70
27	N-44	8,04	0,27	7,49	67,40	0,30	7,08	0,45	1,48	0,02	5,97	0,64	0,27	227	10	98	37		78	361		861	40	197	0,04	0,36	99,81
28	N-47	49,57	0,86	18,55	23,20	1,78	0,33	0,17	0,42	0,12	0,27	0,14	0,05	79	12	189	59		11	13	18	142	184	321	0,06	3,39	98,91
29	P-13	26,03	0,26	9,35	53,03	0,30	3,87	0,21	0,57	0,23	2,64	0,01	0,07	261	18	140	91		24	201		249	112	167	0,11	0,49	97,17
30	P-22	3,62	0,35	8,22	64,36	0,30	10,51	0,80	1,55	0,02	8,36	0,74	0,25	298	10	230	124		72	461		843	45	227	0,05	0,06	99,19
31	P-23	29,92	0,34	9,34	39,66	0,40	10,24	0,22	1,41	0,08	6,62	0,30	0,05	285	13	156	49		42	237		182	40	121	0,07	0,55	99,20
	$\bar{x}$ =	27,45	0,45	11,20	47,15	0,71	3,88	0,40	0,99	0,21	3,01	0,19	0,10	234	25	152	72	43	50	217	14	429	116	254	0,12	2,90	
	s =	±14,61	0,22	3,95	15,94	0,67	2,87	0,40	0,94	0,21	2,46	0,18	0,10	165	21	91	41	28	32	160	6	284	67	148	0,08	2,18	
	v =	53	48	35	34	95	74	99	95	100	81	95	99	71	84	60	57	65	64	74	43	66	57	58			
	c =	27,72	0,44	8,13	5,00	2,09	3,63	2,83	2,59	0,10	0,11	0,06	0,03	425	25	55	90	13	90	375	7	135	70	165			
	$\bar{x}$ **/c** =	0,46	0,62	0,73	6,70	0,20	0,76	0,11	0,32	1,67	12,35	3,02	1,54	0,55	1,01	2,76	0,80	3,29	0,55	0,58	1,91	3,18	1,66	1,54			

1 Total iron oxide 2 No void cell or value too low 3 Not analyzed in all samples

$\bar{x}$: Arithmetic mean, s: Standard deviation, v: Variation coefficient (= s.100/ $\bar{x}$), c: Clarke value (Mason and Moore, 1985), $\bar{x}$ / c: Enrichment ($\bar{x}$ / c >1) or dilution ($\bar{x}$ / c <1)

(Pfeufer, 1997; Ranjbar, 2002; Wellenkampf and Souzo, 2002). The most regular distribution is displayed by Fe_2O_3 and Al_2O_3 (coefficient of variation v = standard deviation x 100 / arithmetic mean= 34 % and 35%). All the other components are considerably variable (v>80). These characteristics mean that this deposit possesses a heterogeneous mineralization and that during a possible operation, it will be difficult to reach a definite average tenor. According to the obtained values of the sample analyses, geochemical data give clues peculiar to sedimentary rocks in the origin of mineralization. These can be enumerated as:

- Positive Al_2O_3-K_2O and Al_2O_3-Ba correlations (Table 3). This shows that these elements are bound to clay minerals. High contents of Al, Ba and Rb and higher percentage of K compared to Na (K/ Na = 2.83, Table 2) and poor correlations between MgO, Cr, Ni, Co and SiO_2 and among themselves (Table 3) do not reflect a magmatic differentiation.

Criteria used to differentiate ortho-rocks from para-rocks are obtained from relations and ratios between certain pairs of elements which behave differently in magmatic and sedimentary environments. Reactions in sedimentary environments take place under higher conditions of oxidation compared to magmatic environment. Pressure and temperature are much lower in the sedimentary environment compared to magmatic environment. The inter-elemental correlations, ratios and Niggli values of the analyzed sample material associate a sedimentary origin. Some selected inter-elemental correlations are shown below.

Correlation analysis

a) *Values of whole rock analysis.-* There are significant positive and negative correlations between numerous components or elemental concentrations of the analyzed samples (Table 3). The important ones are shown in figure 11. The most significant negative correlation is observed between Fe_2O_3 and P_2O_5 (which constitute valuable raw materials) and silicate-forming SiO_2, Al_2O_3, main alkaline components and their trace elements. This means that Fe and P became concentrated and silicates and alkalis became diluted. For example, while Fe_2O_3 and SiO_2 display negative correlation, SiO_2 and Al_2O_3 concentration variations are positive (Figure 11 a, b). Furthermore, there is also a significant

Table 3- Correlation coefficients between components of Pýnarbaþý ore samples. For sample number n= 31, positive correlation coefficient |r| >0,355 with 95% probability (dark: important coefficients)

SiO_2																		
0,658	**TiO_2**																	
0,673	**0,842**	**A_2O_3**																
-0,**968**	-0,690	-0,748	**Fe_2O_3**															
0,238	0,013	0,169	-0,238	**MgO**														
-0,544-	0,585	-0,550	0,430	-0,178	**CaO**													
0,016	-0,088	0,173	-0,081	0,367	0,121	**Na_2O**												
0,150	0,116	0,459	-0,295	0,131	0,210	0,424	**K_2O**											
-0,270	-0,048	-0,205	0,308	0,191	-0,184	-0,281	-0,383	**MnO**										
-0,613	-0,547	-0,601	**0,521**	-0,427	**0,903**	0,001	-0,022	-0,193	**P_2O_5**									
-0,238	-0,132	-0,270	0,154	-0,072	0,410	0,011	-0,044	-0,204	**0,417**	**F**								
-0,011	-0,145	0,177	-0,069	0,270	0,249	0,400	**0,798**	-0,058	-0,065	-0,161	**Ba**							
-0,209	0,003	-0,221	0,264	-0,115	-0,092	-0,342	-0,378	**0,749**	-0,005	-0,257	-0,095	**Co**						
0,254	**0,603**	**0,644**	-0,358	-0,245	-0,189	0,112	0,350	-0,184	-0,140	-0,085	-0,020	-0,069	**Cr**					
-0,380	-0,080	-0,188	0,409	0,016	-0,166	0,071	-0,345	0,485	-0,033	-0,116	-0,209	**0,644**	0,299	**Ni**				
-0,576	-0,530	-0,443	0,526	-0,170	**0,662**	0,342	0,267	-0,015	**0,636**	-0,020	0,355	0,129	-0,021	0,253	**Sr**			
-0,827	-0,593	-0,529	**0,785**	-0,247	0,458	0,094	-0,114	0,146	**0,638**	0,213	-0,091	0,223	-0,158	0,372	0,565	**V**		
-0,069	0,170	0,036	0,131	0,334	-0,533	-0,122	-0,443	**0,696**	-0,432	-0,247	-0,291	**0,609**	-0,020	0,732	-0,214	0,08	**Zn**	
0,318	0,442	0,334	-0,297	-0,223	-0,462	-0,210	0,008	0,003	-0,295	-0,067	-0,180	0,234	0,133	0,216	-0,290	-0,102	0,322	**Z r**

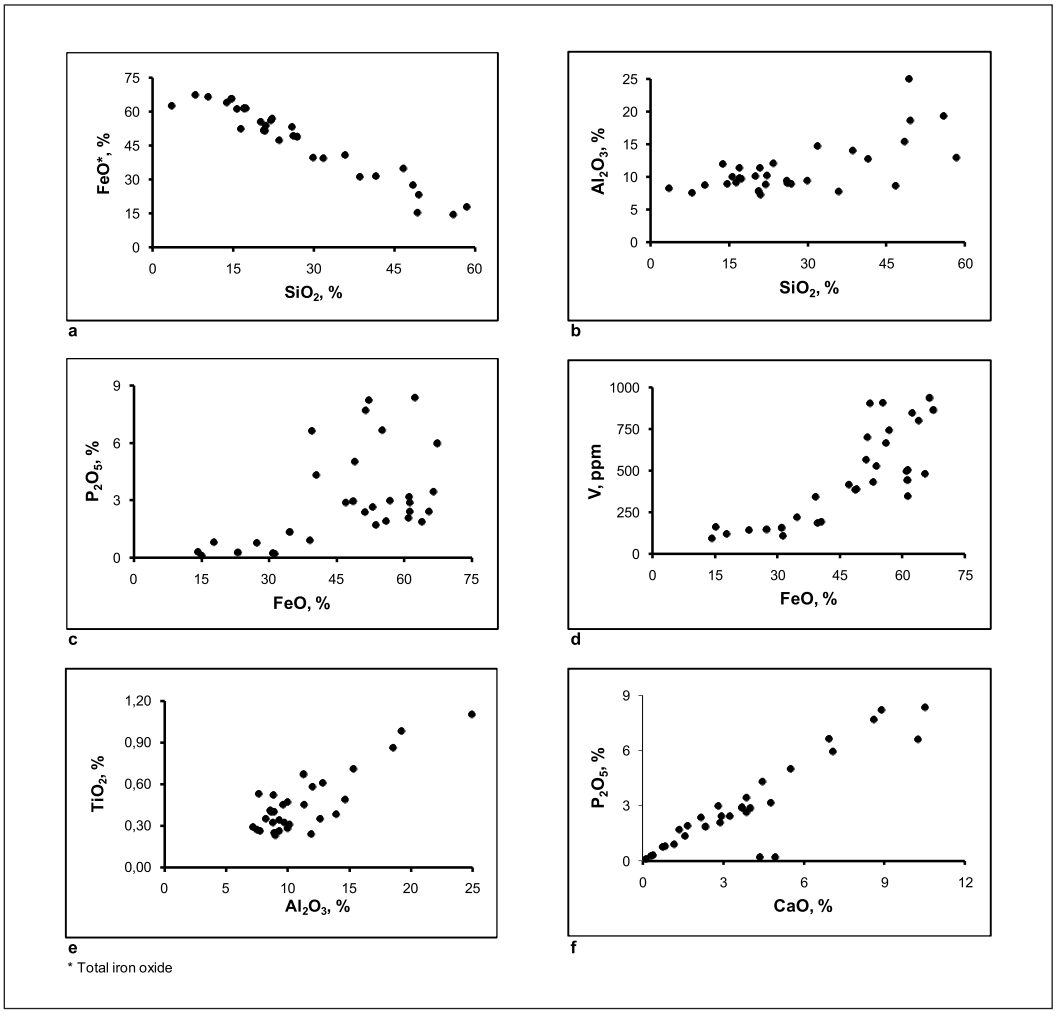

Figure 11 - Correlation diagrams of some selected major and trace elements.

positive correlation (r=0.521) between FeO and P_2O_5 (Figure 11 c). This indicates that these two components were concentrated in parallel with each other in the same environment. In Figure 11, it is seen that V became concentrated in magnetite. Similar ionic radii of V^{5+} (74 pm) and Fe^{3+} (72 pm) played a part in this. The positive exponential correlation between V and FeO indicates that V reached the degree of saturation. On the other hand, it is observed that Ti^{4+} (65 pm) preferred Al^{3+} (63 pm) compounds, for example, muscovite and chlorite (Figure 11 e). The field with high Al_2O_3 - low TiO_2 in the variation diagram corresponds to the sedimentary field (Fernandez and Moor, 1998; Çelebi et al., 2005).

Likewise, the positive correlation between CaO and P_2O_5 results from apatite; and from the linear correlation, it is understood that this also reached the degree of saturation (Figure 11 f). The FeO-V correlation (r=0.785) in magnetite is better than the P_2O_5-F correlation (r=0.417) in apatite (Table 3). Here, the fact that F was bound also to micas and ions of O, Cl, OH and CO_3

partially replaced F influenced the distribution negatively. In addition to these, it is seen from Table 3 that owing to radius similarity and common geochemical behavior, Ba with K (r=0.798), Cr with Al (r=0.644) in micas and Sr with Ca (r=0.662) in apatite, concentrated.

None of the elemental ratios, which are considered important with regard to origin, points out magmatic origin. The ratios of Ca/Sr=127 and Ba/Rb=4.7 correspond approximately to the average continental crust values (117 and 7) (Table 2). Likewise, average Ni/Co=2.9 and Ti/V=6.2 values are lower than the average values of magmatic rocks (2 and 7). In basic rocks, Sr/Ba>1. This ratio is 0.90 in Pýnarbaþý, which reflects the ratio in sedimentary rocks.

Niggli values fall within the field of sedimentary rocks of pelitic origin in the alk-al-c/fm variation triangle (Figure 12). This is supported by the distributions in the ACF and mg-c concentration diagrams, as well (Çelebi et al., 2005).

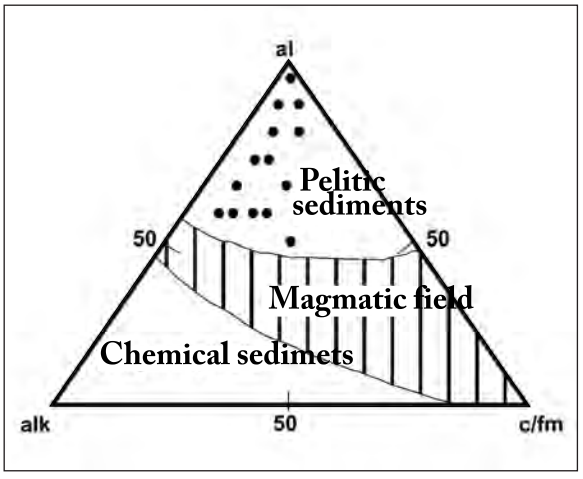

Figure 12- Distribution of wallrock values in Niggli alk-al-c/fm triangle

b) *Values of Fe and P_2O_5 core analyses.*- The samples, the analysis values of which are given in Table 2 are representative samples taken from various parts of the deposit. There-fore, it is not possible to examine the 3. dimension (i.e. its variations with depth) of the deposit by means of these samples. Third dimension examinations are only possible by means of drill core analyses results. However, since only the analyses of valuable raw materials Fe and P_2O_5 are performed on these values (Büyükkýdýk and Aras, 1984), it is only possible to examine the relationships of these two components.

There is also a significant positive correlation between analysis values of Fe and P_2O_5 core samples (Table 2) (Table 3 and Figure 13 a). This indicates that Fe and P_2O_5 concentrated in a parallel manner and most probably came from the same source.

As shown above, in all holes, except SP-7, Fe and P_2O_5 concentrations are positive, but they become negative with depth (Figure 5 and 13 b, c). The drill holes in the north are richer with regard to Fe and P_2O_5 tenor and more disseminated compared to the holes in south. No significant correlation (proportional effect) is observed between average grades and standard deviations of the drill holes (Figure 13 d). This feature resulting from the alternation of ore-rich lenses and lean disseminated mineralizations will complicate to maintain an average ore tenor during a possible operation.

Variation of ore reserves with depth is considered to be the indication of an orientation. Orientation is an expression of the dependence of tenors on a distance like sample interval h. This feature requires the use of complex geostatistical methods in the ore reserve estimation for the deposit.

Distribution of rare earth elements (REE)

Magnetite seems to be poor in rare earth elements (REE). Chondrite-normalized REE concentrations are shown in Table 4. According to this table, total REE concentration is lower than 200 ppm. However, magnetites of similar

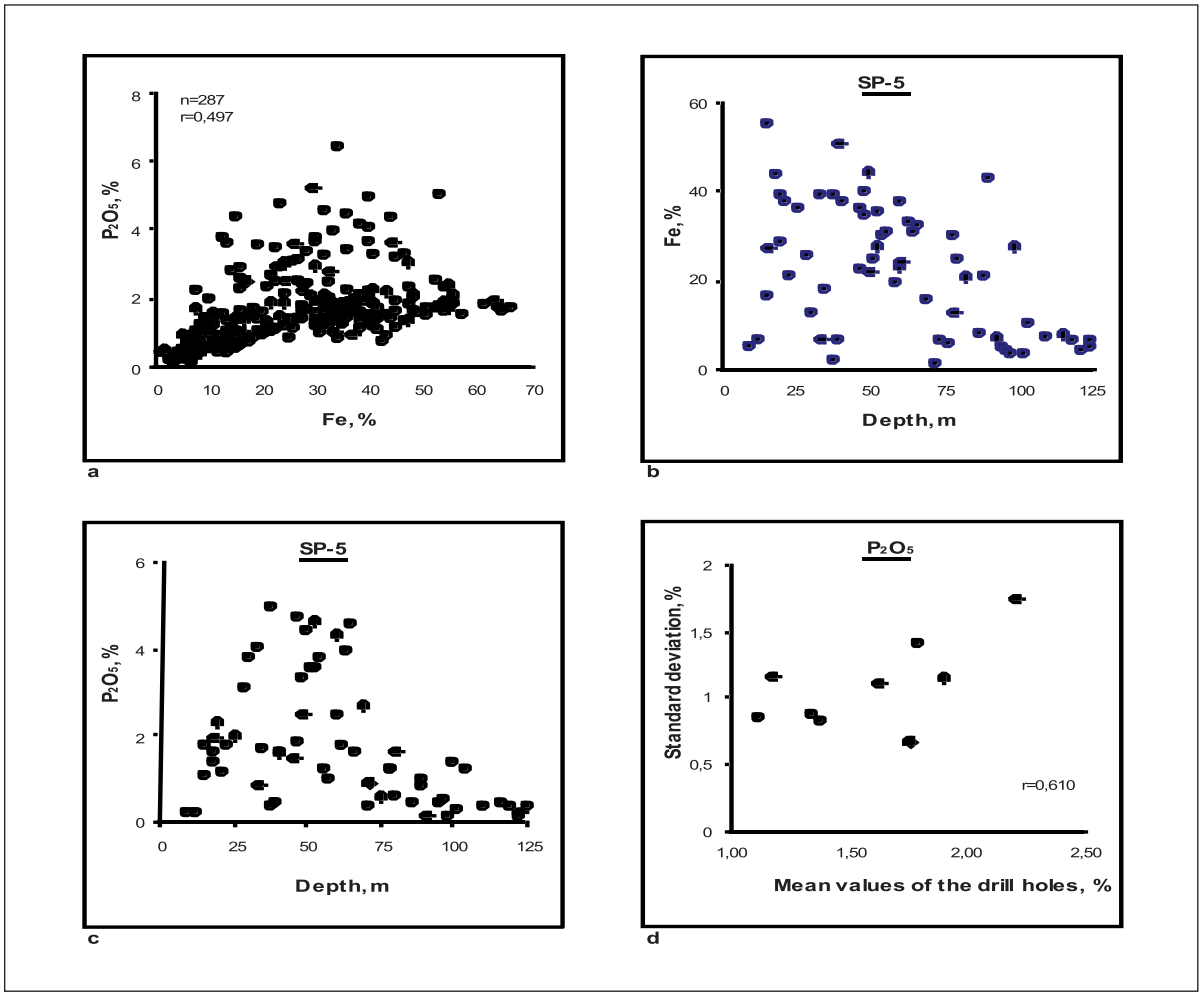

Figure 13- Variation of Fe and P_2O_5 with depth.

deposits, for example, Avnik magnetites contain over 500 ppm and Kiruna magnetites contain over 2000 ppm REE (Frietsch and Perdahl, 1995). This low RRE content denotes that the REEs in Pýnarbaþý magnetites did not reach the saturation point. The reason for this may be, for example, low grade of metamorphism, low REE concentrations in the parent rock and in the ore-bearing fluids. In addition, apatite's intake of REE should also be taken into consideration. However, REE distributions in the selected samples are normal. Coefficient of variation varies between 40% (Tm) and 66% (La). This reflects that magnetite possesses a homogeneous composition.

It is observed that light REEs concentrate better than heavy REEs in Pýnarbaþý. The first 4 REE, La+Ce+Pr+Nd, constitute 75% of the total REE concentration. On the other hand, mean ratio of La/Yb=3.89 is low. This reflects that the elements were not well differentiated (Ekambaram et al., 1986). This ratio is 1.48 in chondrites and approximately 30 in Avnik.

A low Eu anomaly is observed in the distribution of Pýnarbaþý REE, normalized according to

Table 4- Rare earth element values in magnetite

	Sample/Pınarbaşı								
Element	**N-24**	**P-1**	**P-16**	**P18a**	**P-23**	**Ort.**	**Avnik***	**Ünaldı***	**Chondrite****
La [ppm]	23	58	21	22	11	26,92	55,33	126,50	0,245
Ce	70	149	58	69	49	78,68	88,00	217,00	0,638
Pr	7	17	7	7	4	8,41	6,67	19,00	0,096
Nd	30	71	30	27	17	34,80	17,00	53,50	0,474
Sm	9	19	8	7	4	9,46	2,00	7,00	0,154
Eu	2	4	2	1	1	2,07	0,15	0,40	0,058
Gd	9	19	8	6	5	9,43	1,44	5,59	0,204
Tb	2	3	2	1	1	1,75	0,24	0,84	0,037
Dy	10	18	10	5	6	9,70	1,22	4,38	0,254
Ho	2	4	2	1	1	2,08	0,25	0,87	0,057
Er	6	10	7	3	4	5,90	0,64	2,33	0,166
Tm	1	1	1	1	1	0,98	0,11	0,35	0,026
Yb	7	11	8	4	4	6,76	0,81	2,31	0,165
Lu	1	2	1	1	1	1,10	0,14	1,73	0,025
La/Ce	0,33	0,39	0,36	0,32	0,22	0,34	0,63	0,58	0,38
La/Yb	3,29	5,27	2,63	5,50	2,75	3,89	68,30	54,54	1,48

*n=3 ** White, 1997

the chondrites (Figure 14 a). This points out high O_2 mobility. High O_2 mobility oxidizes Eu^{2+} (0.121 nm) to Eu^{3+} (0.109 nm) and causes it to pass into early phases. Consequently, in the environment Eu becomes diluted and cannot be enriched in the crystallization phases, for example, in magnetite. For that reason, Eu gives negative anomaly. Along with this, a slight, positive Ce-anomaly is also observed in the distribution. This shows that Ce is present in the environment as +4-valent and that sea water is not efficient, because sea water causes negative Ce-anomaly (Frietsch and Perdahl, 1995).

In Figure 14 b, REE distribution of Pýnarbaþý magnetites is compared with REE distributions of similar deposits in Turkey. There, it is seen that, in Pýnarbaþý magnetites REE differentiation is slightly negative, Eu anomaly is weak and heavy REEs are more concentrated. This demonstrates that Pýnarbaþý apatite-bearing magnetite mineralizations developed differently from mineralizations of the Bitlis Massif deposits.

The average REE concentration of 900 ppm of Pýnarbaþý apatites is 4.5 times more than that of magnetites. Differences are observed in REE distributions of the phases of magnetite and apatite, xenotime, monazite and allanite, which are known as REE- carrier minerals (Çelebi et al., 2005; Kalkan, Aðcýl and Çelebi, 2004). While light REEs concentrate in magnetite, monazite and allanite, in apatite and xenotime concentrate heavy REEs. Here, crystal structures and ionic radii of the minerals played an important role. For example, heavy REEs having smaller radii concentrated in apatite and xenotime with smaller ionic lattices (Ca^{2+} [0.108 nm] and Y^{3+} [0.098 nm]), and light REEs concentrated in monazite and allanite having larger crystal structures ($REEO_9$ polyeder) (La^{3+} [0.113 nm], Ce^{3+} [0.109 nm] and Th^{4+} [0.108 nm]).

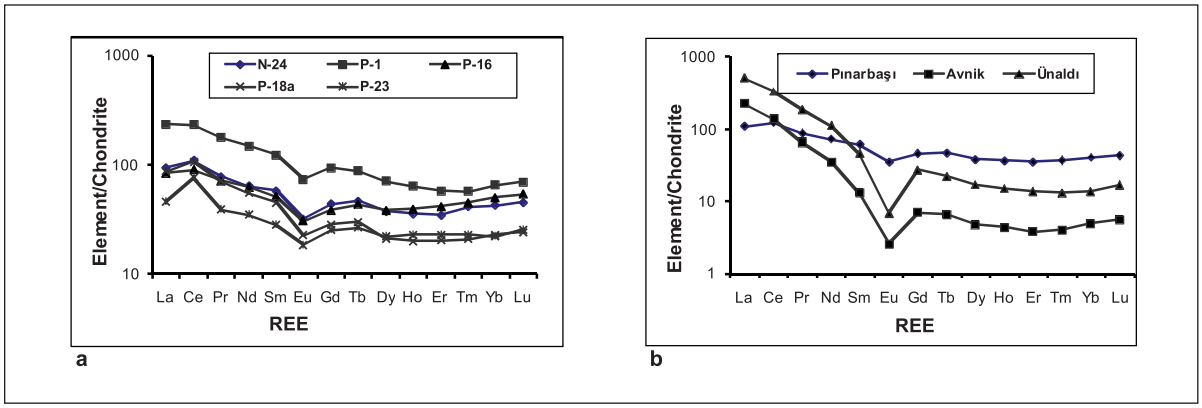

Figure 14 - Distribution of chondrite-normalized rare earth elements of magnetites, a: in Pýnarbaþý magnetites, b: in apatite-bearing magnetite deposits of Turkey (table 3)

Frequency distribution

Fe and P_2O_5 analyses were performed on all of the approximately 300 core samples taken from 9 holes drilled by MTA until 1983 in the Pýnarbaþý deposit (Büyükkýdýk and Aras, 1984). In the present paper, 287 of these were chosen for evaluation.

Distribution calculations performed according to Sturges rule give both Fe and P_2O_5 weak ore type and 2 main populations (Figure 15 a, b). This feature is maintained both in cumulative frequency distribution (Figure 15 c) and in logarithmic frequency distribution (Figure 15 d). This indicates the presence of two different ore types. For example, lean (disseminated) and rich (banded) ore types. These mineralizations may also be the product of 2 different functions.

When looked at logarithmic Fe distribution, it is seen that it approaches normal when distribution symmetry changes (Figure 15 c), whereas P_2O_5 distribution becomes normal (Figure 15 d). This shows that P_2O_5 is distributed more regularly compared to Fe. Log normal distribution is considered a development peculiar to magmatic functions (Ahrens, 1954 *a* and *b*). Consequently, this result can be interpreted as the reflection of a magmatic activity.

Fe distribution is flatter than the theoretical normal distribution, whereas P_2O_5 distribution is peaked. This result expresses that Fe is accumulated in several minerals, whereas P_2O_5 is accumulated only in apatite. Microscopic findings also confirm this.

STRUCTURAL ANALYSIS

In order to determine some important structural features of the ore distribution in the Pýnarbaþý apatite-bearing magnetite deposit, such as the best sample interval, margin of error and alternation, for the values of Fe and P_2O_5 core analyses, according to the equation,

$$\gamma_{(h)} = \frac{1}{2n}\sum_{i}^{n}(x_i - x_{i+h})^2$$

in drill holes, vertical variograms and in the deposit horizontal variograms (in N-S direction) were computed. In this formula, n= number of samples, x_i= analysis value, x_{i+h} = value of the sample at a distance h to xi sample, h= sample interval (m, Figure 16).

The computed variograms show similarity in Fe and P_2O_5 distributions, high nugget effect (~25%), optimum range (around 10 m), trend and alternation.

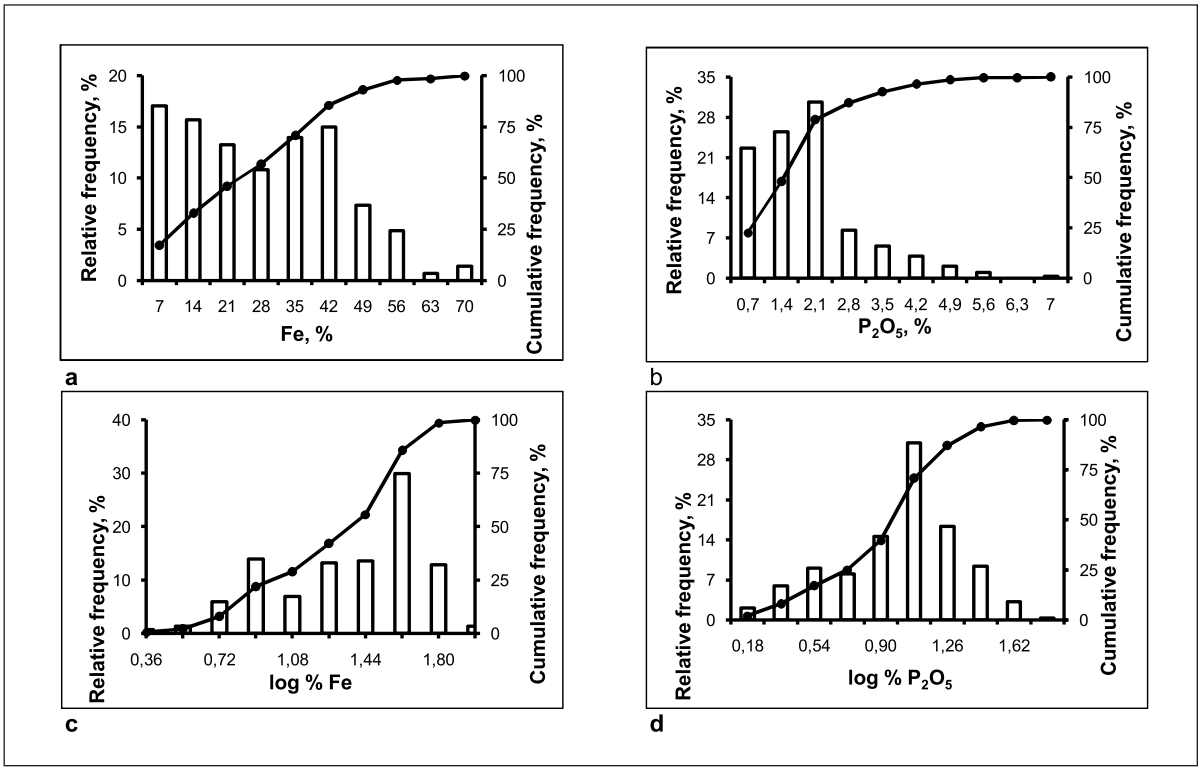

Figure 15- Fe and P_2O_5 frequency distributions of core samples (n=287)

Nugget effect is the beginning point of the average variogram curve on the ordinate (approximately and in %). Optimum range is the point where values become independent; and trend is the variation of the ore with depth. This is understood from the fact that variogram values approach zero with the increasing depth. Alternation shows itself with increasing and decreasing variogram values and it means the alternation of ore horizons with zones devoid of ore (i.e. wall rock) (Figure 16 a and b). These characteristics in an ore deposit are attributed to log normal distribution by Wellmer (1989), Akýn and Siemens (1988) and David (1977).

The alternation towards depth is also observed in the variograms of average drill-hole values taken in north-south direction (Figure 16 c and d). Here, optimum borehole interval is around 150 m. Margin of error in this direction is estimated about 10%. It is not possible to observe the variation in east-west direction due to lack of sufficient number of boreholes.

ECONOMIC POTENTIAL OF THE DEPOSIT

Geological, geochemical and drilling data constitute the basis for the evaluation of the deposit.

Reserves and tenor distribution

MTA explored Pýnarbaþý apatite-bearing magnetite deposit by means of 9 drill holes amounting to 1517 m in total. Nine holes are not considered sufficient for this deposit. Structural analyses show that optimum sample interval is 10 m, and optimum drill hole interval is 150 m (Figure 16). Consequently, the present drill hole interval reaching 300 m is too large. New reserves may

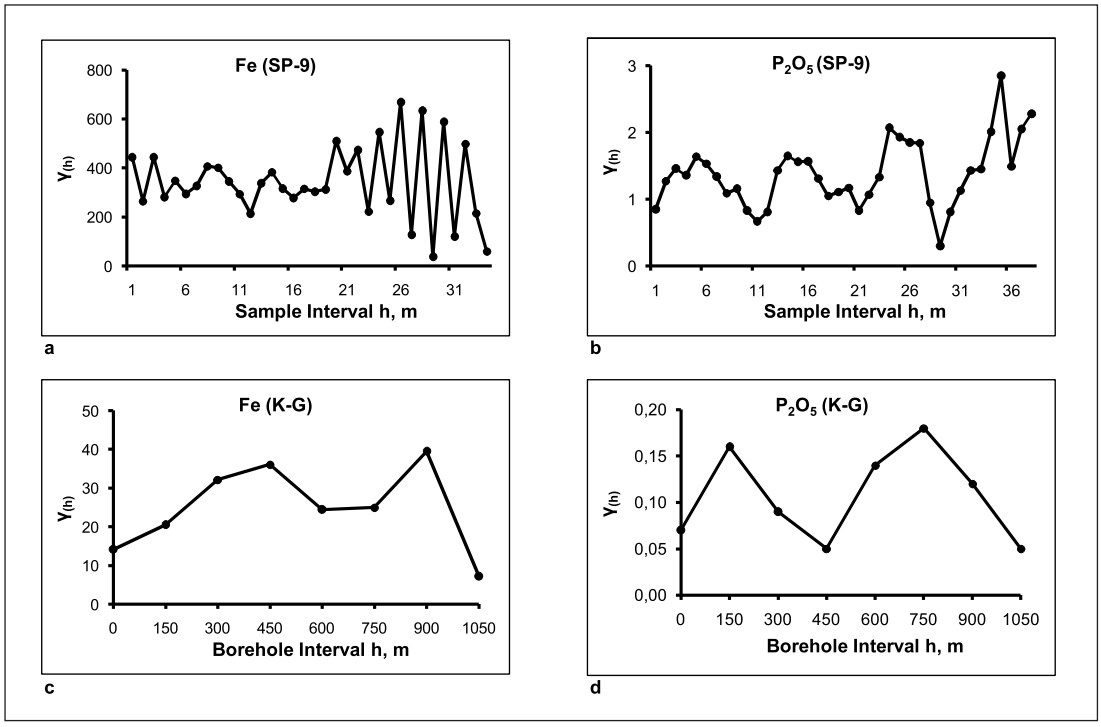

Figure 16- Fe and P_2O_5 variograms computed in some selected holes (a, b) and in N-S direction give the optimum sample interval as approximately 10 m, and optimum drill hole interval around 150 m.

be gained with additional drill holes and developing the drilling network westwards. In addition, the computed reserve quantities are not classified as proved reserves due to low core recovery (v= core length x 100 / drilling advancement). At least 80% core recovery is required for proved reserves (Wellmer, 1989); however, average core recovery is 45.61% at Pýnarbaþý.

Pýnarbaþý apatite-bearing magnetite deposit was studied by a lot of researchers with regard to economic potential (Sýnacý et al., 2003, Güneþ, 1994; Büyükkýdýk and Aras, 1984). Within the scope of this research, taking the principles in Figure 5 as a basis and using parallel section method, a magnetite reserve of 78 Mt having 35.07% Fe and 1.57% P_2O_5 (for ores having over 20% Fe) was calculated by Sýnacý et al. These results, checked with triangular-prism method, are in accordance with the findings of the previous researchers. Güneþ (1994) gives 66.2 Mt (total) magnetite reserve having 36.04 % Fe and 2.07% P_2O_5; Büyükkýdýk and Aras (1984) give 69.2 Mt (total) magnetite reserve having 28.56 Fe and 2.01% P_2O_5. Accordingly, in Pýnarbaþý deposit, there exist metals (Fe, V) and valuable mineral raw materials (F, P_2O_5, REE) approximate quantities of which are given in table 5.

These data show that the quantity of the reserves of the deposit is sufficient for exploitation, but the tenors are low. Çelebi (1989), Pfeufer (1997) and Ranjbar (2002) experimentally demonstrated that various apatite-bearing magnetite ores could be enriched by floatation and along with magnetite concentrate, apatite concentrate could also be obtained. Akar (1983) proved that Pýnarbaþý ores could also be enriched and that P concentration in magnetite could be lowered below 0.05%. According to

Table 5- Valuable raw material content of the deposit according to various researchers.

	Fe [Mt]	**P_2O_5** [Mt]	**V*** [kt]	**F**** [kt]	**NTE**** [kt]
1.	27.30	1,22	30	114	3
2.	23,90	1,37	27	100	3
3.	19,80	1,39	22	120	3,10

1 Sınacı et al., 2003 **2** Güneş, 1994 **3** Büyükkıdık and Aras, 1984 *in magnetite, **in apatitte

Pýnarbaþý magnetites are pelletizable. Accordingly, magnetite and phosphate concentrates with properties adequate to be marketed under present conditions can be obtained.

In this study, the possibilities of gaining present Fe and P_2O_5 raw material values of the deposit are examined. These are vanadium (V) content of magnetite; and fluorine (F) and rare earth elements (REEs) contents of apatite. The results of the examination revealed that 3.46 % F concentration of apatite is normal, but 0.08% V concentration of magnetite and 0.09 REE concentration of apatite are low. In addition, yttrium shows a significant concentration with 0.10%. Concentrate production of some minerals, such as monazite (La-Ce-Th[PO_4]), xenotime (Y[PO_4]) allanite/orthite (Ce-epidote), can be experimented. In addition to these, radon gas (Rn), released during the disintegration of uranium (100 ppm) which is contained in apatite, may be utilized in earthquake early warning researches and in the exploration for new deposits.

Possible mining parameters

In case of a possible mining, the deposit can be strip-mined thanks to considerably low ratio of overburden/ore <1/1. However, in order to get the ore in depth, underground mining will be necessary. The variation of the ore with depth and the state of the overburden is given in Figure 5, section AA' and Figure 6. The extracted ore should be enriched. In this way, phosphate percentage of the magnetite concentrate will be lowered and its quality will be upgraded as well as the lean ore will be utilized.

Along with the proved and probable reserves, there are inferred reserves with low tenor (< 20% Fe) around the deposit and at greater depths (Figure 6). The major problem for magnetite ores, which can be readily enriched by means of magnetic separators, is the phosphorous, not wanted in blast furnace. P should be <0.05%. But, P can also be separated as explained above. However, the fact that the apatite is fine-grained will increase the cost. Although P is harmful for steel production, it is the raw material for phosphoric acid and superphosphate. Turkey procures all of its phosphate demand by import (Çelebi, 2007). That's why P is a highly important raw material. Hence it would be useful to take it into consideration.

Vanadium does not possess a concentration to be a value-adding component for steel production. On the other hand, recovery possibilities for energy storage (battery) can be researched (Çelebi, 2001). Furthermore, fluorine content of apatite seems to be adequate for F production. It can be processed in a hydrofluoric acid plant to be set up and some of the expenditures can be covered by the profit to be obtained from it.

Pýnarbaþý apatite-bearing magnetite deposit can be defined as a medium-scaled iron deposit. This deposit is a great potential and an important resource for a country like Turkey which procures its requirement of iron ore, phosphate and fluorine by import. The deposit with an approximately 3.7 Mt / a optimum capacity will have an optimum life of approximately 18 years (Çelebi et al., 2005).

Significant investment for infrastructure is needed prior to operation. Reinforcement of existing transportation roads, construction of new ones, especially construction of a railroad, supplying water and energy are investments having top priority. For water, the nearest source Çat Dam and for electrical energy, Karakaya Dam can be considered. The ore can be processed under optimum conditions at Ýsdemir (Ýskenderun). And a telpher may be set up to transport ore to a loading station to be established in Sürgü or Doðanþehir.

Such a project, first of all, by making use of Turkey's own resources, will save foreign exchange on a large scale for the iron ore importing country. Related industry investments, such as phosphorous and fluorine processing plants which will come to the district because of mining will contribute to the development of the area. Lastly, an iron and steel plant, which will be set up in Malatya and will process iron ores of Hasançelebi iron deposit,as well, may be taken into consideration.

CONCLUSION AND SUGGESTIONS

The valuable mineral raw materials of Pýnarbaþý apatite-bearing magnetite are slightly matitized magnetite and fluorapatite, bound in chlorite-sericite schists. The most important gangue minerals are fluorapatite and quartz. Results of analyses give average contents of Fe and P_2O_5 as ~ 35% Fe and 3% P_2O_5. Magnetite ores contain high level of Al and numerous trace elements, such as V, Zn and N.

According to the results of geological, mineralogical and geochemical examinations, Pýnarbaþý apatite-bearing magnetite deposit is a medium-scaled, classical Kiruna-type apatite-bearing magnetite deposit. Formation of this type of deposits is a controversial subject. Despite numerous geological, mineralogical and geochemical studies continuing for more than 100 years, the formation of 'apatite-bearing magnetite deposits' or 'Kiruna-type deposits' could not be explained nor could a generally accepted 'formation model' be developed. Current discussions are concentrated on 'magmatic intrusion' and 'sedimentary' models.

Metamorphism complicated the synthesis of the original development by obliterating the traces of the old geological developments. However, field and microscopic observations such as chlorite-sericite wall rock, horizontal position of the ore deposit, bedded structure and especially, apatite's fine-grained structure; and such geochemical findings as high Al concentration of the wall rock and low trace element content of magnetite associates a sedimentary origin. Hydrogen isotope analyses reflect sedimentary rock values and support geochemical findings. These findings indicate that parent rocks of present-day metamorphic rocks of chlorite-sericite schists are sediments of pelitic origin or tuffs.

Fe and P required for the primary enrichment of recent magnetite and apatite were most probably carried as ions and deposited simultaneously with the wall rock. The harmonious distributions of Fe and P in the deposit support this thesis. Both of these components decrease with depth. Banded structure or wall rock-ore alternation reflects a rhythmic change and strengthens the possibility that deposition took place in a calm environment. The iron ore which formed first was most probably hematite and the primary minerals of apatite were phosphates.

Lastly, in Cretaceous the temperature which increased with ophiolite development, the reducing effect of pH and Eh values, at least 0.4 GPa pressure and conditions of metamorphism at 370 °C transformed hematite into magnetite and phosphates into apatite. As orientational forces of metamorphism arranged the wall rock with schistosity and foliation, the ore accommodated itself to the orientation as massive, banded and disseminated. With subsequent E-W comp-

ression movements, erosion and transportation, the deposit took its present shape.

Mineralogical examinations show that deposit units are primarily composed of oxides and silicates. The ores with geochemically pure composition consist of magnetite, hematite (martite and specularite) and goethite. The content of fluorapatite, the most important gangue mineral of magnetite, reaches in places up to 30%. It is followed by quartz, chlorite, sericite and micas. Rutile, zircon, monazite and xenotime are rarely observed.

Geochemical analyses show that Al, Mg and Ca follow Fe and P. Alkali content is around 1.5%. In the deposit P was enriched the most with 17- fold compared to Clarke values. Fe 9-fold, F 8-fold and V was 4-fold enriched. On the other hand, Na 7-fold K and Mg were 3-fold impoverished. The most important trace element of magnetite, which is considerably pure, is V with average 800 ppm. Apatite is also present as a minor element with 3.46% concentration of F. Furthermore, rare earth elements with an average concentration of 900 ppm in apatite may be considered significant.

Elements present a logarithmic distribution. Correlation analysis shows the existence of a significant positive correlation between numerous pairs of elements. The optimum negative correlation exists between Fe and SiO_2. However, there is a significant positive correlation between Fe and P. This shows that Fe and P developed parallel to each other. Fe-V correlation is better than F-P, which indicates that F concentrated in micas as well as in apatite.

Radiometric (Ar-Ar) age determination gave 66 and 48 Ma. Of these, the older 66 Ma is explained with the metamorphism realized with ophiolite development (Campanian). And 48 Ma is accepted as the age of a secondary metamorphism, retrograde metamorphism or tectonic mobilization (Eocene).

Structural analyses give the spherical variogram type which reflects a hole effect. These show that optimum sample interval is 10 m, optimum drill hole interval is 150 m and there exists a proportional effect and orientation.

Pýnarbaþý deposit can be defined as a classic Kiruna-type deposit of sedimentary origin. Similar deposits are Kiruna, Cerro des Mercado, El Laco and Bafq deposits. Similar deposits in Turkey are Avnik and Ünaldý deposits. The deposit is not considered to be economically mined under present conditions due to its low content of F and high content of P. However, by-products such as P, F, V and rare earth minerals which can be recovered along with Fe increase the value of the deposit and earn it the feature of an important mineral raw material source of the future.

ACKNOWLEDGMENTS

This study was realized within the scope of the project YDABÇAG-101Y119 of Tübitak. For that reason, we are grateful to Prof. N. Yetiþ, President of Tübitak. We would like to extend our sincere thanks to Prof. Dr. Mehmet Önal (Ýnönü U.) for his great help during field works, Engineer, Msc. E. Kýlýnç (Kromsan, JSC/ Mersin) for his interest during sample preparation and Asst. Prof. G. Matheis (Berlin Technical U.) for his support during laboratory works.

Manuscript received April 22, 2008

REFERENCES

Ahrens, L. H., 1954*a*. The lognormal distribution of the elements (1). Geochim. et Cosmochim. Acta, 5, 49-79.

_____, 1954*b*. The lognormal distribution of the elements (2). Geochim. et Cosmochim. Acta, 6, 121-131.

Akar, A., 1983. Adýyaman-Çelikhan-Pýnarbaþý mevkiindeki apatitli manyetit-hematit cevherinin

zenginleþtirme etüdü. MTA Report no. 4915, Ankara (unpublished).

Akýn, H. and Siemes, H., 1988. Praktische geostatistik. Springer Verl., Berlin, 304 s.

Aktaþ, G. and Robertson, A. H. F., 1984: The Maden Complex, SE Turkey: Evolution of a neotethyan active margin. Dixon, J. E. and Robertson (eds.). The geolo-gical evolution of the Eastern Mediterranean Spec. Publ. Geol. Soc. London 17, 375-402.

Brinkmann, R., 1971. Das kristalline Grundgebirge von Anatolien. Geol. Rudsch. 60, 886-889.

Brownlow, A. H., 1996. Geochemistry. 2nd Ed, Prentice Hall, Inc., New Jersey, 580 p.

Büyükkýdýk, H. and Aras, A, 1984. Adýyaman-Çelikhan-Pýnarbaþý apatitli demir madeni jeoloji raporu. MTA Report, No. 1803, 24 s (unpublished) Ankara.

Çelebi, H., 1989. Ansaetze zur Rohstoffwirtschaftlichen Bewertung der Magnetit-Apatit-Lagerstätte Avnik, Ost-Türkei, Erzmetall 42/2, 78-85.

_____, 2001. Vanadyum: Doðada bulunuþu, üretimi, kullanýmý ve Türkiye'deki potansiyeli. MMO Adana Þubesi Bülteni 4, 9-13.

_____, 2007. Mineralische Rohstoffsituation in der Türkei. TU-International 52, 12-14.

_____, Helvacý, C. and Uçurum, A., 2005. Bulam (Pýnarbaþý) Apatitli Manyetit Yataðýnýn Vanadyum, Nadir Toprak Elementleri ve Flüor Açýsýndan Ýncelenmesi ve Ekonomikliðinin Araþtýrýlmasý. Tübitak projesi, YDABAG-101Y119, Ankara (unpublished), 82 s.

David, M., 1977. Geostatistical ore reserve estimation II. Elsevier, Amsterdam, 364 p.

Ekambaram, V., Brookins, D. G., Rosenberg, P. E. and Emanuel, K. M., 1986. Rare-earth elements geochemistry of fluorite-carbonate deposits in Western Montana, USA. Chem. Geol. 54, 319-331.

Fernandez, A. and Moro, M. C., (1998). Origin and depositional envirenment of Ordovician stratiform iron mineralization from Zamora (NW Iberian Pensula). Min. Deposita 33, 606-619.

Förster, H. and Jafarzadeh, A., 1994. The Bafq Mining District in Central Iran - a Highly Mineralized Infracambrian Volcanic Field. Econ. Geol. 89, 1697-1721.

Frietsch, R. and Perdahl, J.-A., 1995. Rare earth elements in apatite and magnetite in Kiruna type iron ores and some other iron ore types. Ore Geology Review 9, 489-510.

Güneþ, Ö., 1994. Bulam (Adýyaman) apatitli manyetit yataðýnýn jeolojisi ve rezerv hesaplanmasý. Yüksek lisans tezi, Fýrat Üniversitesi Fen Bilimleri Enstitüsü, Elazýð (unpublished), 59 s.

Gözübol, A. L. and Önal, M., 1986. Malatya-Çelikhan alanýnýn jeolojisi. Tübitak projesi no TBAG-647, Ankara (unpublished).

Kalkan A., H. and Çelebi, H., 2004. Türkiye'deki apatitli manyetit yataklarý ve jeokimyasal özellikleri. 1. Ulusal Jeokimya Sempozyumu, Bildiri Özleri, 49.

Koþal, C., 1967. Elbistan-Doðanþehir arasý demir prospeksiyonu ve jeolojisi. MTA raporu, no. 498, (unpublished) Ankara.

Mücke, A. and Younessi, R., 1994. Magnetite-apatite deposits (kiruna-type) along the Sanandej-Sirjan zone and in the Bafq area, Iran, associated with ultramafic and calcalkaline rocks an carbonatites. Mineralogy and Petrology 50, 219-244.

Önal, M., Þahinci, A. and Gözübol, M. A., 1986. Yeþilyurt-Çelikhan (Malatya -Adýyaman) dolayýnýn hidrojeolojik incelenmesi. Jeoloji Müh. 29, 5-12.

_____ and Gözübol, M. A., 1992. Malatya Metamorfitleri üstündeki örtü birimlerinin stratigrafisi, yaþý, sedimanter fasiyesleri, depolanma ortamý ve tektonik evrimi. TPJD Bült. 1/2, 119-127.

_____, Þaþmaz, A. and Önal, A., 2002. Pýnarbaþý (Çalikhan-Adýyaman) apatitli manyetit cevheri-

nin mineralojisi, jeokimyasý ve kökeni. Yerbilimleri Dergisi 40/41, 207-226.

Öztürk, M., 1982. Adýyaman-Çelikhan-Bulam demir aramalarý manyetik etüt raporu. MTA raporu no: 7367 (unpublished) Ankara.

Perinçek, D., 1979. Çelikhan-Sincik-Koçali (Adýyaman ýli) alanýnýn jeoloji araþtýrmasý. ÝÜ Fen. Fak. Mec. B 44, 127-147.

Pfeufer, J., 1997. Phosphat im Eisenerz der Lagerstätte Leonie im Auerbach (Ober-pfalz). Spurenelemente in Lagerstätten, GDMB 80, Clausthal-Zellerfeld, 41-52.

Ranjbar, M., 2002. Dephosphatisation of Iranian Iron Oxide Fines by Flotation. Erz-metall 55, 11, 613-616.

Shannon, R. D., 1976. Revised effective ionic radii and systematic studies of interatomic distances in halid and chalcogenides. Acta Crystallogr. A 32, 751-767.

Sýnacý, H., Çelebi, H., Alpaslan, M., Helvacý, C. and Uçurum, A., 2003. Bulam (Pýnarbaþý) Çelikhan/ Adýyaman Apatitli Manyetit Yataðý'nýn jeolojik özellikleri ve ekonomik potansiyeli. Mersin Üniversitesi 10. Yýl Sempozyumu Bildiri Özleri, 68.

Tolun, N., 1955. Besni-Adýyaman-Samsat arasý bölgelerinin jeoloji etüdü. MTA raporu no: 2251 (unpublished) Ankara.

Wellenkampf, F. J. and Souzo Barroso, M. A. de, 2002. Column Flotation of Apatite. Erzmetall 55, 10, 553-558.

Wellmer, F.-W., 1989. Rechnen für Lagerstaettenkundler 2. Clausthaler tekt. Hefte, Clausthal-Zellerfeld, 460 s.

Winkler, H. G. F., 1976. Petrogenesis of metamorphic rocks. Fifth edition, Springer Verl., New York, 348 p.

Wright, S. F., 1986. On the origin of iron ores of the Kiruna Type - An additional discussion. Econ. Geol. 81, 192-206.

Yýlmaz, Y. and Yiðitbaþ, E., 1990. SE Anadolu'nun farklý ofiyolitik - metamorfik birlikleri ve bunlarýn jeolojik evrimdeki rolü. Türkiye 8. Petrol Kongresi bildirileri, TPJD, 16-18 Nisan 1990, 128-140.

Yazgan, E. and Chessex, R., 1991. Geology and tectonic evolution of the southeastern Taurides in the Region of Malatya. TPJD Bült. 3/1, 1-42.

Mineral Res. Expl. Bull., 141, 53-68, 2010

MICROTHERMOMETRIC CHARACTERISTICS OF THE OXIDIZED TYPE W-SKARN, IN SUSURLUK, BALIKESIR, TURKEY

Ayþe ORHAN*, Halim MUTLU* and Nurullah HANÝLÇÝ**

ABSTRACT.- The Susurluk skarn deposit developed at the contacts of the Çataldað Granitoid and Mesozoic carbonate rocks is represented by endo and exoskarn (proximal zone, distal zone and vein skarn) zones. The endoskarn zone which occurs in a limited area is characterized by clinopyroxene, plagioclase, sphene, orthoclase and quartz minerals. The exoskarn zone is composed mainly of clinopyroxene, vesuvianite, wollastonite and some accessory minerals such as calcite, quartz, plagioclase, orthoclase, scapolite, biotite, muscovite, sphene and chlorite and ore minerals of scheelite, chalcopyrite and bornite. The presence of anhydrous minerals such as garnet and clinopyroxene is indicative of prograde stage, and the absence of hydrous minerals such as epidote, amphibole and biotite indicates that retrograde stage was not developed. Microthermometric data on exoskarn zone reveal that boiling at temperatures of 587°-592°C took place at the first stage of skarnization. Solutions of the first stage in which scheelite mineralization occurred are characterized by homogenization temperatures of 587 to ≥ 600°C and salinity range of 11-16 wt% NaCl equivalent. At the second stage of skarnization, homogenization temperatures and salinities were recorded as 371 to ≥ 600°C and 36 to >70 wt% NaCl equivalent, respectively. High salinity values are attributed to boiling phenomenon. The Te values of fluid inclusions may indicate a solution composition of $CaCl_2$+NaCl+KCl+H_2O and significant amount of carbonic additions to the system, CO_2 (Te: -66 to -58°C) and CH_4 (Te: -188 to -178°C). The Susurluk skarn deposit which entirely shows shallow skarn system characterized might have been formed at a pressure of around 1 kbar.

Key words: Susurluk skarn deposit, fluid inclusion, W-skarn, boiling, Çataldað Granitoid.

INTRODUCTION

In many skarn deposits two different types of alteration are developed in association with pluton evolution (intrusion, crystallization and cooling). The first is prograde stage (also known as early stage) which is characterized with anhydrous minerals (e.g. garnet, pyroxene) deposited from high-temperature and high-salinity solutions. The second is retrograde stage which is distinctive with hydrous minerals (e.g. epidote, amphibole, biotite) crystallized from lower-temperature and lower-salinity solutions. The source of solutions operating in these stages is mostly magmatic and meteoric or combination of both (Einaudi et al., 1981; Einaudi and Burt, 1982; Meinert, 1992).

Homogenization temperature (Th), first melting temperature (Te) and last ice melting temperature (Tm-ice) data from fluid inclusion works are quite useful for reliable assessment of skarn formation conditions as well as nature and salinity (wt % NaCl equivalent) of the solutions. Studies particularly on Sn and W skarns indicate that salinity and temperature are systematically decreased in distal parts of the pluton from prograde to retrograde stage (from proximal to distal zones) (Higgins, 1980; Mathieson and Clarck, 1984; Kwak, 1986; Layne and Spooner, 1991; Larsen, 1991; Fu et al., 1993; Singoyi and Zaw, 2001; Timon et al., 2007).

In this study, fluid inclusion measurements were carried out on samples collected from the

* Eskiþehir Osmangazi Üniversitesi, Mühendislik Mimarlýk Fakültesi, Jeoloji Mühendisliði Bölümü, Eskiþehir
** Ýstanbul Üniversitesi, Jeoloji Mühendisliði Bölümü, Avcýlar Kampüsü, 34320, Avcýlar-Ýstanbul

Susurluk (Serçeören village-Susurluk-Balýkesir) skarn deposit (Figure 1) and skarn development was discussed by basing on the available fluid inclusion data pointing to the nature of the skarn-forming solutions (temperature, salinity and composition). Previous works in the region are geological studies, (Ergül et al., 1980; Ergül et al., 1986; Akyüz 1995) industrial raw material (wollastonite) surveys (Erdinç 1978; Çakýr and Genç 1983) and petrographic investigation of the skarn zone (Erdað, 1976; Arýk, 1995; Orhan and Mutlu 2009). Skarn mineralization in the area was first studied by Erdað (1976) who proposed that diopside, garnet, vesuvianite and wollastonite at the contact between granitoid and marbles form a typical contact metasomatic occurrence. The same worker stated a mineral assemblage consisting of forsterite, quartz, tremolite, scapolite, biotite, calcite and plagioclase and trace amount of ore minerals such as molibdenite, scheelite, bornite and specularite also occur in the skarn zone. According to Arýk (1995) epidote also develops in the skarn zone, and host rock is in dolomitic composition. Although mineralogical and petrographic characterizeds of the skarn zone at Susurluk have been determined previously, nature of skarn-forming solutions and skarn formation processes have not been investigated. Orhan and Mutlu (2009) described skarn zones on the basis of mineral abundances and their textural properties and proposed that exoskarn zone has a calcic character and only the products of prograde stage (e.g. garnet, pyroxene) were formed related with the intrusion and crystallization of the Çataldað Granitoid. Orhan and Mutlu (2009) also state that intrusion and continuous crystallization of Çataldað Granitoid into shallow depths prevented development of retrograde stage products (e.g. epidote, amphibole, biotite). The same authors investigated chemical composition of garnets and pyroxenes from various mineral zones and concluded that mineralization at Susurluk is of oxidized W skarn character and ore minerals (W and Cu) were formed at different stages of magma crystallization.

In this study, based on previously described mineral zones (Orhan and Mutlu 2009), fluid inclusion studies were conducted on pyroxene, wollastonite, vesuvianite and quartz from a number of skarn zones in Susurluk deposit. Homogenization temperature (Th), inclusion salinity (wt% NaCl equivalent) and possible solution compositions are compared with those from similar W-skarn deposits and skarn formation conditions and processes are discussed.

GEOLOGY OF THE STUDY AREA

Palaeozoic Fazlýkonaðý Formation, Mesozoic limestone and marbles, and the Oligocene-Miocene Çataldað Granitoid are the main rock units in the study area (Figure 1). The Fazlýkonaðý Formation forms the basement and is composed of schists and intercalated marble bands and lenses (Ergül et al., 1980, 1986; Akyüz, 1995). Petrography reveals that schists are made up of amphiboleschist, micaschist, quartz-micaschist and talcschist. According to Akyüz (1995), metamorphism occurred at pressures of 4-6 kilobars and temperatures around 550-650°C.

Mesozoic carbonates which are represented by crystallized limestone and marbles are characterized with white-beige colored, coarsely crystalline and laminated structure. The Susurluk skarn deposit was formed at north of the Serçeören village along the contact zone between the Çataldað Granitoid and the above mentioned carbonate units (Figure 1). The Çataldað Granitoid is one of post-tectonic intrusions in northwest Anatolia which were formed as a result of Alpine orogeny (Erdað, 1976; Ergül et al., 1980, 1986; Akyüz, 1995; Ercan et al., 1990). It shows peraluminous / metaluminous composition and calc-alkaline affinity and hololeucocrate and leucocrate character. The granitoid which covers an area of about 450 km^2 at east of Susurluk is composed of a series of dike and sills. The mineral assemblage of muscovite + margarite + biotite (siderofillite) + andalusite at

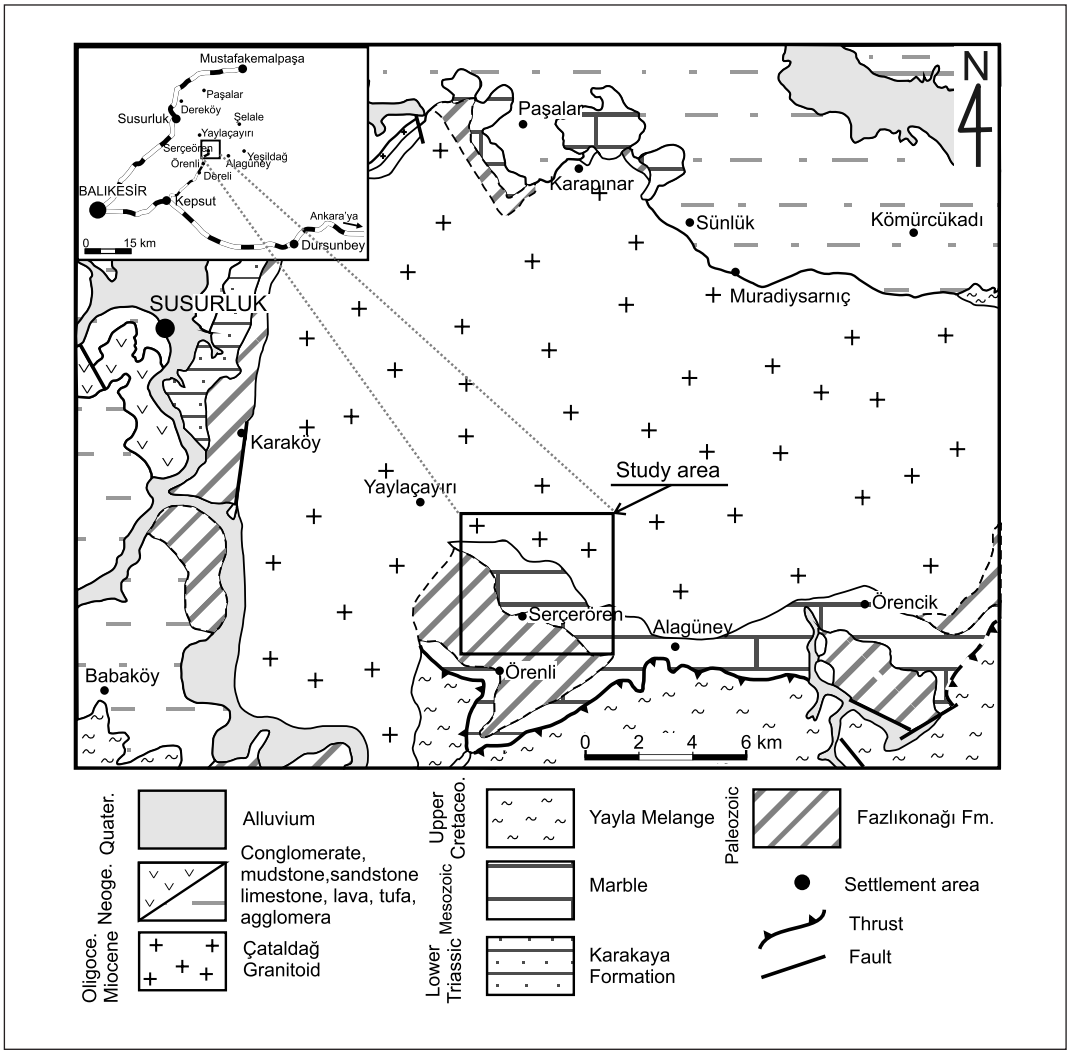

Figure 1- Location and general geology maps of study area (after Ergül et al., 1986).

the contact between the Çataldað Granitoid and schists might indicate that the granitoid was formed at pressures less than 3.5 kilobars and temperatures around 550-650°C (Akyüz, 1995). The cooling age of intrusion is found as 21.2-25.9 Ma by K-Ar method (Boztuð et al., 2009) and 20.9 Ma by Rb-Sr isochron method (Mutlu and Orhan, 2009).

The granitoid has a holocrystalline texture at the core changing to porphyric texture to the margins. It shows significant schistosity towards the contacts. Toward the skarn zone cataclasis is evident and feldspars and biotites are coarsened. The changes in textural properties are also accompanied by mineralogical variations. The core of pluton is composed of quartz, plagioclase, K-feldspar, hornblende and biotite ± pyroxene ± apatite ± sphene ± tourmaline ± opaque minerals. Biotite, that is replaced by hornblende, becomes a major mineral in the margins of the facies in porphyritic texture. Some biotite granite samples from the margins contain secondary muscovite. Mineral abundance and

geochemical classifications indicate that the granitoid is represented by granitic and granodioritic compositions (Erdað, 1976; Ergül et al., 1986; Akyüz, 1995; Orhan, 2008; Boztuð et al., 2009) which may locally change to syenogranite (Arýk, 1995; Ergül et al., 1980; Ercan et al., 1990). Towards the skarn contact, it displays notable changes in mineralogy. The quartz abundance is significantly decreased while K-feldspar content varies over a wider range and some secondary minerals such as epidote, pyroxene and calcite and chloritization and sericitization become prominent. In skarn zone and some of veins cutting the granitoid apatites are coarsened and calcite precipitations are developed.

MATERIAL AND METHOD

For fluid inclusion measurements polished thin sections of 80-150 µm were prepared from samples collected from different zones of the Susurluk skarn deposit. Fluid inclusions measurements were carried out with Linkham THMG-600 heating-freezing apparatus (at temperatures between -196 and +600°C). Liquid nitrogen and a thermal resistor were used for cooling and heating, respectively. First melting (Te-eutectic temperature) and final melting of ice (Tm-ice) temperatures of inclusions were measured during cooling while homogenization temperatures (Th) were measured during the heating stage. Calibration of the heating-freezing apparatus was done by measuring melting points of pure CO_2 inclusions hosted by quartz. Measurements yielded a precision of ±0.2°C for melting temperatures and ±0.4°C for homogenization temperatures.

SKARN ZONE CHARATERISTICS

Both endo and exoskarn zones occur in the Susurluk skarn deposit. The endoskarn zone with massive and undulated structure is observed at the contact and within the granitoid. In this zone which is represented by clinopyroxene (hedenbergite), plagioclase (labradorite-bytownite), sphene, orthoclase and quartz minerals magmatic texture is well preserved. The exoskarn zone occurs as monomineralic zones or veinlets and lenses and veins within the marbles or irregular bands parallel to the marble layers. The exoskarn zone is composed chiefly of garnet, clinopyroxene, vesuvianite and wollastonite which are accompanied by quartz, plagioclase, orthoclase, scapolite, sphene, biotite, muscovite and chlorite. Scheelite, chalcopyrite and bornite are main the ore minerals in this zone. In proximal zone, zoned garnets are replaced by pyroxene, inclusions of vesuvianite are common within garnets, pores and fractures of garnet are mostly filled by quartz and chloritization and carbonatization are the most common types of alteration. Wollastonite and vesuvianite are observed in distal zones and veins in marbles. Wollastonite usually has a coarse flaky form while vesuvianite with zoned structure appears to replace pyroxene. Towards the contact where marbles are banded pyroxene, vesuvianite, wollastonite, biotite and muscovite are found (Orhan and Mutlu, 2009). Macro and micro textural and mineralogical studies reveal that the Susurluk skarn deposit closely resemble worldwide known W-skarn occurrences (Einaudi et al., 1981; Einaudi and Burt, 1982; Meinert, 1992). The anhydrous minerals (e.g. garnet and pyroxene) in the deposit were formed during the prograde stage which is associated with intrusion and crystallization of the Çataldað Granitoid while the absence of hydrous minerals (e.g. epidote, amphibole, and biotite) implies that retrograde stage was not occurred during the cooling (Orhan and Mutlu; 2009). When compared to other well known W-skarns (e.g. Kara skarn, Northwestern Tasmania; Singoyi and Zaw; 2001), the exoskarn of the Susurluk skarn deposit is represented by two stages (Figure 2) which are given below:

First stage: Garnet (grossular) + clinopyroxene (hedenbergite) ± vesuvianite ± wollastonite ± quartz ± scapolite ± calcite ± sphene ± scheelite

Second stage: Garnet (grossular-andradite) + clinopyroxene (diopside)+vesuvianite + wollastonite + calcite + chalcopyrite + bornite ± quartz ± plagioclase ± orthoclase ± scapolite ± sphene ± chlorite ± biotite ± muscovite

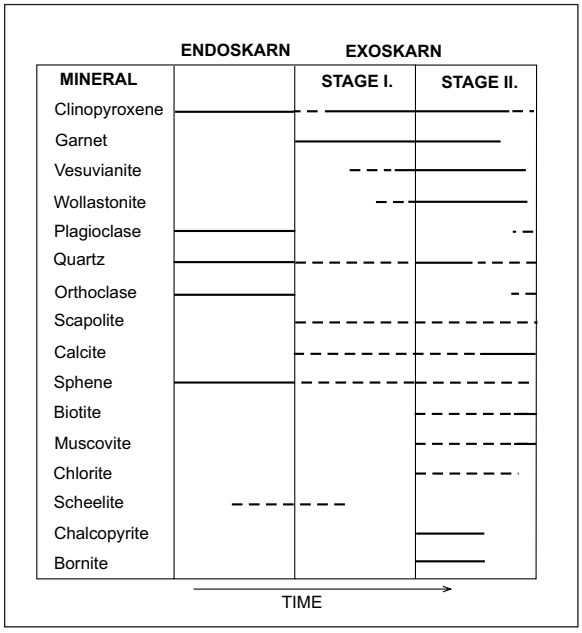

Figure 2- Schematic diagram showing paragenetic relationships of skarn and ore assemblages at Susurluk skarn deposit (after Orhan and Mutlu, 2009).

MICROTHERMOMETRIC MEASUREMENTS

Microthermometric measurements on the Susurluk skarn deposit were conducted on proximal and distal zones of exoskarn and clinopyroxene, quartz, vesuvianite and wollastonite minerals in the vein skarn (Figure 3). Prior to analysis, fluid inclusion types were classified as primary or secondary inclusions according to criteria proposed by Roedder (1984) and Van den Kerkhof and Hein (2001). All the measurements were performed on primary fluid inclusions.

Inclusions are generally irregular-shaped in quartz and vesuvianite, irregular and rectangular or square shaped in clinopyroxene and irregular or tube shaped in wollastonite (Figure 4). The length of inclusions is in the range of 10 to 216 µm. When viewed at room temperature primary inclusions were determined to contain liquid+gas (Type-I) and liquid+gas+soild (Type-II) phases (Figure 4). In Type-II inclusions solid phase is comprised by halite and/or sylvite minerals. In proximal zone of exoskarn clinopyroxene and vesuvianite contain both Type-I and Type-II inclusions while quartz and wollastonite contain only Type-II inclusions. Measurements in distal zone and vein skarn were conducted on clinopyroxene and wollastonite which produced Type-II inclusions.

Homogenization Temperatures and Salinity Values

Homogenization temperatures of Type-I inclusions in clinopyroxene and vesuvianite from the proximal zone were measured as 587°C to ≥ 600°C (n=4) and 438°C to ≥ 600°C (n=2), respectively. Type-I inclusions were generally homogenized into liquid phase and inclusions in one clinopyroxene sample were homogenized to both liquid (592.2°C) and gas (587°C) phases (Table 1).

Homogenization temperatures of Type-II inclusions in skarn minerals of the proximal zone range from 572 to ≥ 600°C (n=15) for clinopyroxene, 369 to 494°C (n=5) for wollastonite, 455 to ≥ 600°C (n=4) for quartz and 403°C (n=1) for vesuvianite (Figure 5). In Type-II inclusions, except for one sample (gas phase sample in wollastonite), homogenization to the liquid phase was observed.

Type-II inclusions in clinopyroxenes and wollastonites of the vein skarn have homogenization temperatures greater than 600°C (Th ≥ 600°C; n=15). Type-II inclusions in clinopyroxenes from distal zone of exoskarn were homogenized to liquid phase at temperatures between 371 and 549°C (n=4) (Figure 5).

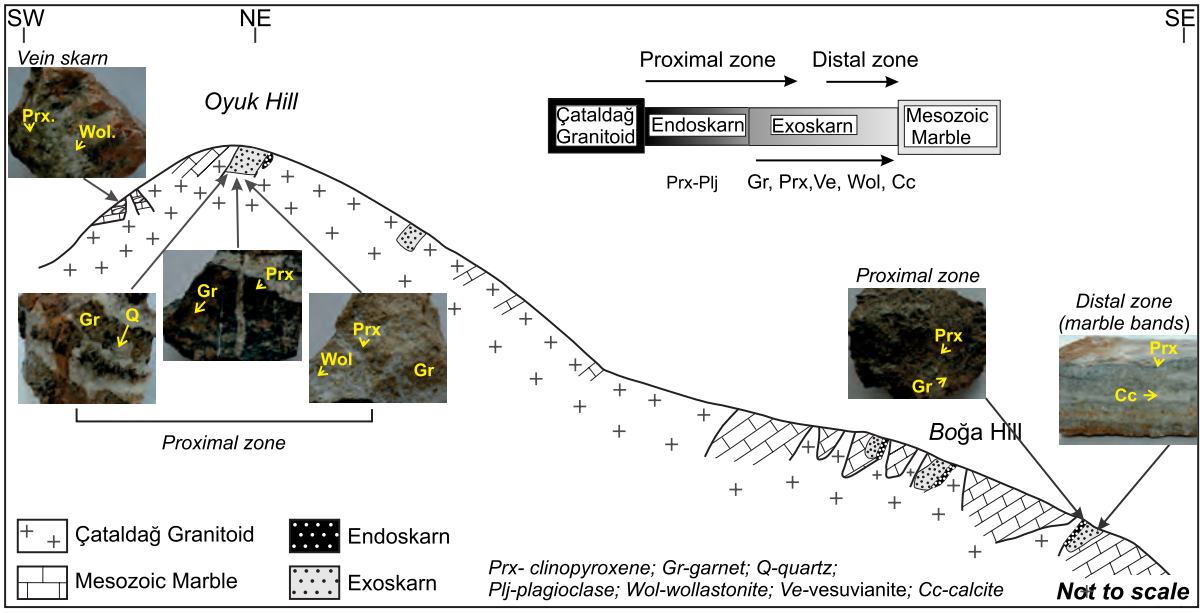

Figure 3- Cross-section showing different skarn zones and locations of samples collected for microthermometric measurements.

Salinity values of liquid+gas inclusions (Type-I) were calculated from the last ice melting temperature (Tm-ice) while those of liquid+gas+soild inclusions (Type-II) were computed from melting temperatures of halite and sylvite crystals (Shepherd et al., 1985; Bakker 2003). Results indicate that in proximal zone clinopyroxenes with Type-I inclusions (n=4) have an average salinity of 14.5 wt% NaCl equivalent and the salinity of vesuvianites (n=2) is 11.1 wt % NaCl equivalent (Table 1; Figure 6).

Since some of solid phases did not melt to a temperature of 600°C, all the salinities of Type-II inclusions in proximal zone could not be calculated. From the melting of the halite salinity of one sample in vesuvianite was found as 36 wt% NaCl equivalent, from the melting of halite and sylvite salinities of two samples in wollastonite were computed as 61-61.5 wt% NaCl equivalent and from the melting of sylvite salinities of two samples in quartz were found as 67 and >70 wt% NaCl equiv. Salinities of inclusions in which halite and sylvite did not melt at 600°C were found to be at least 70 wt% NaCl equivalent (Shepherd et al., 1985) (Table 1).

Salinities of clinopyroxenes (n=4) in distal zone are between 51.5 and >70%, salinities of clinopyroxenes in vein skarn are in the range of 58 (n=1) to >70% (n=6) and those of wollastonites (n=3) are from 57 to 66 wt% NaCl equivalent (Table 1).

First Melting (Te), Last Ice Melting (Tm-ice) and Clathrate Melting (Tm-clth) Temperatures

It is a challenging work to determine low-temperature (<0°C) phase transitions (Te and Tm-ice) within the inclusions. Therefore, a total of 33 Te (samples from proximal and distal zones and vein skarn) and 7 Tm-ice (samples from proximal zone) values could be determined in fluid inclusions from the Susurluk skarn deposit (Table 1).

Te values Type-I inclusions in clinopyroxene and vesuvianite from the proximal zone are represented by a narrow temperature range of -68 to

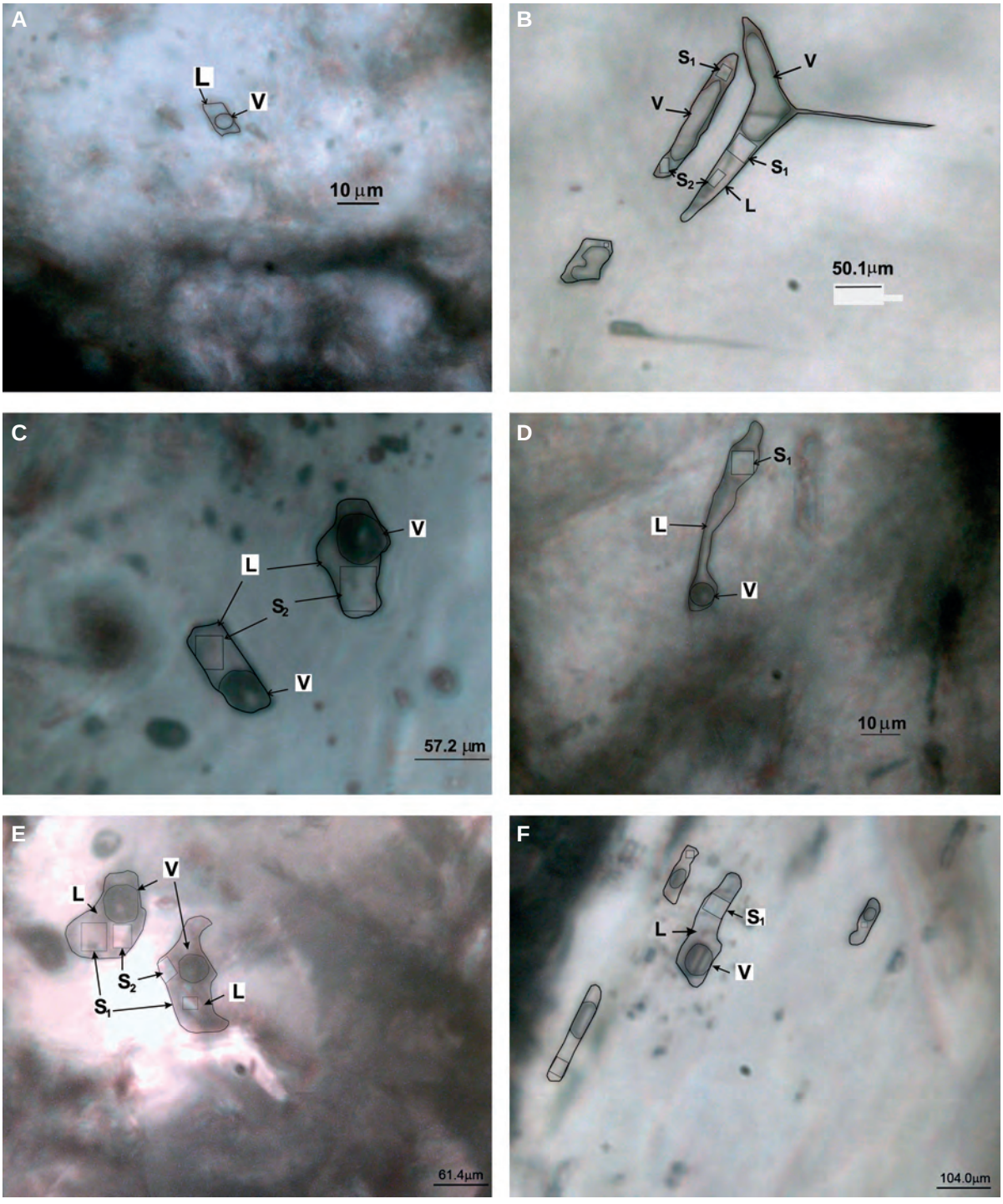

Figure 4- Fluid inclusion photomicrographs of skarn minerals from the Susurluk skarn deposit. (A) Type-I inclusion in clinopyroxene; (B) Type-II inclusion in clinopyroxene from distal zone; from proximal zone (C) Type-II inclusion in quartz; (D) Type-II inclusion in vesuvianite; (E) Type-II inclusion in wollastonite; (F) Type-II inclusion in wollastonite from vein skarn (S1: Halite, S2: Sylvine).

Table 1- The microthermometric data of Susurluk skarn deposit.

Skarn Zone	*Host mineral*	*Inclusion Type*	*Te (°C)*	*Tm-ice (°C)*	*Tm-clth (°C)*	*Tm-solid (°C)*	*Th (°C)*	*Th-phase*	*Salinity (equivalent wt %NaCl)*
PROXIMAL ZONE	Quartz	II	n.d.	n.d.	-	432.6 (S)	454.6	**V→L**	67
		II	n.d.	n.d.	-	463 (S)	≥600	-	>70
		II	n.d.	n.d.	-	489.5 (S)	489.5	**S→L**	>70
		II	n.d.	n.d.	-	545 (S)	545	**S→L**	>70
	Clinopyroxene	I	-58.2	-10.7	-	-	587	**V**	13.98
		I	-60.2	-10.7	-	-	≥600	-	13.98
		I	-58.8	-12.9	-	-	592.2	**L**	16
		I	n.d.	-10.9	-	-	≥600	-	14
		II	-180.4	n.d.	-	536.6 (H) 483.9 (S)	≥600	-	>70
		II	-69.5		9.0	522.2 (S)	≥600	-	>70
		II	-67.2		9.0	520.9 (S)	≥600	-	>70
		II	-65.4		10.7	n.d.	≥600	-	-
		II	-69.4		6.1	517.7 (S)	≥600	-	>70
		II	-69.9		10.0	504.5 (H) 488.2 (S)	≥600	-	>70
		II	-69.2		8.3	488.8 (S)	572.2	**V→L**	>70
		II	-48.8	-14.4	-	> 600 (H)	≥600	-	>70
		II	-188.1		19.8	n.o (H, S)	≥600	-	-
		II	-176.5	n.d		n.o (H)	≥600	-	-
		II	-176.4	n.d		n.o (H)	≥600	-	-
	Wollastonite	II	-67.4		10.8	373.5 (H) 368.5 (S)	439	**V→L**	61
		II	-69		11	365.8 (H) 365.7 (S)	369.1	**V→L**	61.5
		II	-81.4		10.5	n.d (H, S)	439.6	**L(?)**	n.d
		II	-62		11.2	424.1 (H) 477.3 (S)	494	**V→L**	>70
		II	-61.6		11.6	381.8 (H) 409.1 (S)	434.6	**V→L**	>70
	Vesu-vianite	I	-	-7.7	-	-	≥600	-	10.49
		I	-68.1	-8.2	-	-	437.6	**L**	11.71
		II	-136	-	-	285.4 (H)	403.1	**V→L**	36

Table 1- continued

Skarn Zone	*Host mineral*	*Inclusion Type*	*Te (°C)*	*Tm-ice (°C)*	*Tm-clth (°C)*	*Tm-solid (°C)*	*Th (°C)*	*Th-phase*	*Salinity (equivalent wt %NaCl)*
DISTAL	Clinopyroxene	II	-126.1	n.d.	-	270.8 (S)	370.8	V→L	51.5
		II	-118.6	n.d.	-	379.2 (S) 375.9 (H)	532.3	V→L	61
		II	n.d.	n.d.	-	548.9 (S)	548.9	S→L	>70
		II	n.d.	n.d.	-	275 (S)	502.9	V→L	52
VEIN	Clinopyroxene	II	-181.7	-	15.8	525.7 (H)	≥ 600	-	58
		II	-182.5	-	16.3	n.o (H).	≥ 600	-	-
		II	-189.2	-	-	n.o (H)	≥ 600	-	-
		II	-130	n.d.	-	n.o. (S)	≥ 600	-	-
		II	-56.1		12.8	567.9 (S)	≥ 600	-	>70
		II	-55.4	.	9.6	n.o. (S)	≥ 600	-	-
		II	-55.5	n.d.	19.4	n.o. (S)	≥ 600	-	-
	Wollastonite	II	-188	n.d.	-	509.8 (H)	≥ 600	-	57
		II	-188.9	n.d.	-	591.1 (H)	≥ 600	-	66
		II	-183	n.d.	-	592 (H)	≥ 600	-	66
	Definitions: **Te:** Eutectic temperature; **Tm-ice:** Final ice melting temperature; **Tm-clth:** Clathrate melting temperature; **Tm-solid**: Solid phase melting temperature; **Th:** Homogenization temperature; **n.d:** Not-determined, **n.o.:** Not-occured, **S:** Sylvine; **H:**Halite; **V**: Vapour; **L**:Liquid; **V→L:** Homogenisation occured by disappearance of vapour to liquid phase; **S→L:** Homogenisation occured by disappearance of solid to liquid phase.								

-58°C (n=4) while Te values Type-II inclusions in wollastonite, vesuvianite and clinopyroxene from the same zone (n=17) vary over a wider range (-188 to -58°C) (Table 1; Figure 7). Te values from the proximal zone are mainly clustered in two distinct fields. 14 inclusions within the first field have temperatures of -66 to -58°C while 4 inclusions within the second field are represented by a temperature range of -188 to -178°C (Figure 7).

Only two Type-II inclusions in clinopyroxenes from the distal zone yielded Te values from -126.1°C to -118.6°C. In contrast, Te values of all samples in vein skarns are significantly out of this range changing -188 to -183°C in wollastonite (n=3) and -189 to -181°C (n=3) and -55 to -56°C (n=3) in clinopyroxene (Figure 7).

Last ice melting temperatures (Tm-ice) were mostly determined in Type-I inclusions from the proximal zone which range from -13 to -10°C (n=4) in clinopyroxene and from -8.2 to -7.7°C in vesuvianite (Figure 7). In the same zone, Tm-ice value of a clinopyroxene sample with Type-II inclusion was measured as -14.4°C.

Final ice melting temperatures of most Type-II inclusions in proximal zone and vein skarn are in the range of +6.1 to +19.8°C (n=17) (Figure 7). In none of the inclusions immiscible liquid phase was determined at room temperature (e.g. CO_2 or CH_4). However, these melting values above 0°C (between +6.1 and +19.8°C) are indicative of Clathrate ($CO_2.5.¾H_2O$) formation at low temperatures which, although not detectable at room temperature, may imply the presence of carbo-

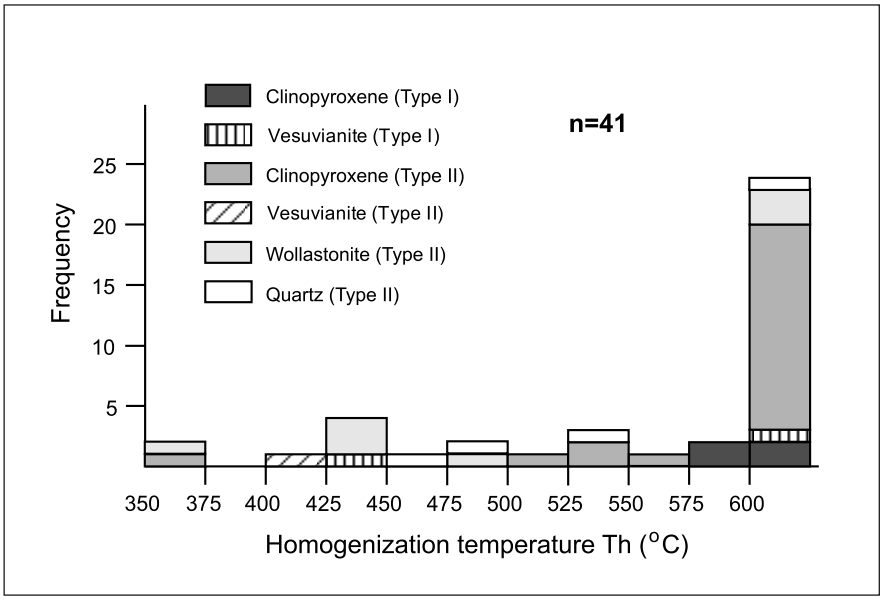

Figure 5- Homogenization temperature vs. frequency histogram of the Type I and Type II inclusions.

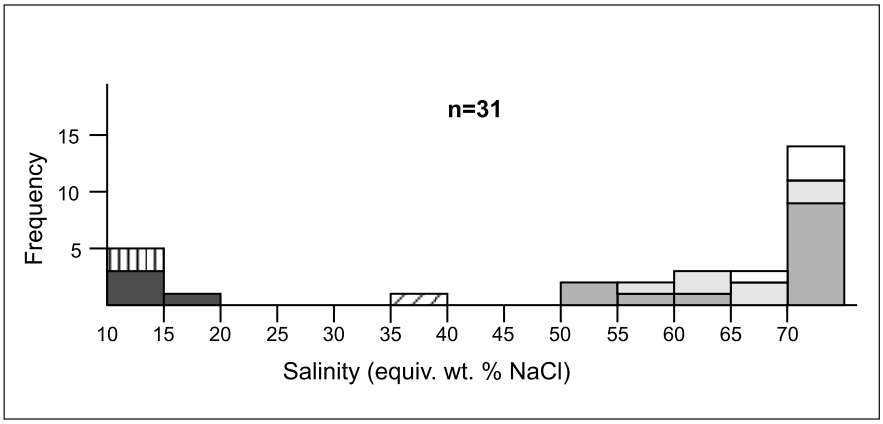

Figure 6- Salinity (equiv. wt. % NaCl) vs. frequency histogram of the fluid inclusions (for symbols see figure 5).

nic compounds (e.g. CO_2 or CH_4) in the solution (Roedder 1984; Shepherd et al., 1985; Van den Kerkhof and Hein 2001).

DISCUSSION AND RESULTS

Skarnization at the contact between Çataldað Granitoid and Mesozoic carbonate rocks (Figure 1) occurs as proximal zone, distal zone and vein skarn. First ice melting temperatures of Type-I and Type-II inclusions in wollastonite and vesuvianite from these zones are generally clustered in two distinct fields (Figure 7). Te values in the first field (ranging from -66 to -58°C) indicate the presence of CO_2 in the solution system (Tm-CO_2: -56.6°C) and those in the second field (from -188 to -178°C) point to occurrence of CH_4 (Tm-CH_4: -182.5°C) (Roedder, 1984; Sheppard et al.,

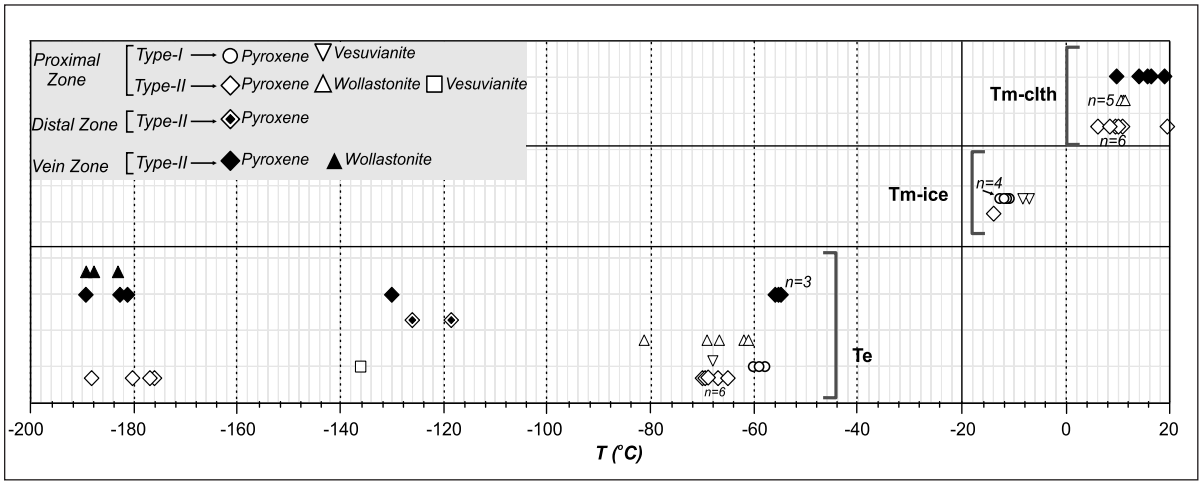

Figure 7- Distributions of the first melting temperatures (Te) of fluid inclusions (for symbols see figure 5).

1985). The fact that last ice melting in these inclusions occurs at temperatures greater than 0°C (between +9 and +19.8°C) (clathrate melting) indicates that significant amount of carbonic phases is also present in the system. Fluid inclusions studies on W-skarns reveal that CO_2 occurrence is associated with W mineralization (Higgins, 1980). It was also stated that that CH_4 is slightly more abundant than CO_2 in reduced systems (Fonteilles et al., 1989). In Susurluk deposit the presence of methane both in proximal zone and distal and vein skarn may be attributed to CH_4 and CH_4+CO_2 development by metamorphism and decomposition of pure marble during the skarnization rather than reduced conditions of the system (Larsen, 1991). A Te value of -48.8°C (Type II) measured on a clinopyroxene from the proximal zone shows that the system contains $CaCl_2$+NaCl+KCl+H_2O (Linke, 1965) which may indicate that carbonate dissolution is operative in skarn formation (Kwak, 1986).

On the salinity value vs. homogenization temperature diagram (Figure 8) solutions are bunched up in distinct fields. Type I inclusions of clinopyroxenes from the proximal zone are represented by a homogenization temperature of ≥ 587°C and an average salinity of 14.5 wt% NaCl equivalent. Type I inclusions in clinopyroxenes are homogenized into both liquid (592.2°C) and gas (587°C) phases at nearly the same temperature (Table 1) indicating boiling occurred in the system. Homogenization temperatures and salinity values of this clinopyroxene and those from the Kara magnetite-scheelite skarn (Northwestern Tasmania; Singoyi and Zaw, 2001) (511 to 616°C Th; 11.9-12.5 wt% NaCl equivalent) are found to be similar. Type I inclusions in clinopyroxenes from the proximal zone plot in the "Primary Magmatic Fluid" and "Metamorphic Fluid" fields (Bodnar, 1999) which represent for the first stage of skarnization. Type I inclusion in vesuvianite from the proximal zone with a homogenization temperature of >437°C and an average salinity of 11.1 wt% NaCl equivalent plots into the "Metamorphic Fluid" field (Figure 8) and these values are nearly similar to those of vesuvianite from stage II of the Kara magnetite-scheelite skarn (Th between 362 and 571°C; salinity between 16.3 and 17.8 wt% NaCl equivalent; Singoyi and Zaw, 2001). Type II inclusions (liquid+gas+(halite± sylvite)) which are commonly observed in proximal and distal zones and vein skarns of the Susurluk deposit have extremely high salinity values (36 to >70 wt%)

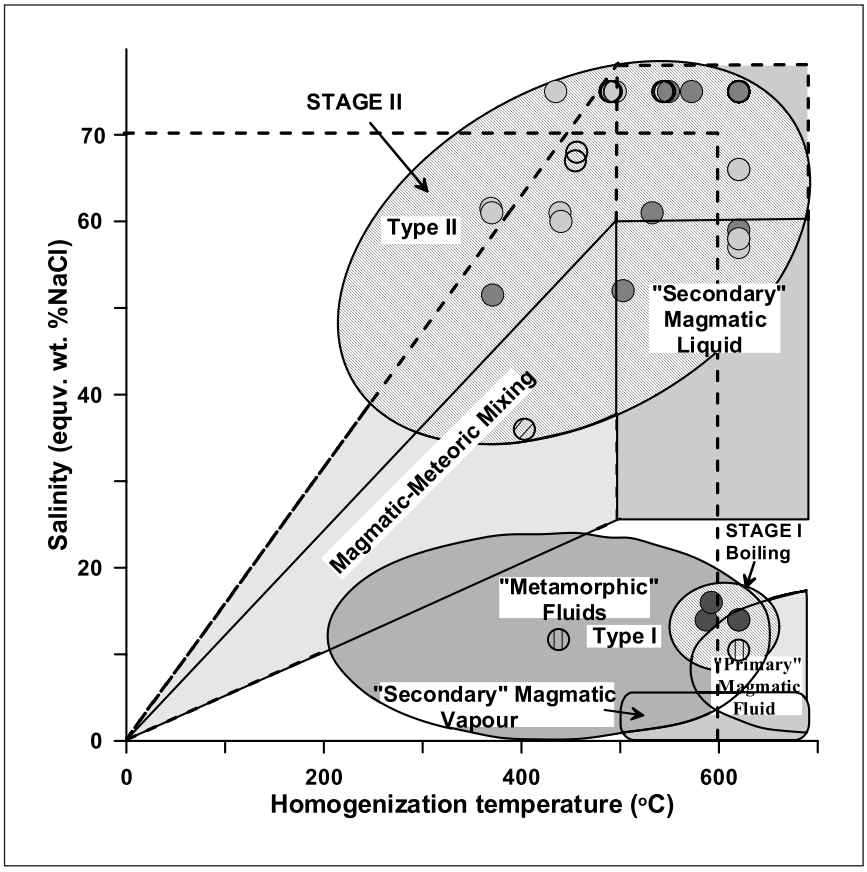

Figure 8- Plot of homogenization temperature vs. salinity values of fluid inclusions from the Susurluk skarn deposit (for symbols see figure 5) (approximate temperature-salinity distributions for hydrothermal solutions of different origins are from Bodnar (1999). Dashed line of "Secondary Magmatic Liquid" and "Magmatic-Meteoric Mixing" belongs to this study).

and plot into the "Secondary Magmatic Fluid" and/or "Magmatic-Meteoric Mixing" fields (Figure 8). In the Susurluk skarn system salinity was found to be increased following the boiling. This behavior of high-salinity magmatic fluid is particularly typical to shallow hydrothermal systems (porphyry copper deposits) (Bodnar, 1999; Wilkinson, 2001) and associated with granitoid crystallization (Kwak, 1986; Bodnar, 1999). Homogenization temperatures and salinity values of Type II inclusions generally decrease from proximal zone to distal zone (Figure 8) which may be indicative of partial mixing of magmatic solutions with cold, dilute meteoric waters (Beane, 1983).

In homogenization temperature vs. salinity value diagram constructed for various types of deposits (Figure 9), Type I and Type II inclusions formed during the first stage of skarnization (587 to ≥ 600 °C and 14-16 wt% NaCl equivalent) are plotted into porphyry and skarn fields above the critical curve. Th-wt% NaCl values of vesuvianite which is associated with anhydrous minerals

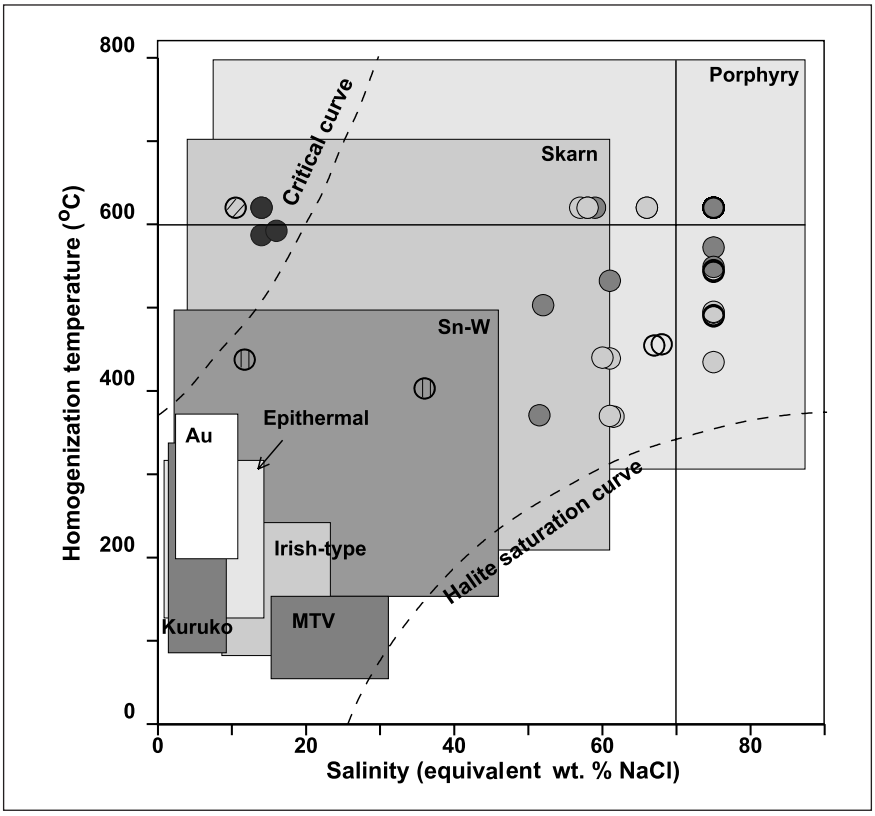

Figure 9- Homogenization temperature vs. salinity (wt. %NaCl) diagram illustrating typical ranges for inclusions from different deposit types (Wilkinson, 2001) (for symbols see figure 5).

indicate Sn-W, skarn and porphyry character (Figure 9). Homogenization temperatures (371 - ≥ 600ºC) and salinity values (52->70 wt%) of solutions from the second stage of skarnization which developed after the boiling plot predominantly into porphyry and partly into skarn fields. Boiling resulted in a sharp increase in salinity and deposition of some sulfide minerals (e.g. bornite, chalcopyrite) in the skarn zone (Kwak and Tan, 1981).

In W skarns scheelite is less abundant at early stage of skarnization but it increases with increasing of amphibole content (Kwak and Tan, 1981; Singoyi and Zaw, 2001). In the Kara (Northwestern Tasmania) skarn deposit, scheelite was formed during retrograde stage at a temperature range of 360 to 230°C and salinities of 0.2 to 19.8 wt% NaCl equivalent (Singoyi and Zaw, 2001). In the Susurluk skarn deposit, scheelite with trace abundance occurs at early stage of skarn formation at temperature of ≥ 587°C and salinity of 14-16 wt% while copper minerals (bornite and chalcopyrite) were formed at different periods of prograde stage from solutions with temperatures above 371°C and higher salinities (52 to 70 wt%).

In shallow skarn systems, boiling occurs at early stage of skarnization by hydraulic fracturing and brecciation of rocks by high-temperature solutions due to a major pressure drop from lithostatic to hydrostatic pressure (Kwak, 1986). Early boiling process at Susurluk may indicate that

skarnization was formed at shallow depths (less than 4 km) under pressures of about 100 MPa (1 kbar) (Figure 10). Oxidized type W skarns are formed under low pressure conditions while large - reserved W deposits mostly occur under reducing systems (Newberry, 1983). According to Newberry and Einaudi (1981), large- reserved W deposits are formed in systems lacking fracturing and under extremely high temperature and pressure conditions (1.5-3 kbar and 550-650°C). In contrast, Susurluk skarn deposit was developed at high temperature (371- ≥ 600°C) but low pressure conditions (1 kbar).

Although mineralized skarn systems have common characterizeds systems with main skarn minerals (W, Cu, Fe, Pb-Zn, Mo and Sn) may show systematic differences (Einaudi et al., 1981) which include parent rock composition, composition and degree of evolution of fluid, skarn formation depth, metamorphism and metasomatism (Meinert et al., 1980). Einuadi et al. (1981) classify W skarns as "reduced" and "oxidized" types while Kwak and White (1982) categorize them as "W-Sn-F" and "W-Mo-Cu" types. Newberry (1998) divided W-F skarns into Mo-poor and Mo-rich subgroups based on their highly incompatible element contents. Most of mined large-reserved W deposits (e.g. Mactung and Cantung deposits in Canada; Sandong deposit in Korea and Fujigatani deposit in Japan) are of "reduced" type and characterized with garnet composition less than 50% andradite, hedenbergite type pyroxene (Hd_{60-90}) and abundant pyrrhotine and trace pyrite contents (Einaudi et al., 1981). In contrast, "oxidized" type

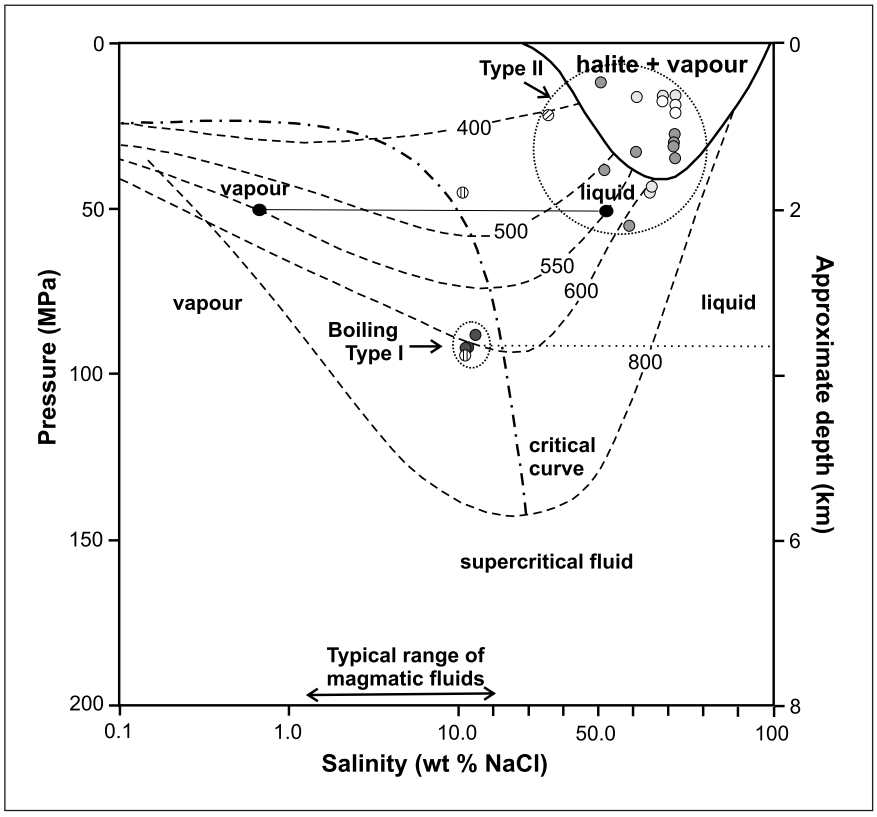

Figure 10- Phase distribution of fluid inclusions under P-T conditions proposed for typical porphyry deposits (Wilkinson, 2001) (for symbols see figure 5).

W skarns mostly contain andraditic garnet (Ad_{80-100}), salic pyroxene (Hd_{20-70}) and abundant pyrite and trace pyrrhotine (Einaudi et al., 1981). Garnets in skarn zones at Susurluk are of dominantly grossular-andradite composition and andradite / grossular ratio of zoned garnets in the exoskarn zone increases from core to rim (Orhan, 2008; Orhan and Mutlu, 2009). High andradite composition of garnets (Eiunadi et al., 1981) and increasing andradite content of zoned garnets from core to rim are suggested to be the indicator of "oxidized" type W skarns (Newberry, 1983). All these findings clearly indicate that scheelite-containing Susurluk skarn is an "oxidized" type W skarn.

ACKNOWLEDGEMENTS

The Scientific and Technical Research Council of Turkey (TUBITAK Project No. 106Y187) and the Eskiþehir Osmangazi University (grant No. 2006-15010) are greatly acknowledged for financial support.

Manuscript received December 11, 2009

REFERENCES

Akyüz, S, 1995. Manyas-Susurluk-Kepsut (Balýkesir) Civarýnýn Jeolojisi. Ph.D. Thesis, Istanbul Technical University, Istanbul, 239 p. (unpublished) Turkish.

Arýk, F., 1995. Serçeören-Örenli-Kansýz (Kepsut-Balýkesir) Yöresi Vollastonit ve Talk Yataklarý. M.Sc. Thesis, Selçuk University, Konya, 107 p. (unpublished) Turkish.

Bakker, R.J., 2003. Package FLUIDS 1. Computer programs for analysis of fluid inclusion data and for modelling bulk fluid properties. Chemical Geology, 194, 3-23.

Beane, R.E., 1983. The magmatic-meteoric transition. Geothermal Resource Council, Special Report no. 13, 245-253.

Bodnar, R.J., 1999. Hydrothermal solutions. in Marshall, C.P., and Fairbridge (eds.), Encyclopedia of geochemistry: Lancaster, Kluwer Academic Publishers, p. 333-337.

Boztuð, D., Harlavan, Y, Jonckheere, Can, Ý.and Sarý, R., 2009. Geochemistry and K-Ar cooling ages of the Ilýca, Çataldað (Balýkesir) and Kozak (Izmir) granitoids, west Anatolia. Turkey, Geological Journal, 44, 1, 79-103.

Çakýr, A. and Genç, H., 1983. Balýkesir-Susurluk-Yaylaçayýr Köyü, Bursa-Mustafakemalpaþa Ýlçesi Paþalar Köyü-Býçkýdere-Farafat Alanýndaki Vollastonit MTA Report No: 7299, 11 p. (unpublished) Ankara.

Einaudi, M.T, Meinert, L.D and Newberry, R.J., 1981. Skarn deposits. Economic Geology, 75, 317-391.

_____ and Burt, D.M, A, 1982. Special Issue Devoted to Skarn Deposits, Introduction-terminology, classification and compositionof skarn deposits. Economic Geology, 77, 745-754,.

Ercan, T., Ergül, E., Akçaören, F., Çetin, A., Granit, S. and Asutay, J., 1990. Balýkesir-Bandýrma arasýnýn jeolojisi, Tersiyer volkanizmasýnýn petrolojisi ve bölgesel yayýlýmý, MTA Dergisi 110, 113-130.

Erdað, A., 1976. Balýkesir-Çataldað Granodiyoritinin (Güney Alaný) Jeoloji ve Petrolojisi. Ph.D. Thesis, Istanbul University, Istanbul, 94 p. (unpublished).

Ergül, E., Öztürk, Z., Akçaören, F. and Gözler, M.Z., 1980. Balýkesir Ýli Marmara Denizi Arasýnýn Jeolojisi. MTA Raporu Derleme No: 6760, 57 p. (yayýmlanmamýþ) Ankara.

_____, Gözler, Z. and Akçaören, F., 1986. 1:100 000 Ölçekli Açýnsama Nitelikli Türkiye Jeoloji Haritalarý Serisi, Balýkesir-F6 Paftasý. MTA Genel Müdürlüðü, 11 p.

Erdinç, H., 1978, Kepsut-Serçeören Köyü (Balýkesir) Çevresinde Yer Alan Vollastonit Zuhurlarýnýn Ön Etüdü. MTA Report No. 6458, 11 p. (unpublished) Ankara.

Fonteilles, M., Soler, P., Demange, M., Dere, C., Krier-Schellen, A.D., Verkaeren, J., Guy, B. and

Zham, A., 1989. The scheelite skarn deposits of Salau (Ariege, French Pyrenees). Economic Geology, 84, 1172-1209.

Fu, M., Kwak, T. A. P. and Mernagh, T. P., 1993. Fluid inclusion studies of zoning in the Dachang tin-polymetallic ore field, People's Republic of China. Economic Geology 88; 283-300.

Higgins, N.C., 1980. Fluid inclusion evidence for the transport of tungsten by carbonate complexes in hydrothermal solutions.Can. J. Earth Sci. 17, 823-830.

Kwak, T.A.P., 1986. Fluid inclusions in skarns (carbonate replacement deposits), J. Metamorphic Geol., 4, 363-384.

_____ and Tan, T. H., 1981. The Geochemistry of zoning in skarn minerals at the King Island (Dolphin) Mine, Economic Geology, 76, 468 - 497.

_____ and White, A.J.R., 1982. Contrasting W-Mo-Cu and W-Sn-F skarn types and related granitoids. Mining Geology, 32, 339-351.

Larsen, R. B., 1991. Tungsten skarn mineralizations in a regional metamorphic terrain in northern Norway: a possible metamorphic ore deposit. Mineralium Deposita, 26, 281-289.

Layne, G.D. and Spooner, E.T.C., 1991. The JC tin skarn deposit, southern Yukon Territory; Geology, paragenesis and fluid inclusion microthermometry. Economic Geology, 86, 29-47.

Linke, W.F., 1965. Solubilities of Inorganic and Metal Organic Compounds. American Chemical Society 2, Van Nostrand, 1914 p.

Mathieson, G.A. and Clark, A.H., 1984. The Cantung E-zone scheelite skarn ore body, N.W.T.: a revised genetic model. Economic Geology, 79, 883-901.

Meinert, L.D., Newberry, R.J., and Einaudi, M.T., 1980. An overview of tungsten, copper, and zinc-bearing skarns in western North America U.S. Geological Survey Open-File Report 81-355, p. 304-327.

Meinert, L.D., 1992. Skarn and skarn deposits, Geoscience Canada, 19, 145-162.

Mutlu, H. and Orhan, A., 2009. Susurluk (Balýkesir) Skarn Yataklarýnýn Duraylý Ýzotop Sistematikleri. Eskiþehir Osmangazi Üniversitesi Araþtýrma Fonu Projesi Raporu, 197 p. (unpublished).

Newberry, R.J., 1983. The formation of subcalcic garnet in scheelite-bearing skarns. Canadian Mineralogist, 21, 529-544.

_____, 1998. W- and Sn-skarn deposits: A 1998 status report. Mineralogical Association of Canada Short Course Series, 26, 289-335.

_____ and Einaudi, M.T., 1981. Tectonic and geochemical setting of tungsten skarn mineralization in the Cordillera: Symposium on tectonics and ore deposits, Tucson, 1981, Proc., 99-111.

Orhan, A., 2008, Susurluk Skarn Yataklarýnýn Mineralojik ve Jeokimyasal Özellikleri (Balýkesir-Batý Anadolu), Ph.D. Thesis, Eskiþehir Osmangazi University, Eskiþehir, 258 p. (unpublished).

_____ and Mutlu, H., 2009, Susurluk (Balýkesir) skarn yataðýnýn mineralojik ve petrografik özellikleri, Eskiþehir OGU Mühendislik Mimarlýk Fakültesi Dergisi, 22(II), 65-91.

Roedder, E., 1984. Fluid inclusions. Reviews in Mineralogy 12, 12- 45.

Sheppard, T., Rankýn, A.H. and Alderton, D.H.M., 1985. A practical guide to fluid inclusion studies. Blackie-Glasgow-London, 239 pp.

Singoyi, B. and Zaw, K., 2001. A petrological and fluid inclusion study of magnetite-scheelite skarn mineralization at Kara, Northwestern Tasmania, Implications for ore genesis. Chemical Geology, 173, 239-253.

Timon, S.M., Moro, M.C., Cembranos, M.L., Fernandez, A. and Crespo, J.L., 2007. Contact metamorphism in the Los Santos W skarn (NW Spain). Mineralogy and Petrology, 90, 109-140.

Van den Kerkhof A.M. and Hein, U.F., 2001. Fluid inclusion petrography, Lithos, 55, 27-47.

Wilkinson, J.J., 2001. Fluid inclusions in hydrothermal ore deposits. Lithos, 55, 229-272.

Mineral Res. Expl. Bull., 141, 69-92, 2010

THE GEOARCHEOLOGY OF THE YENÝKAPI EXCAVATION SITE IN THE LAST 8000 YEARS AND GEOLOGICAL TRACES OF NATURAL DISASTERS (ÝSTANBUL - TURKEY)

Doðan PERÝNÇEK*

ABSTRACT.- During the excavations of the Istanbul Archaeological Museum for the Marmaray Project, which will connect two sides of the Bosphorus by rail tube tunnel, an ancient Byzantine Port (Port of Theodosius)** was explored around Yenikapý, district of Istanbul. The aim of the study is to understand the stratigraphical sequence observed in the excavation site, to recognize the traces of natural events observed within the sequence and to reach the geoarcheological data that will provide contribution to the archeological studies by geological findings. The sequence studied in the Yenikapý Excavation site was divided into 9 different units. The sequence is transgressive from 1st to 7th unit and regressive from 7th unit, to upper part of the 8th unit. These investigated sequences have been deposited during the last 8000 years. 32 ancient shipwrecks were detected in three different geological layers of nine units which were dated to the 6th century, 7th, 8th, 9th centuries and 10th, 11th centuries respectively. The 4th unit was formed under the effect of an earthquake and following tsunami waves occurred in A.D. 557. It is considered that some of the districts of Istanbul which are very close to shore have submerged by the effect of tsunami waves during the earthquakes in A.D. 553 and 557. It was also considened that the reason of the sinlang of the was 25 Byzantine vessels a very strong storm that affected the coasts of Istanbul city. The traces of this storm are detected in 5th and 6th units.

Key words: Yenikapý, geoarcheology, tsunami, ancient shipwreck, amphora, Byzantine.

INTRODUCTION

The Port of Theodosius belonging to Byzantine era has been unearthed in ongoing excavations in Yenikapý district of Istanbul under the administration of Istanbul Archeological Museums for the Marmaray project which will connect both sides of Istanbul strait by rail tube passage (Figure 1).

By the directorate of Istanbul Archeological Museums, in Yenikapý district, 1.5 km inward from the shoreline, to the north of the railway, nearly 30 shipwrecks were encountered during excavations in the area where Metro and Marmaray stations will be constructed formerly named as "Langa Orchard" (Pulak, 2007; Asal, 2007; Baþaran et al, 2007; Kocabaþ and Kocabaþ, 2007; Gülbahar, 2007). The "Port of Theodosius" (Kocabaþ and Kocabaþ, 2006) belonging to Byzantine Era is also called as the "Port of Eleutherios" in some published papers (Müller-Wiener, 2001). The Port of Theodosius was probably founded by Theodosius I (379-395) in a naturally occurred bay in Yenikapý (Asal, 2007). According to archeological evidences the port mentioned has intensively been used after A.D. 4th century (Gökçay, 2007). A marble stele of 4 B.C. gives some clues about the construction date of the Port (Gökçay, 2007).

The author visited the Yenikapý excavation site in April, 2005 to get an information about the reason of the sinking of the vessels and started to collect geological data in order to answer to the questions relevant to subject. Within the following months of his first visit, he has been invited by the Directorate of Istanbul Archeological Museum. The geological investigations have been formalized with this invitation. The

* Çanakkale 18 Mart University, Faculty of Engineering and Architecture, Terzioðlu Campus, 17020, Çanakkale

** Among historical places mentioned in the article, the “Theodosius Port” of Byantian era is called as the “Yenikapý Port” with its present name and “Lycos River” is called the “Bayrampaþa River”.

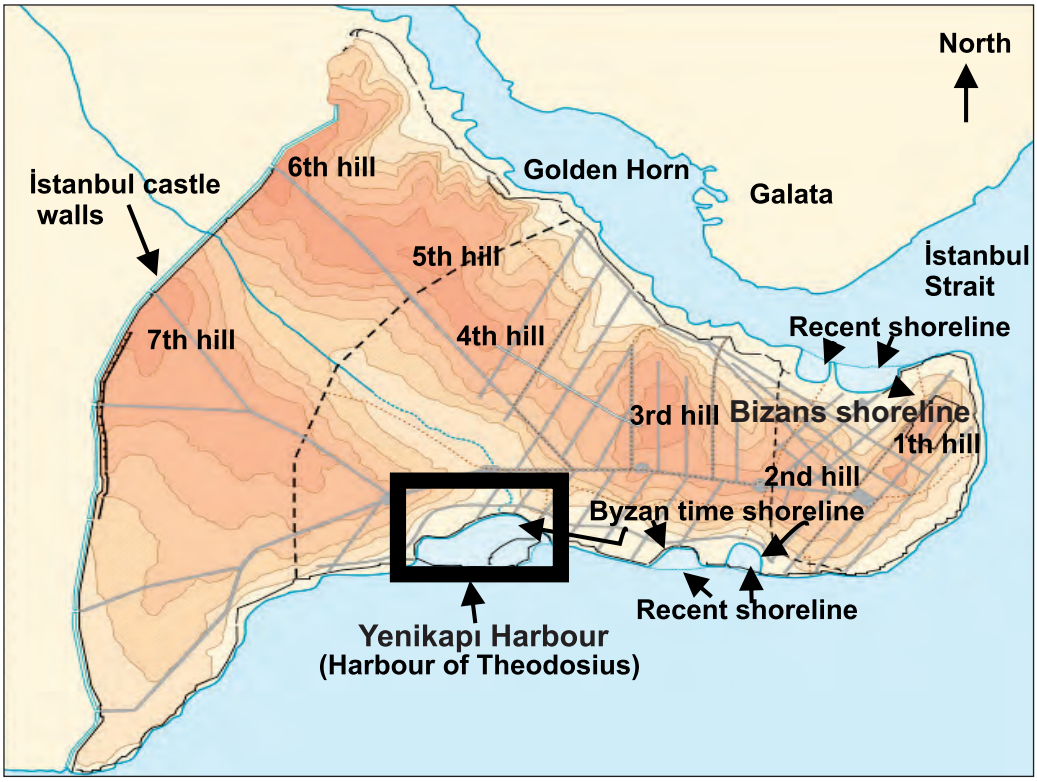

Figure 1- Topography of Istanbul in Byzantine era and port of Theodosius (Janin, 1964). The location of the Port was marked as rectangle.

purpose of this study is to collect geological data related with the site of excavation, to understand their relations with archeological evidences, to transfer geological information to archeologists working in the area and to provide a support, to find out the reason of the sinking of the vessels and to reveal the geological history of the site of excavation. Geological investigations have been intensified after necessary permissions had been taken from the Ministry. Thus the author has been the first authorized geologist who worked on the site of the excavation. In 2007, a student from the Geological Engineering Department of 18 Mart University carried out a graduation thesis on the site of the excavation with the permission of the Ministry. The interest of earth scientists into excavations in Yenikapý district has increased a lot in the following years, then a group of scientists from Istanbul University proposed a profect and started to work here with the presentcauthor in 2007 by basing on his permission.

In studies carried out in Yenikapý area, the distinguishing features of units were determined and lithological differences were revealed. Based on these, 9 different units were detected on the site of excavation. Sedimentological data were compiled based on field observations and the relations of units were studied in detail. Mainly data collected in the field, related results and interpretations since 2005 will be presented in this article.

The Marmara region has been shaken by earthquakes several times throughout the history. The first known earthquake occured in A.D. 29, and the first earthquake which its details

have been registered, had experienced the region in 1st of February 363. Byzantine sources state that Istanbul thoroughly has been collapsed in 10 quakes until the earthquake in 1265, and some of tsunamis affected the shores of Istanbul during these earthquakes (Altýnok, 2005; Yalçýner et al., 2002). Tsunami waves which were formed by earthquakes mentioned in historical documents should have remained traces on land. Sediments which it was brought by tsunami waves from the sea should have been preserved in some areas of Istanbul. It will be possible to reach many unknowns when these traces are found (Perinçek et al., 2007).

STRATIGRAPHIC SUCCESSION

Sections in six stations were measured in the Yenikapý excavation site and generalized stratigraphic section was obtained making numerous point observations (Figures 2, 3). 9 different units were distinguished from bottom to top on the site of excavation in terms of lithological features. Late Miocene - Holocene units form the Pre Quaternary basement of the excavation site. All units forming the site of excavation will be introduced in detail starting from the 1st unit at the bottom.

1st Unit

The 1st unit is represented by dark gray to black colored sandy mud in patches (Figures 2, 4). Crushed, dark brown rush stalks are observed in mud indicating to a swamp environment. After the unit had been deposited in lagoonal environment, the study area has been submerged under water as a result of a transgression. It was observed that living beings in marine environment had previously burrowed in mud of the lagoonal environment, and these burrows had been filled by the sands of the 2nd unit. In these burrows, abundant shell fragments and small gastropods with sand are recognized (Figure 4). The unit starts with pebble, coarse pebble and sand (sand ratio is small) at least in two places at the site of excavation. Regularly arranged pebbles are observed in mud which is too rare to form a layer in patches. Surface of pebbles are in white color and are composed of crystallized limestone and Miocene limestone. Their fracture surface is gray to whitish gray in color. The contact between the 1st unit and the 2nd unit is clear. Beneath this unit Late Miocene deposits are seen. These are represented by claystone and siltstones. There is also a possibility about the unit that may be the equivalent of the Kuþdili formation of Holocene age (Meriç et al., 1991).

Swamp deposit is represented by mud silty mud, sandy mud, muddy sand and sand bands are observed in patches. Besides, channels are observed within the deposit. The filling material of these channels is silt, sand and pebble with muddy matrix and has a direction of N-S. These data indicate that the center of the lagoon is to the south of the study area. The pebble in channels, mostly are less rounded and poorly sorted. In some channel fills, some angular coarse pebbles also exist. Angular grains have been transported from close areas or thrown into channel by people. Over the surfaces of the pebbles in channel fills, carbonate accumulation/coating is observed. The lime carried in channel by water has been accumulated on pebbles which have fresh gray surface and turned their colors into white. The surface of pebbles is irregular and no any reworking are seen after transportation into the channel and coating by lime. The channels are not deep. These are flat laying channels having 3-15 cm depths. Channels filled by gravel laterally grades into pebbly sand and sand. The granular size decreases from bottom to top of the channel. Sand layers which are laterally lensoidal in marsh form wide shallow channels as well. The sand in question is usually represented by quartz grains and well sorted. Abrasion marks in mud layers at channel bottoms are distinctive but the boundary here is irregular. However, the upper boundary was detected as regular. Besides, there are silty, less

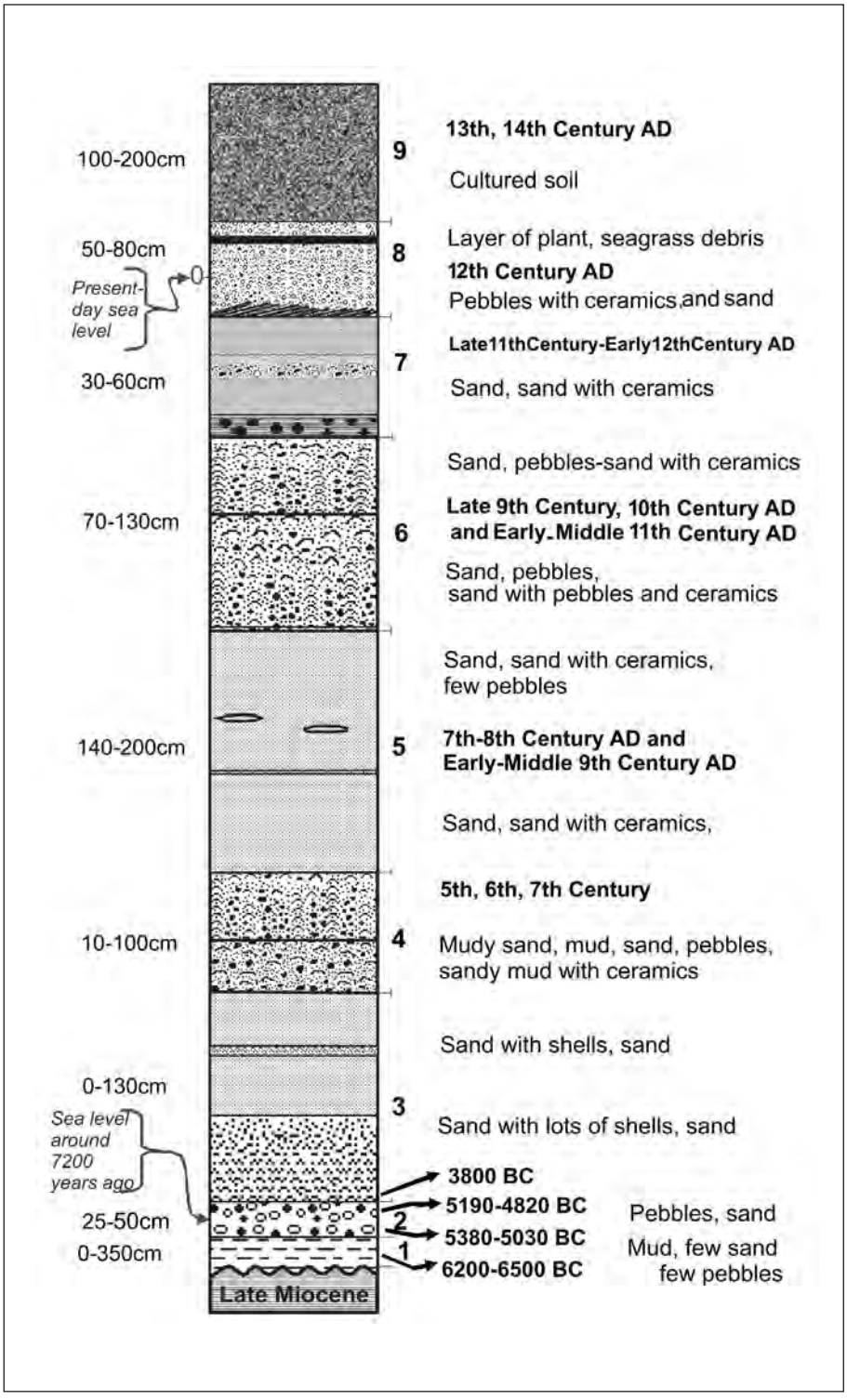

Figure 2- Generalized stratigraphical section of the Yenikapý Excavation site.

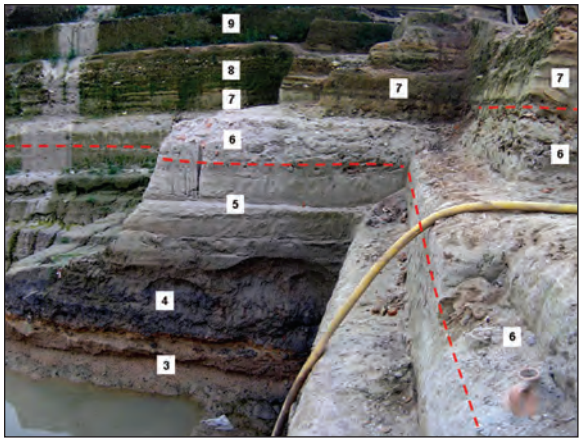

Figure 3- Close up view of succession from 3rd to 9th units.

Figure 4- Relation of the 1st Unit (dark gray colored marsh) and pebbly, sandy unit denoted as number 2. Nests of living organisms (burrows) are observed while the 2nd unit deposits in the upper parts of the marsh. These burrows were filled by sand and fragmented shells.

muddy sands with regular lower and upper boundaries in marsh deposit. These were interpreted as sheet sands that had been deposited during flood.

The thickness of the 1st unit varies between 0 to 3.5 m. Regions where the thickness reaches 3.5 meters are observed to the east of the excavation site. The 2nd unit directly overlies the Late Miocene deposits in areas where the 1st unit does not exist. Marsh deposits are observed at eastern parts of the Yenikapý excavation site. Coastal marshes can easily be traced at this location. The settlement area which can be observed along the coastal marshes falls into the eastern-northeastern part of the marsh (Çelik, 2007; Prof. M. Özdoðan, 2007, oral interview). Usually, Late Miocene deposits crop out at the bottom of the settlement area.

At the bottom of the marsh, 6 tree roots and part of trunks close to root section were found. However, the upper sections of trunks did not exist. As a result of the increase in water level, the contact of the lagoon along the coast has been cut off due to the development of spit and the mud began to deposit in the area. After the formation of lagoon environment, trees remained in the marsh land decayed as these were subjected to excess submersion in water. That is why only roots and trunks close to roots have been preserved. Tree branches were also recognized in some locations in the marsh land other than roots. In some places shells of bivalves were recognized in the marsh land. The shells in question are observed both as dispersed and also in the form of aggregation. It is considered that strong waves in stormy times have transported material into the marsh land from sea and shells have also been transported into the lagoon within materials.

2nd Unit

Flat and sub rounded pebbles and coarse pebbles of the 2nd unit overlie the unit deposited in lagoon environment (Figures 4, 5, 8). Pebbles are mostly composed of formed of recrystallized limestones and sometimes reach to a small block dimensions. The matrix among pebbles is sandy. The burrows are observed on pebbles and coarse pebbles. This case shows that pebbles have remained in marine environment for a long time. Fossils have been preserved in many burrows (mollusc Teredo navalis, Prof. C.

Morhange, March, 2008, oral interview). It is observed that both ends of pebbles are usually equally sized and disc shaped. This indicates the bidirectional wave action but not the unidirectional erosion of river flow. Although pebbles mentioned have been transported to the area by a river, there are distinct features showing that these pebbles have been eroded by wave actions and flattened. The total thickness of pebble layer is around 25 - 50 cm.

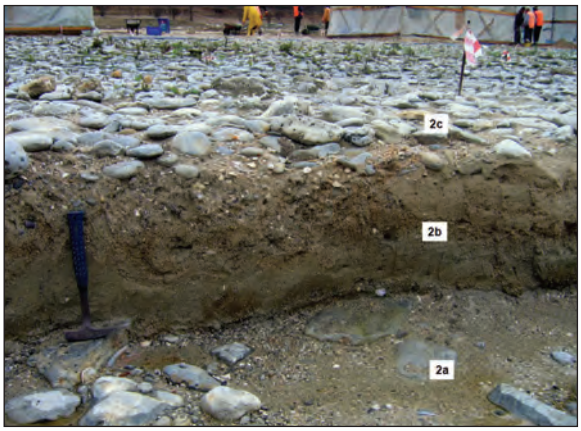

Figure 5- The 2nd unit can be divided into three sub units as there is sand among gravel layers in some parts of the excavation site. Therefore the unit has been denoted as 2a, 2b, 2c.

The unit can be divided into three sub units (2a, 2b, 2c) in some sections of the excavation site due to the presence of sand. There was observed pebble at the bottom (2a) then sand in the middle (2b) and again pebble at top (2c). The pebble sizes at the bottom reach 30 x 20 x 7 cm. However, pebble sizes located at top of the sand layer in the middle are mostly 10 x 5 x 2 cm. The ratio of both pebble layers decreases as going to the south in seaward direction. Whereas on land, pebble at the bottom and sand layer located in the middle are pinched out and fine grained pebbly layer at the top directly overlies the 1st Unit at the bottom. The reason for pinching out of pebble at the bottom and the decrease in pebble ratio towards sea is due to the regression. The pebbly layer named as 2c disappears before 2a pebble layer on seaward and laterally grades into sand. This lateral change has developed as a result of transgression. Pebbles show a transition into sand towards open sea but overlaps with each other in landward. The shore line of the sea which caused the precipitation of the pebble layer at top might be located very near or inside the site of excavation. Since the excavation has not yet reached the area in question the accurate information will be obtained in further stages of the excavation. Mollusc burrows are observed in both pebble layers (mollusc Teredo navalis). Some of the smaller granules of the pebble layer at top have probably been formed by the transportation, abrasion and re-deposition of pebbles at the bottom.

It is considered that the 2nd Unit was deposited in beach environment. After the transgression that had caused the deposition of this unit the environmental conditions were deepened and the 3rd unit on top was deposited. The upper boundary of the 2nd unit is as distinct as the lower boundary.

C14 analysis was performed in samples taken from shells of mollusc (*Teredo navalis*) which were observed in burrows over pebbles in the unit. After the calibration of C14 dating, the layer 2c was dated as 5190 B.C. - 4820 B.C. with 94.5 % probability (Sample no: Yenikapý U2 798; Petricola). However the sample taken from the layer 2a of the 2nd unit was dated as 5380 B.C. - 5030 B.C. (sample no: Yenikapý U2A 801; Ostrea) with 95.4% probability (Prof. C. Morhange, July, 2008, written communication). Ceramics found at different levels of the 2nd unit and at levels closer to the bottom of the 3rd unit were ages as 5200 B.C. - 3800 B.C. (Prof. M. Özdoğan, 2008, oral communication). These are important data indicating that the transgression started at least 7200 years ago. The reason for the transgression is because the rise of water level in the Sea of Marmara started to rise 11000

- 8000 years ago (Stanley and Blanpied, 1980; Ryan et al, 1997, 2003; Çağatay et al., 2000). The reaching of the seawaters to the coasts of the Theodosius port happened 7200 years ago.

3rd Unit

There is the sandy level of the 3rd unit containing abundant sea shells with a thickness of 60 cm over the 2nd unit (Figures 2, 3, 6, 7, 8). The thickness of the 3rd unit varies between 0 - 130 cm It is observed that the 3rd unit pinches out and the 4th unit directly lies on the 2nd unit to the northeast of the site of excavation. The unit begins with a layer formed by complete shell and fragments of shell with 80% at the bottom having a thickness of 10 - 50 cm. The amount of sand in the fragmented shell layer increases upward. It is also observed that the shelly level becomes thinner and disappears in some places. There is a sand layer over it with a total thickness of 60 -70 cm. Shell layers and lenses were observed in variable thicknesses within the sandy level. The 3rd unit generally shows a fining upward sequence. Very little amount of amphora fragments were recognized within this unit. An oxidation level was observed in the upper part of the 3rd level. It might be considered that the reason of this oxidation of ferrous material in the 4th unit and stained the 3rd unit in its below.

Figure 6- The relation of the mud bearing dark gray 4th unit with lower and upper units is observed.

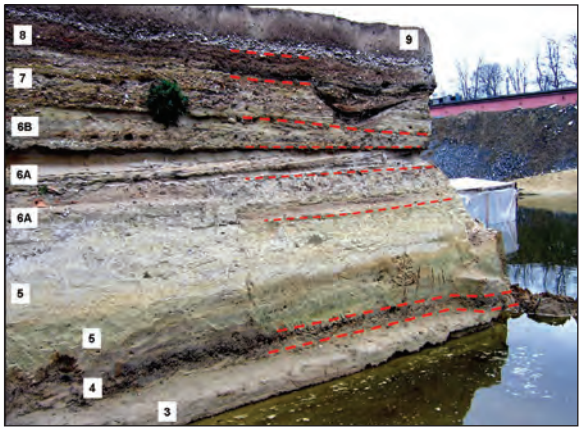

Figure 7- Vessels which are considered as has submerged by the storm are observed in the 6th unit. In photo succession from 3rd unit to 9th unit is observed. At upper right corner a channel excavated during the deposition of eight units and its filling is viewed.

Figure 8- The relation of pebbly unit denoted as the Unit number 2, the 3rd Unit represented by sand and the 4th Unit which was deposited with a distinct contact is seen in photo. Oxidation around the bottom of the dark colored muddy 4th unit is noticed. The 4th unit is overlain by light colored 5th Unit. The 6th Unit is observed at the topmost.

4th Unit

Gray colored, muddy sand and sand belonging to the 4th unit exits over the 3rd unit (Figures 2, 3, 6, 7, 8, 9, 11). Dark gray to black colored level rich in black colored organic material takes place

Figure 9- The camel skeleton at the 4th Unit (Gökçay 2007, R11) is observed in dark colored mud. The bones of the camel skeleton are not in messy form.

at the base of this layer. The matrix of this coarse grained layer is made up of mud, silt, sand and less pebble. This unit is very poorly sorted. The unit is represented by the coarse sand and muddy sand in some places. There are also detritic particules in pebble and block size. The size of some particules may even reach 1 m. An angular ceramic fragment, a tree with length of 150 cm. and a spetia type amphora in 40-50 cm in size may possibly be observed next to a marble block 1 m in length (Katalog, 2007). In addition to things mentioned above, there are also abundant shells, sometimes complete amphora and fragments of amphora, coins, metal pots, ceramic pots and fragments, fragments of kerosene lamp, rounded marbles, piece of decayed wood, fragments of glassy pots, hawser and stone anchors of ships found at this level (Pulak, 2007; Asar, 2007), pine cones, marine and terrigenous fossils, animal bones, plant pieces and leaves transported from land and kernels of different fruits (Figure 11). There was found 4 horses as completely preserved and a skeleton of camel in muddy layers of the unit (Figure 9) (Çelik, 2007; Gökçay, 2007; Perinçek et al., 2007; Perinçek, 2008). The bones of skeletons found in the site are not dispersed. The leash of one of the horses was found next to them and the feed basket of the other horse was detected next to it as transported as the horse was drifted towards sea.

The lower boundary of the unit is distinct and irregular (Figure 6, 8). There are some evidences showing that previously deposited 3rd unit has been eroded by submarine currents. Channels which were formed after being scraped by current activity were filled by the material of the 4th unit following the erosion. The depth of these channels varies in between 10 - 30 cm. These channels might have been engraved by sea base currents formed after the tsunami. Although the lower boundary of the 4th unit is distinct (Figure 8), the upper boundary usually gradually passes into 5th unit (Figure 6, 7, 8). Along the gradual transition zone, laminating sand and muddy sand layers between 4th and 5th units are observed. Sometimes this transition is observed without lamination.

The thickness of the 4th unit varies in between 10 cm to 1 m. The mud present within the unit has changed the color of all ceramics observed in one portion of the site brown to dark gray in color. Besides, the mud in the unit has also colorized the 3rd unit at the bottom into dark gray infiltrating through pores of the sand. Metals parts in the 4th unit has decayed and penetrated through 3rd unit at the bottom. Thus, the oxidized surfaces were formed parallel to the contact between the two Units. The 4th unit is divided into 2 sub units to the southwest of the study area. The lower one of these sub units 30 cm and the upper one is 40 cm in thickness. Muddy sand and less archeological findings (ceramic etc.) and blocks of stone unfamiliar to the environment also exist at the lower level. The upper layer is more pervasive and distinguishable at the site of excavation. The information given in previous paragraphs are mostly related with this upper layer and there are many materials in it. Many dock piles were found in different units within the marine sand at the Yenikapý excavation site. Many of piles in the 4th unit disappear at the

boundary of the overlying 5th unit (Figure 10). Tsunami might be the natural event which has deteriorated the piles at the same height.

Figure 10- The 4th Unit is considerably thin in some places. Docks constructed at the Port in the 6th century and earlier have been destructed by tsunami and piles of the dock were later covered by the deposits of the 5th Unit. The relation of the 4th, 5th and 6th Units are observed in photo. Piles marked by "X" have been destructed by tsunami and next piles marked by "Y" have been constructed.

C14 analysis was performed in one of the samples taken from woods in the 4th unit (Yenikapý U4 795). After the calibration the sample was dated as A.D. 420 - A.D. 570 with 95.4 % probability. Another sample taken from the same unit was dated in an interval of A.D. 400 - A.D. 450 with 68.2% probability (Prof. C. Morhange, July 2008, in written communication). The first sample had been taken into account since the probability was high. The 4th unit was dated as A.D. 5 - 7 centuries according to the ceramic, coin and similar archeological materials in it (Katalog, 2007). When historical earthquakes and tsunamis were studied (Altýnok, 2005; Yalçýner et al. 2002), records of strong earthquake and tsunami were encountered as 543, 545, 549, 553, 555 and as 557 B.C. There was not recorded any important tsunami happened in A.D. 5 - 7 centuries. The 4th unit

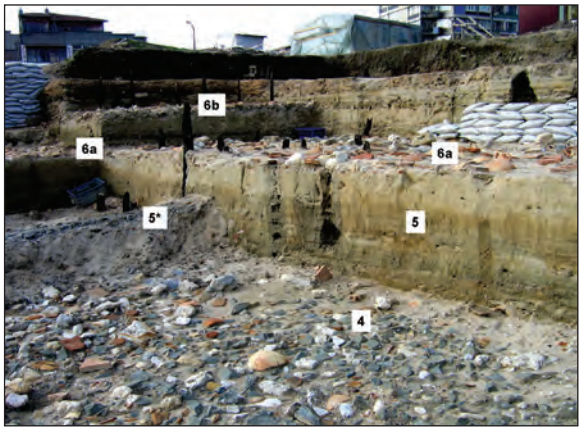

Figure 11- The photo shows the relation of 4th, 5th and 6th Units. The section marked by 5* indicates the wooden part belonging to 7th and 8th centuries in the 5th Unit. At the bottom of 4th Unit, there is observed ceramic, various furniture, coins, processed angled marble, pebble and unprocessed wooden parts transported from land and processed wooden material belonging to destroyed ships in the sea and piles.

most probably was formed due to the earthquake which occurred in A.D. 557 and following tsunami waves. The dome of Ayasofya (Hagia Sophia) Museum was weakened by the earthquake in December 557 then collapsed in May 558 (Wikimedia, 2008). Therefore, although many earthquakes and tsunamis happened in 6th Century, the earthquake in A.D. 557 have been brought foreground in this article. Taking records of historical earthquake, tsunami and C14 dating into account, it was brought into foreground that the important part of the 4th unit was formed in A.D. 6th Century.

5th Unit

Sand belonging to the 5th unit overlies the 4th unit (Figures 2, 3, 6, 7, 8, 10, 11). Minor cross bedded sand was observed in the unit. Lens shaped levels composed of shells exist toward upper layers. Besides; pieces of ceramic were also observed. The 5th unit is composed of well sorted fresh sand and its thickness changes in between 140 - 200 cm The archeological findings

are not much in this unit when compared with the 4th unit at the bottom. It usually has a gradual transition with the 4th unit at the bottom but mostly has a distinct contact with the 6th unit above it. The distinct boundary indicates an important event. The 5th unit contains intercalations of sand with thin muds and lensoidal gastropod accumulations 5 mm in length. Besides, there are many shells as dispersed in the sequence. It is observed that fresh sand and very little muddy sand intercalate with each other and the bedding is markedly visible in some part of the excavation site. The transgression in the Yenikapý excavation site has begun with the 2nd unit and has continued during depositional periods of 3rd, 4th and 5th units.

Relics of 5 shipwrecks were encountered at 4 different places within the 5th unit. One of the ships which it has recently been studied within this unit by archeologists was dated as 7th century (Pulak, 2007; Asal, 2007). While some of the remnants are in the form of whole vessel, some are the parts of the ship. Laminated layers have been formed just above the shipwreck by the abrasion of wood and the aggregation of the abraded material. When these dark brown surfaces were investigated it is observed that granules were originated from abraded wood. Other than the shipwreck within the unit, the wooden materials have been detected mostly parallel but sometimes with an angle to the bedding plane. It is commonly considered that wooden parts are dock piles. The reason for sinking of ships has been noted that there has been a storm affecting the shores of Istanbul (Perinçek, 2008). The 4th unit underlying the 5th unit was most probably deposited in A.D. 6th century. As for the ships found in the 6th unit that was deposited above the 5th unit were dated as 10 - 11th centuries by archeologists (Pulak, 2007; Asal, 2007; Kocabaþ and Kocabaþ, 2007; Gülbahar, 2007). Thus, it is possible to date the 5th unit between A.D. 7 - 9 centuries. There are rare findings in ships which have been unearthed in this unit. Only in one location, many well preserved amphorae have been found close to the wrecked dock (Figure 12).

Figure 12- During the excavation, well preserved several amphorae were found in the 5th Unit near dock that was destructed.

6th Unit

This unit takes place above the 5th unit and contains many pieces of amphorae (Figure 2, 3, 7, 11, 13, 14, 15). The thickness of the 6th unit varies in between 70 - 130 cm. The sequence is generally represented by sand. Besides; it contains intercalations of clayey sand and silty sand and has a plenty of shells. Levels full of shell are laterally discontinuous. Plenty of angular ceramic pieces are observed in the 6th Unit. Sporadically rounded pebble and granules, angular to sub-rounded rock fragments, bones and ceramic levels are present in the unit. Considerably intense pieces of ceramic, almost complete amphorae are observed in three different levels in the unit. Sporadically, angular rock fragments that have been transported from shore and structures on the coast into the sea by stormy waves also exist (Figure 11, 13). Pieces of ceramic have usually been accumulated in a way that convex sides would look upward. Cross bedded sands in the form of ripple mark were observed in ceramic levels. The thickness of this sand layer varies in between 20 - 35 cm. The

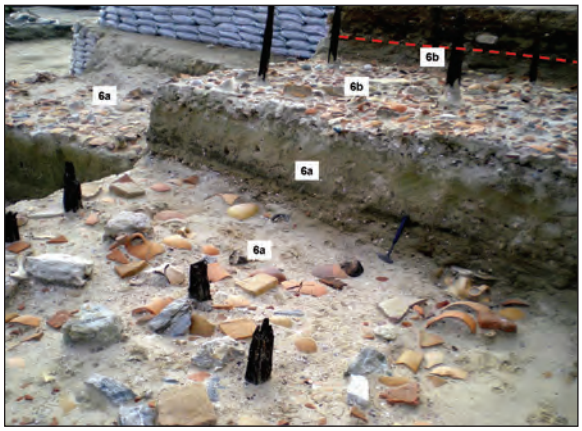

Figure 13- The 6th Unit can easily be divided into 2 sub units (as 6a and 6b) to the north of the study area. The division can be made by layers which masses of ceramic, pieces of amphora and angular stones are dense. Levels in which there are several coarse materials were deposited as a result of storm. The sand however has been deposited in normal sea conditions after the storm. Ceramic (6a and 6b) and sand layers (6a and 6b) of both sub units were marked by the same symbol in figure.

Figure 14- A view from shipwreck existing in fine to medium grained sand within the 6th Unit. There were found pieces of ceramic, walnut shells, cherry kernels and pieces of alga (posidonia) in the sand which precipitated after the storm in the vessel

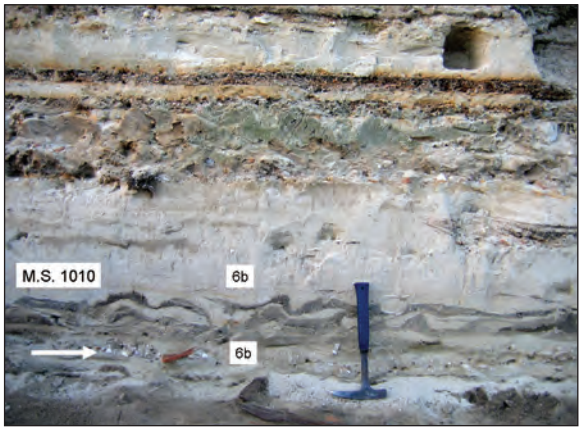

Figure 15- Seismite sedimentary structures are observed in the 6a sub unit. This data indicate that Istanbul surround has been influenced by earthquake during the precipitation of this unit. When historical records are taken into account, it can be considered that the earthquake which formed the seismites seen in the photo occurred in A.D. 1010. The section marked by white arrow indicates the level of ceramics dispersed at the sea bottom after the storm. These data show that first the storm then the earthquake occurred.

sand layer in some places intercalates with muddy sand and shows lamination. It is observed that the cross bedded sand sometimes contains black to dark gray colored lenses. These lenses include decayed, carbonized and disintegrated sea weed and other pieces of plant. Besides; 25 shipwrecks were found in the unit. Shipwrecks were determined as these belong to 10th century (Pulak, 2007). The macro cross bedded sand was also observed other than the micro cross bedded sand in the sequence of the 6th unit. The presence of macro cross bedding and non-mudy sand precipitated in shipwrecks were interpreted as indicators for the occurrence of storm.

The unit in some parts of the excavation site is represented by 70 cm. thick intensive pieces of ceramic levels. In these parts, it has not been possible to differentiate the unit into subunits. In places where the unit was divided into 2

subunits, it was seen that two ceramic levels overlapped each other and were difficult to separate them laterally. The unit can be divided into two subunits in many places (Figures 7, 11, 13). In areas where the separation was made it was observed that there had been no ceramics following the pieces of ceramic levels (6a) but very less amount of sand (6a). The ceramic level at the bottom and the sand on it was separated as "6a". The "6b" level containing plenty of ceramic pieces exists after "6a" sand level and is covered by sand (6b). On the other hand, sand layers which cover ceramic levels have been deposited at a longer period of time under conditions of marine environment. Two big storms that affected the shores of Istanbul in 10th or in mid 11th centuries might be the reason of formation of "6a" and "6b" ceramic levels (Perinçek, 2008). Following storms "6a" and "6b" sand accumulations occurred under normal coastal-marine conditions.

"Seismite" sedimentary structures observed at lower layers which were separated as 6a and 6b indicate that Istanbul and its surrounding area was subjected to two important earthquakes during the deposition of this unit. Uncemented sediments having too much water in the pores had lost their primary sedimentary structures and the sequence was subjected to deformation. Thus, seismites was formed before compaction and cementation (Figure 15). It is thought that seismites observed at 6a and 6b levels seperataly are related with the earthquakes in 989 and in 1010 (Yalçýner et al., 2002 and Altýnok, 2005). Many seismites were found over the ceramic level located at the bottom of "6b" and at the bottom of "6b" sand layer (Figure 15). This data indicate that the earthquake happened after the storm.

Ballast stones were detected around the shipwreck. Ballast stones are usually rounded to subrounded as these are collected in sea or river beds. However, angular bile stones were found in some vessels. Some of the ballast stones dispersed from the ships are made up of serpentinite. As it is known, serpentinite and basic rocks do not crop out around Istanbul. Therefore, it is certain that those ballast stones had been transported by ships taking the goods from the harbours, out of the city.

More than two ceramic levels were observed within the 6th unit. There are 3 ceramic levels at the bottom, in the middle and at the uppermost part of the 6th unit. The 7th unit begins after the ceramic level at the uppermost layer. It is difficult to distinguish the boundary between the 6th and 7th units where the mentioned ceramic level does not exist.

7th Unit

In some of the observation stations, ripple marks are observed at section where it coincides with the boundary between 6th and 7th units and in the 7th unit. The boundary of 6th and 7th units can not be detected easily. The transition of the boundary is gradational.

The 7th unit is represented by sand and sporadically laminated sand (Figure 2, 3, 7, 16). Dispersed fragments of ceramic and ceramic levels, rounded pebbles and dark gray layers rich in organic material are observed sporadically. The thickness of the unit varies between 30 - 60 cm. Ceramic fragments are both angular and of some were rounded as being eroded by the wave action. It is considered that the 7th unit was deposited at the end of 11th century - beginning of 12th centuries and shows a gradational transition with the 8th unit over it in some places.

The ballast stones are also present in this unit and this is another important thing that had been noticed. Rocks which were transported to the port by vessels had been dropped on port while ships were being loaded. Lithologies of some rocks show that some of these ballast stones do not belong to Istanbul district.

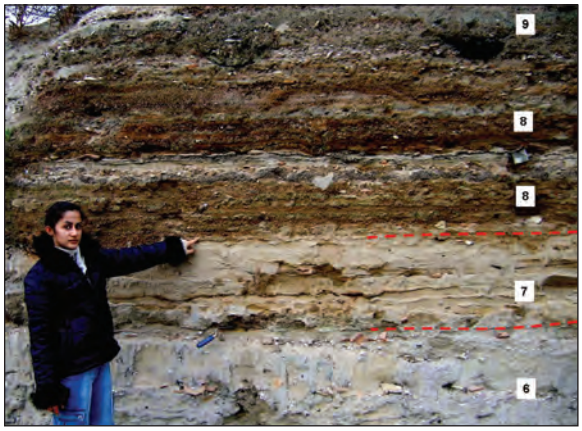

Figure 16- 7th and 8th Units have both lateral and vertical transitions. 8th Unit is pebbly and majority of pebbles are represented by pieces of ceramic. Ceramics dispersed into the sea with various reasons have then been rounded by waves in time. The 7th Unit in the photo can easily be differentiated from the 6th Unit at the bottom and 8th Unit at top in terms of color and texture. The 9th Unit exists at the topmost level.

8th Unit

The 7th unit traverses into 8th unit which is 50-80 m thick. The unit is mostly made up of pebble, rounded pebble, granule and lesser amount of sand. There are black colored intercalations and lenses composed of decayed and carbonized sea weeds and plant residuals. Plenty of glassy spines (sponge spicule) were encountered in these intercalations (Prof. E. Meriç, 2007, written communication; Perinçek et al., 2007). The characteristic of the 8th level (Figure 2, 3, 7, 16) is that it consists of sand and pebbles formed generally by rounded ceramic pieces. 80 to 90 % of most pebbles which were made up of ceramics have been processed by wave actions and corners are rounded. The color of the unit is red, dark gray and black; the red color originates from abraded and rounded ceramics. The said distinct key horizon is over the vessels in the 6th Unit which was dated as 10th and 11th centuries. Rounding and flattening of pebbles made up of ceramic occurred after the processes of wave erosion that had lasted for a long time following the sinking of vessels. Besides, it is considered that pieces of ceramic pots which have accidentally fallen at the port were passed through the same process in the first half of the 12th century. Most of ceramic pieces belong to the Port and can be considered that one portion of these have been carried to the Port along river.

Channels which have been formed during the deposition of the 8th unit have sporadically eroded the 7th unit and sediments that belong to 8th unit have been accumulated in these channels. The channel fill contains intercalations of sand, gravel and decayed sea weeds. The depositional environment of the 8th Unit might be the coastal - beach environment which was developed under the effect of stream action. According to Algan et al. (2009), the 8th unit reflects the conditions of fluvial environment and had been formed by the deposition of materials which was transported by Bayrampaþa river (Lykos river) flowing along the Vatan Street until the beginning of 1950s. The thickness of this fluvial deposit that underlies the 9th unit (molasse fill at the top) is 1 to 3 meters (Algan et al., 2007; Algan et al., 2009). At the lower part of the sequence, Meriç et al. (2007), determined the presence of less amount of *Chara* sp. which was a plant organism. The most important characteristic of *Chara* sp. is that it has lived and still lives around the mouth of streams at coastal zones. Besides, the observation of ostracods living both in fresh and brackish waters in upper levels supports this idea. Consequently, the presence of the stream mouth in the Yenikapý excavation site and around is strongly considered.

9th Unit

9th Unit made up of terrigenous soil is recognized after the 8th unit (Figure 2, 3, 7, 16). The 9th unit is represented by 1-2 meters thick cultivation soil. In the cultivated soil around the study area many architectural structures and archeological findings belonging to Late Middle Age and later

have been investigated (Çelik, 2007; Gökçay, 2007).

DISCUSSION

At the northeastern part of the Yenikapý excavation site, it is observed that the 3rd unit is pinched out to north and east and 4th unit directly lies on the 2nd unit. The 2nd unit has been deposited B.C. whereas the 4th unit was deposited A.D. 6th - 7th centuries. Accordingly; there is a time gap of at least 1500 years between the 2nd and the 4th units. Since, in the studied area, the 4th unit directly overlies the 2nd unit the archeological evidences give quite different ages (Archeologists working at excavation, 2008, 2009, oral communication). It is observed that a vessel belonging to 6th or 7th centuries has been settled directly on the 2nd unit in the same area. It was also investigated that the 5th unit becomes thinner from west to east. Generally all units become thinner from south to north in a way that it reflects the topography of the sea bottom. Other than these, the 5th unit also becomes thinner in east-west directions.

The settlement area of people who lived on the edge of marsh land falls into the eastern and northeastern parts of the marsh area. Usually Late Miocene sequence crops out at the bottom of the settlement area. Depending on the water level changes in summer times, northern edges of the marshland as well have seasonally been used as settlement area on swamp mud. The boundary of marsh land importantly changes in summer and winter times depending on the season and the rate of precipitation. When the water level decreased in summer, people on the edge of marsh would approach the area submerged under water to benefit from the area. There are evidences which support this observation in the study area. One of them is the arrangement of stones within the marsh deposits towards the center of the marsh. People living in the region have usually collected angular stones and put them on the edges of muddy marsh land although its water had receded. Thus, they approached the edge of the lake stepping on these stones. The reason of doing so is most probably to hunt for fish, bird and other living animals. The reason of stones to be mostly angular is an important indicator that these have been placed by people. The other indicator showing that the boundary of marsh has changed in summer is the presence of cemetery, granary and cremations in the area where water receded. The marsh land that had dried up in the summer has been used by people. Swamp mud was observed both below and above the cemetery. It is not possible that the cemetery has been buried in the mud. The corpse which has been placed on wooden grid in the form of litter had been buried there digging swamp mud when the water has receded in the summer. This litter is considered to have been attached on the ground by nailing small piles as shown in Figure 17. Any other aim of the piles is not known at present. People who lived in the region followed by the retreating of water in the summer have created seasonal storage areas for themselves. Wheat and similar materials were stored in these storages. The swamp mud exists below and above these storages which the archeologists unearthed in Yenikapý district. It is not possible to

Figure 17- A human skeleton is seen within the 1st Unit belonging to Neolithic era as placed on wooden grid. Wooden grid may have been stitched up by piles "K" into mud ground. Both the top and bottom of the skeleton and wooden grid is covered by marsh.

store grains in humid conditions. Therefore, it has been considered that these storages were temporal storage used in the summer.

There are some uncertainties about the origin of crystallized lime pebbles in the 2nd unit. There is not any data showing that the crystallized limestone crops out in and around the excavation site in geological maps. Lack of information about the origin of pebbles at this stage might have originated from the deficiency in available geological maps. It is considered that one portion of stones on beach might have been arranged and used by people although there is not any possibility for people to carry pebbles available in the 2nd unit to nearby the site of excavation. The presence of a river which has enough flow rate to carry the flattened limestone blocks of pebbly, blocky levels in the study area is out of question. The traces of the river are observed in the site of excavation and its presence is mentioned in historical records. However it does not have enough flow rate to carry limestone blocks to its recent place. There has not been collected enough data so far about their origins and on how flattened coarse pebble and blocks had been transported to their recent places. Exposures of the crystallized limestone could not be observed that might be the source to pebbles along the shore near the Port and around the tributary area of the river mentioned above. For the source of pebbles, it can be interpreted that the exposure of it might be in the sea to the south. During marine transgression that caused the precipitation of the 2nd Unit, particles detached from the exposures of crystallized limestone located under the sea at south by wave action have formed marine sediments which advanced landward without being transported much.

Archeological evidences which have been found in the 2nd unit belong to Neolithic Era Fikirtepe culture which was 8000-600 years ago than today (Algan et al., 2009). The architectural ruin with its pebbly foundations which has lasted so far possesses a rectangular plan in patches and sometimes rounded plan at a level where two units exist (approximately 6.3 m). Its bearing system was formed by wooden pillars which have been supported by stones. However, walls have been made by masonry branches plastered with mud originating from burnt bricks obtained during excavation (Çelik, 2007; Prof. M. Özdoðan, 2007, oral communication). Architectural ruin shows a similarity with the architecture of Aþaðý Pýnar Neolithic era found in Kýrklareli (Çelik, 2007).

The oldest ceramic pot fragment found in the Yenikapý Prehistoric settlement area shows a similarity with pot samples in Fikirtepe settlement area (Prof. M. Özdoðan, 2007, oral communication). Late Miocene claystone in and below the 2nd unit and skeletons found in 4 cemeteries (2 of them are small) which were dug into the mud of the 1st unit most probably belong to 6200 - 6400 B.C. according to Prof. Özdoðan (Hürriyet, 2008). In 2009, there was found an 8500 years old cemetery at the level of 1st unit in the excavations carried out at the construction area of the Yenikapý Marmaray Station as well. The executive person of the excavation Mr. Yaþar Anýlýr claimed that this cemetery which was very important for the archeological history of Istanbul was much older than Yarýmburgaz, Fikirtepe Neolithic Excavation site and was the oldest cemetery found in Istanbul. According to Mr. Anýlýr the skeleton which has been placed on the Neolithic wooden grid has not any other example (Hürriyet, 2008). As a summary, people lived on a topographic plain at 6.5 meters below the recent sea level, 7200-8500 years ago in the site of excavation. As a result, the transgression that had started within the 2nd unit and the following submersion of the land has mostly occurred mostly 7200 years ago.

In the muddy layers of the 4th unit the skeleton of 4 horses and one camel has been found as one piece (Çelik, 2007; Gökçay, 2007; Perinçek et al., 2007; Perinçek, 2008). It was also noticeable that feeding basket of one horse and the

halter made up of rope of the other horse had remained next to horses. These animals have been brought to marine environment with muddy, sandy, pebbly coagulated materials and have rapidly been buried by unprocessed trees and leafs transported from land. The neck of the camel might give some information about how it has died (Figure 9). The neck was found in a position that it had turned toward its body in the direction of tail. The animal should have taken this position before he had died and his body had been cooled. It is deliberated that both camel and horses had been into the sea in excess mud then have rapidly died under the water. Different interpretations are made for each skeletons found in the study area. According to one of them, the animals belonging to skeleton have been thrown away here. If it had been so, then the feeding basket and the halter would not have existed there. Besides; according to another interpretation, if animals mistakenly had fallen into the sea then these should have bulged and remained on the water. Animals that had died in this way would decay in time and bones would break away by wave actions. However, the skeletons of animals are as one piece.

Although some ceramic fragments were covered by shells in the 4th unit some of them are not. It is considered that ceramics not covered with shells have not remained on water for a long time but have been buried into sand and gravel as soon as they have been transported there after the tsunami in the region. On the other hand, shelly ceramic fragments have most probably been transported to marine environment previously, stayed in contact with water for long time then mollusks have hung on these ceramics. Ceramics covered with shells are considered to be older than the others. Most probably; shelly ceramic pieces in sand at the sea bottom belonging to 4th and 5th centuries have been scraped off the sea bottom at tsunami which has occurred after the earthquake in 6th century. These pieces have then mixed with ceramics of the 6th century and re-deposited at the sea bottom and have finally formed marine and terrigenous deposits of the 4th unit with abundant ceramics and pebbles. When the surface of processed marble fragments have carefully been studied within the unit, it was observed that upper faces of these fragments had been hung by seashells but had no shells on lower faces when these were lifted up. Pieces of amphora found in the 4th unit have behaved mostly like shells settling in the sea during the precipitation of the unit and these have been deposited at the sea bottom in a way that convex sides would look upward. One portion of these pieces has been lifted up and the material below has been investigated. The abundant plant pieces were observed under some fragments which were transported from land. Plant pieces in syrupy mud which have been transported into the sea had been trapped under amphora fragments before they got a chance to float on the water. Since some amphora pieces have not totally contacted with the sea bottom one or two types of the living marine organisms have invaded and colonized there. Colonization of only one species was observed at the lower part of some fragments.

The 4th unit to contain mud in significant amounts, to have a poor sorting and full skeletons indicate the presence of a low energy environment that occurred in a short time and the event related with it. It does not seem possible this event to be highly energetic storm. All other possibilities are tsunamis and floodings. Based on data given above, it is considered that the 4th unit was deposited under the control of tsunami which occurred after the earthquake. Tsunami waves coming from open and deep sea have carried sea shell, mud and sand towards land scraping the bottom of the sea. When tsunami waves which carry these materials had reached the Port they have destructed some vessels and docks there and have carried them to shore and landward. Tsunami waves reaching the land have lost its force after it had advanced a bit more and had receded back to sea. Waves which

have returned to sea have also carried living creatures on land, goods such as amphorae and oil lamps on shore for commercial purposes, trees and other terrestrial materials. Syrupy mud returning to sea has carried the accompanied material to open shallow sea and on the depressions of the sea bottom on port. Materials which may float such as tree and animal did not have any chance to do so thus, have rapidly been buried - precipitated together with mud and all materials within mud. The probability of rapid burial of animals into mud which were carried into sea by tsunami is much higher than by floodings. However, if these had been carried into the sea by floodings then the animals would have died, expanded and floated over the water. Thus, there would have been less chance for skeletons to be as one piece. On the depressions of the sea bottom first coarse material then fine grained sand and mud were accumulated. At the strike of strong tsunami wave, the sections of dock piles at the port which have remained under water were broken by the effect of tsunami wave. Thus, the broken part has been mixed with the material which the tsunami had brought and removed away. However the portion in the sand had been buried under tsunami deposits after the tsunami has ended. Later on, portions of these wooden piles which were close to the sea bottom and in contact with water have partly been deteriorated by the living marine organisms. Then, these piles were completely covered by deposits of the 5th unit (Figure 10). It was observed that some piles have completely been detached off the sea bottom where these were placed and pile slots had been filled by deposits of tsunami level.

Significantly deteriorated shipwreck and processed wooden materials (dock piles) were found in the 4th unit. Shipwrecks observed in two locations were probably carried towards land by tsunami then brought back to port by the receding waters. Ships have significantly been crashed during this process. Therefore, ships in the 4th unit have been damaged more than the ships settled at upper level which belong to B.C. 7, 8, 9, 10 and 11. There are very less findings close to shipwreck which belongs to 4th unit. Findings are observed everywhere without directly related with shipwreck. In one section of the excavation site nearly 100 baked soil gas lamps were found although there was not any wreckage. It is considered that these lamps have been drifted into the sea by the tsunami wave from a table of lamp seller near the coast but not related with the ship.

The 4th unit at Yenikapý excavation site the exposure is divided into 2 sub units. There are many entries of earthquake and tsunami at 6th century in historical records. Since two different layers are distinctly separated at some exposures, it is considered that there has been more than one tsunami that affected the port at 6th century. There is a need for additional data to be gathered to reach the final decision about this event. Observations will continue to demystify this issue in further stages of the study.

It is claimed that one portion of the 4th unit was deposited after the tsunami (Perinçek et al., 2007; Perinçek, 2008). However it is necessary to make detailed study on it. The event that caused the formation of the unit might be the flooding that occurred just after a heavy rain. The presence of excess mud in the unit and materials carried from land (branches of tree, leaf, angular rock fragments, ceramic pots and etc.) might reinforce the idea of flooding. If there is such a possibility then there should be a section where there is only terrigenous material at any location of the port within the marine deposit in the study area. Whereas; the layer distinguished as the 4th unit was formed by the complex mixture of marine and terrigenous material. The 4th unit can be divided into two sub units to the southwest of the study area. The sequence below the unit is made up of mud and sandy mud and there is little angular rock and ceramic fragments. The sequence which is in the same unit is observed throughout the study area and the thickness varies in between 10 - 80 cm. Marine and

terrigenous material is mixed in the upper part of the sequence and composed of muddy sand, sandy mud and sand. It contains sediments varying from pebble to large cobbles and many archeological findings. It is considered that this unit was deposited followed by a significant geological event. Perinçek mentions that this important event could be tsunami after earthquake (National Geographic, Turkey, 2007; Hürriyet, 2007).

The Lycos River is the reason of occurrence of mud in the 4th unit. The Theodosius Port was constructed at the 4th century (Asal, 2007; Gökçay, 2007). After the Port had been constructed, significant amount of mud might have been accumulated on the western part of the Port possibly because of breakwater located at the southwest. This muddy layer corresponds to the lower half of the 4th unit. The mud accumulation at the eastern part of the port might have occurred due to the breakwater located at the southwestern part of the port to stop the wave energy entering to the port. However, at the eastern part of the port the wave energy is higher relative to western part since it is the entrance of the port. There fore, this case caused the sequence at east to be less muddy. Let us once assume that Lycos River located at east of the port might have been effective in filling up the port with muddy sand at the 5th and 6th centuries. According to this; ones who have used the port after the 6th century might have changed the direction of the river setting a wall in order to overcome negative effects of Lycos River to the port at location where the river reaches the sea between the port and the mouth of the river. Thus, they have tried to remove the material which the river transported from the port. After this probable structuring the mud accumulation at the port has rapidly decreased and the 5th unit composed of fresh marine sand might have been deposited. After discussing this possibility, the possibility of muddy sand in the 4th unit to be tsunami becomes stronger when data in hand are reevaluated.

Shipwreck and the material being thrown away from these ships are encountered at sequence belonging to 5th unit. Storm is the reason for ships to sink down (Perinçek, 2008). Macro cross bedded sand at the deposit and the sand precipitated in sunken ships indicate the presence of storm. There is less findings in the unit. Many well preserved amphorae were found near the destroyed dock which occurs at only one location (Figure 12). There has not yet been found any shipwrecks near amphorae but since these were found at the foot of docks it was considered that amphorae had been brought to dock to be loaded on to ships. The dock has been destroyed after the storm and amphorae which were ready to be loaded to ships have been as dispersed over the sea bottom.

Shipwrecks were encountered in areas where ceramic fragments and amphorae are intensely present in the 6th unit. Frame timbers of these ships has mostly been preserved. There was observed nutshells, cherry kernels and carbonized sea weeds (Posidonia) with sea shells in the sand which filled up the vessel. There was also found laminated sand, amphora, ceramic fragments and various goods other than sand in vessel. As a result of two storms occurred in 10th century and in the mid of 11th century ceramic fragments dispersed after the sinking of 25 vessels and these fragments had been buried in the sand of the 6th unit and had well been preserved (Perinçek et al., 2007, Perinçek, 2008). The sand is usually available in undamaged sections of ships and mud is quite less. These sand layers have been deposited at high energy zone which the storm had made. It was understood that the sand which the storm had lifted up at sea bottom has generally covered the bottom of vessels and therefore, these parts have been well preserved from the effect of waves and living organisms and not decayed. However sections of vessels which are covered with sand and directly in contact with water were broken apart by wave and water actions. It was also observed that organisms living in the sea

and fed on woods have destroyed these parts by boring. The traces of borrow are very distinctive. The wooden material shivered by wave action has formed laterally discontinuous laminae by being deposited within sand at top. Amphorae that had fallen into the sea from ships and not buried into the sand have been fragmented more by the wave action thus, the edges of ceramics have been rounded. Big ones of complete amphorae and fragments of amphorae exist in and near the sunken ships. Generally, getting away from the sunken area the size of amphora and other ceramic pieces gets smaller and their density decrease. This observation shows that ceramic pieces found in the 6th unit at the excavation site were dispersed from sunken ships over the port base by the effect of storm. Consequently; it is observed that there is less possibility that these pieces have been thrown away at port by hand. In deeper parts of the port and towards open sea there are many ceramic pieces. However, there are less or almost no angular blocks and coarse angular pebbles. Approaching the shore, there is observed a significant increase in numbers of angular blocks and coarse angular pebbles. The storm which sank ships has made significant damage at coast and has drifted rock pieces which had been detached from structures at coasts. These pieces could not be carried into deeper parts but were deposited near the coast as these were big in size. However, in the 4th unit there is not such an arrangement. Angular blocks and coarse pebbles have been dispersed as disordered and disproportionally is near or away from the coast. There are 3 ceramic levels in the 6th unit. Vessels that exist with ceramic layers at the lowermost layer were dated as B.C. 10th century by Pulak (2007). The relation of the ceramic level at the uppermost part of the 6th unit which also forms the bottom of the 7th unit does not have a definite relation with the storm. The formation of this layer might be due to the deposition of ceramics by wave actions which were spilled off the sea because of storms in previous times.

Prof. A. Ergin, from the Institute of Marine Sciences of the Middle East Technical University, has contributed to the idea of the author from a different perspective saying that the storm was the reason for vessels to sink at 7th and 11th centuries at Port of Theodosius assessing data of coastal engineering (NTV, 2009). Prof. Ergin has also determined the dominant wind direction in the area as south-southwest in his assessments. According to wave data, he estimated that the storm wave heights towards port had changed between 3-4 meters outside the port within the periods of 100, 500 and 1000 years. Prof. Ergin has detected that the height of waves in harbor had decreased to 1.5 m. by means of breakwater and concluded that waves at such a height could sink vessels at the port. He said that the harbor had been overwhelmed by strong waves in harbor as resonance waves and waves reflected from the walls of the port were combined with storm waves from the sea (NTV, 2009).

Following the 7th unit, data indicating the regression was encountered in the 8th unit too. The most significant of these data indicate that the sea has receded back. The 8th unit down laps the boundary of the 7th unit and partly along the upper boundary of the 6th unit. The 8th unit has been deposited in coastal environment under river action near the study area. The material which has been transported to the shore by Lykos River and shore currents has been flattened by being processed and formed beach deposits. This level is very poorly sorted. The 8th unit which contains seashells, ceramic fragments and partly sand intercalations was truncated by minor channels in upward direction. Intercalation of pebble layers with ceramic pieces, carbonized marine alga and terrestrial plant residuals intercalate with sand layers. Carbonized layers also form intercalations at 7th and 8th units. The ratio of these intercalations is much more in the 8th unit. Sponge spicules are encountered in sand which contains decayed dark brown and black colored layers.

It is known that Lycos River has discharged near the harbor at Yenikapý but, the trace of materials transported by the Lycos River near the excavation site was not observed very much in deposits. Shores of Istanbul extend in W-SW and E-NE directions. Dominant wind directions in the Sea of Marmara are northward based on long term averages. Ostro and Tramontane winds reach the shores of Istanbul with an angle and form shore currents. These northeastern currents sweep the material away which the Lycos River had transported, carry them in northeast direction and spread it out. According to data available, the Port of Theodosius is at the western part where the Lycos River has reached the shore. Therefore; the material which the river had carried has been distributed by shore currents in the opposite direction of the port. That is why alluvial deposits in the 8th unit are less recognized in the study area. Algan et al. (2007) mentioned about the Lycos River deposits in the 8th unit. Perinçek et al. (2007) and Perinçek (2008) claimed that the material observed in the 8th unit had been deposited at coast by the river action.

It is observed that the 8th unit in total and the 7th unit in partial did not exist under the basement of light house which was unearthed during excavations in Yenikapý. However the 6th unit remains under the basement of the light house. The 8th unit and one portion of the 7th unit were deposited after the light house had been constructed. The age of deposits of the 6th unit belongs to 10th and to the first half of the 11th century. Accordingly; the construction of the light house had been made before the first half of the 11th century. Data regarding the level of the sea at time of construction has been collected during investigations around the light house. There are traces of wave erosion on the walls of the light house. Besides; the traces of marine organisms which have lived by attaching themselves on the wall of the light house were found over the basement of it which was submerged in water. The attachment levels of sea shells on the wall are compatible with levels of wave erosion. The highest level which these organisms were attached shows the sea level at that time. It is seen that the sea level has not changed since the 11th century when the level of the sea at time of construction of lighthouse with the recent sea level was compared.

There exists a church at the excavation site which dates back to the end of 12th century (Archeologist M. Gökçay, 2008, oral communication) and beginning of 13th century (Gökçay, 2007). It was seen that this church had been constructed over the 8th unit when the basement of this church was investigated. The construction of the church has been after the deposition of 8th unit or towards last stages of the deposition. The 8th unit is younger than the lighthouse but older than the church. Therefore, it is considered that the age of the 8th unit would be the beginning, second quarter or mid of the 12th century. According to Erel et al. (2009), the Port of Theodosius was fully filled by natural deposits carried by river, sea and anthropogenic wastes from the northern settlement area due to the increase in population in B.C. 1200. Algan et al. (2009) stated that after the 11th century the Port has started to fill up fully with alluvials which the Lycos River has carried and the coast line has again receded seaward.

Traces of Lycos River are not encountered in the 9th unit. The unit is composed of cultivated soil and molasses which were carried by humans to Langa Orchards. If the Lycos River had continued its activity in 13th and 14th centuries then the traces of alluvial deposits should have been in this unit. But it is not so, then two possibilities may be in question. First, the river bed of Lycos has been changed under human control. Second, material which was carried by river is mostly fine grained and has easily been distributed by sea waves.

The 2nd unit deposited in coastal environment is the production of transgression. The sea level

has increased as waters of Black Sea or Mediterranean Sea entered the Marmara Basin 11.000-8.000 years ago (Stanley and Blanpied, 1980; Ryan et al., 1997, 2003; Çağatay et al., 2000). Increasing sea level reached the shores of the Port of Theodosius approximately 7200 years ago. As a result of transgression people who lived on a topographic plane 6.5 m. below the recent sea level had to leave their living areas. As a result of continuing sea level increase the 3rd, 4th, 5th and 6th units have been deposited under shallow marine conditions. After the 6th unit, the material carried by rivers that reached the shore has been carried away being reworked by wave and shore currents and accumulated on coastal plain. Thus, the coast line has receded back to sea. Since the sea level was constant in this period, the material accumulated along shore has caused regression. The structures of down lap encountered in layers of the 8th unit are data which show the coast line change and regression.

CONCLUSIONS

9 units which were differentiated in the study area are represented by different lithological groups. It is considered that the 1st unit at the bottom is older than 6200 B.C. in age. However, the cultivated soil at top represents the sequence that has been deposited so far since 13th century.

The 1st Unit represented by the marsh sequence was deposited in lagoon - lake environment. People lived around the shore of the mentioned lagoon at a topographical plain 6.5 m. lower than the present sea level at least 7200 years ago than today. The people used coastal zones and it was also detected that they had also used lagoon lakes due to the retreat of sea water in summer times detecting traces of life. The 1st unit lies on the deposit represented by Late Miocene aged clay, silt sequence. However, the 2nd unit directly lies on that clay-silt deposit in areas where marsh deposits do not exist. Marsh deposits are encountered to the east of the site of excavation, whereas; 1st unit is not observed to the west of the site.

The 2nd unit started to deposit by the transgression which developed due to increase of sea levels in the Sea of Marmara which began 7200 years ago than today. The sequence investigated in Yenikapý excavation site is transgressive from 1st to 7th unit. However, a regressive sequence is observed starting from the 7th unit to the upper part of the 8th unit. The regression is not due to change in the sea level but the existence of abundant material that have been transported and deposited. This material was accumulated along the beach and caused the coast line to be seen as if it had receded seaward.

Archeologists working at the excavation site have detected ceramics for the 4th unit indicating A.D. 5-7th centuries (Katalog, 2007). Afterwards; archeological data obtained in the 4th unit have been correlated with geological data. It was found that a significant portion of this unit belongs to A.D. 6th century due to C14 dating results from samples taken. Archeologists aged vessel and plenty of ceramic materials as A.D. 10th century and as the beginning of 11th century from the 6th unit which is located at upper levels of the deposit (Pulak, 2007; Asal, 2007; Gülbahar, 2007). To date all units, the dating results of 4th and 6th units have been used to date all other units. Thus, the depositional age of the 5th unit was determined as A.D. 7th and 8th centuries and in the first half of the 9th century although the unit has not enough ceramic to perform radiometric dating. The wooden materials and vessels detected in the 5th unit were determined as A.D. 7th century and this age was proposed for all other vessels (Asal, 2007).

The 4th unit was investigated and it was obtained that data indicating deposits at this level were related with the tsunami. Fragments of ceramic, pebbles, wooden materials and pieces of bones are present chaotically and indicate a rapid sedimentation. The sediments in which a

skeleton of camel and 5 horses exist in the excavation site belong to the 4th unit. Tsunami waves which had reached the coast after the earthquake have then carried camel and horses towards sea when these were still alive as it recedes and caused these animals to be buried mixing with suspended marine and terrigenous materials in water. Pieces of skeleton and woods mixed with water have been deposited in the matrix without having an opportunity to float on the sea. The earthquake and the following tsunami waves that occurred in A.D. 557 are probably responsible for the formation of one portion of the 4th unit. After the earthquakes that occurred in A.D. 553 and 557, some districts of Istanbul which are very close to seaside were affected by the tsunami waves (Perinçek et al., 2007).

Shipwrecks and their loads which had been dropped off ships were encountered in the deposits of 5th and 6th units. Existence of macro cross bedded sand layers in the sequence and the deposited sand in shipwrecks to be free of mud are two important evidences indicating the occurrence of storm. Due to decrease in energy the sand which was lifted up by waves during storm has been accumulated in vessels with no mud after the storm. Amphorae in the 6th unit to be either in one piece or as less damaged, the decrease in sizes of ceramic as moving away the wrack and this distribution to occur independently from the distance to the shore indicate the presence of storm.

The sinking of Byzantine vessels detected in the 6th unit in Yenikapý excavations is due to the presence of severe storm. Data obtained from the 6th unit so far indicate that vessels have sunk due to storm (Perinçek et al., 2007). Two different storms that happened in mid 10th and 11th centuries damaged approximately 25 vessels. The sinking of vessels found in deposits of the 7th unit is also due to swashes and waves that had occurred in the port.

ACKNOWLEDGEMENT

The author gratefully thanks to the staffs of the Istanbul Archeological Museum administrating the Yenikapý Ancient Port excavation, to Dr. Ýsmail Karamut, the director of the Museum, to Metin Gökçay, the executive archeologist in the site of excavation, to archeologists Gülbahar Baran Çelik and to Candan Kozanlý, to geologist Zeynep Gökgöz for their contributions during the study. The author would also like to express his special thanks to independent archeological team, Prof. Engin Meriç, Assoc. Prof. Cemal Pulak, Assoc. Prof. Ahmet Cevdet Yalçýner and to Prof. Mehmet Doğan, the teaching staff of Istanbul University for their invaluable cooperation and supports.

C14 dating of samples taken from 2nd and 4th units was performed by Prof. C. Morhange. The author cordially thanks him for his supports.

Manuscript received June 12, 2009

REFERENCES

Algan, O., Yalçýn, M. N., Yýlmaz, Y., Perinçek, D., Özdoğan, M., Yýlmaz, Ý., Meriç, E., Sarý, E., Kýrcý-Elmas, E., Ongan, D., Bulkan-Yeþiladalý, Ö., Advisor, G., and Özbal, H., 2007. Antik Theodosius Yenikapý Limaný'nýn jeoarkeolojik önemi; Geç-Holosen ortam deðiþimleri ve Ýstanbul'un son 10 bin yýllýk kültürel tarihi. Gün ýþýðýnda Ýstanbul'un 8000 yýlý. Marmaray, Metro, Sultanahmet Kazýlarý. Vehbi Koç Vakfý publication, pp.242-245.

_____, _____, Yýlmaz, Ý., Kýrcý-Elmas, E., Sarý, E., Ongan, D., Bulkan-Yeþiladalý, Ö., Özdoğan, M., Yýlmaz, Y., and Perinçek, D., 2009. Holosen'de Deðiþken Bir Kýyý Ortamýnýn Antik Theodosius Limanýndaki (Yenikapý-Ýstanbul) Ýzleri. 62. Türkiye Jeoloji Kurultayý, 13-17 Nisan 2009, MTA - Ankara, pp.60-61

Altýnok, Y., 2005. "Türkiye ve Çevresindeki Tarihsel Tsunamiler", TMMOB Ýnþaat Mühendisleri Odasý, Türkiye Mühendislik Haberleri Dergisi:

Tsunami Special Issue, Yýl 50/2005-4, No. 438, pp.33-37.

Asal, R., 2007. Ýstanbul ticareti ve Theodosius Limaný. Gün ýþýðýnda Ýstanbul'un 8000 yýlý. Marmaray, Metro, Sultanahmet Kazýlarý. Vehbi Koç Vakfý publication, pp.180-189.

Baþaran, S., Kocabaþ, U. and Kocabaþ, I. Ö., Yýlmaz, R., 2007. Ýstanbul Üniversitesi, Yenikapý Bizans batýklarý projesi: Belgeleme, yerinden kaldýrma, koruma-onarým ve rekontsrüksiyon çalýþmalarý. Gün ýþýðýnda Ýstanbul'un 8000 yýlý. Marmaray, Metro, Sultanahmet Kazýlarý. Vehbi Koç Vakfý publication, pp.190-195.

Çaðatay, M. N. Görür, N., Algan, O., Eastoe, C., Tchapalyga, A., Ongan, D., Kuhn, T. and Kuþcu, Ý., 2000. Last glacial-Holocene palaeoceanography of the Sea of Marmara: timing of the last connections with the Mediterranean and the Black Sea. Marine Geology, 167: pp.191-206.

Çelik, G.B., 2007. Yenikapý'da günlük yaþam. Gün ýþýðýnda Ýstanbul'un 8000 yýlý. Marmaray, Metro, Sultanahmet Kazýlarý. Vehbi Koç Vakfý publication, pp.214-229.

Erel, L., Eriþ, K. K., Akçer, S., Biltekin D., Beck, C. and Çaðatay M. N. 2009. Bayrampaþa (Lykos) Deresi Havzasý ve Aðzýndaki Yenikapý (Theodosius) Limaný Kýyý Alanýndaki (Marmara Denizi) Deðiþim Süreçleri. 62. Türkiye Jeoloji Kurultayý, 13-17 Nisan 2009, MTA - Ankara, pp.58-59.

Gökçay, M., 2007. Ýstanbul Üniversitesi, Yenikapý kazýlarýnda ortaya çýkarýlan mimari buluntular. Gün ýþýðýnda Ýstanbul'un 8000 yýlý. Marmaray, Metro, Sultanahmet Kazýlarý. Vehbi Koç Vakfý publication, pp.166-179.

Hürriyet, 2007. Marmara'da tsunami tehlikesi kesinleþti. Issue of Kaplan, S., 07 Kasým 2007.

_____, 2008. Metro kazýsýndan taþ devri iskeletleri çýktý. Issue of Kýnalý, M., 06 Aðustos 2008.

Janin, R., 1964. Constantinople Byzantine. Topographical map of Constantinople during the Byzantine period. Paris. http: // tr.wikipedia.org / wiki / Dosya: Byzantine_Constantinople_eng.png

National Geographic Türkiye, 2007. Yenikapý'da Tsunami Ýzleri. Issue of Ayman, O., Kasým 2007, 70p.

Katalog, 2007. Yenikapý buluntularý. Gün ýþýðýnda Ýstanbul'un 8000 yýlý. Marmaray, Metro, Sultanahmet Kazýlarý. Vehbi Koç Vakfý publication, pp. 247-299.

Kocabaþ, U. and Kocabaþ, Ý. Ö., 2006. Ýstanbul Üniversitesi, Yenikapý batýklarý belgeleme, konservasyon, restorasyon ve rekonstrüksiyon projesi 2006 yýlý çalýþmalarý. Sualtý Bilim ve Teknolojisi Proceedings, pp.115-121, Galatasaray Üniversitesi, Ýstanbul, 2006.

_____ and ____, 2007. Ýstanbul Üniversitesi, Yenikapý Bizans batýklarý projesi kapsamýndaki gemilerin yapým teknikleri ve özellikleri. Gün ýþýðýnda Ýstanbul'un 8000 yýlý. Marmaray, Metro, Sultanahmet Kazýlarý. Vehbi Koç Vakfý publication, pp.196-201.

Meriç, E., Perinçek, D., Avþar, N., Nazik, A. and Yokeþ, M. B., 2007. Yenikapý Batýklarý Alt ve Üst Bölümlerinde Gözlenen Güncel Çökellerin Foraminifer, Ostrakod ve Mollusk Ýçeriði, 11. Sualtý Bilim ve Teknolojisi Toplantýsý, Proceedings. 3-4 Kasým 2007, pp.128-139.

_____, Oktay, F. Y., Sakýnç, M., Gülen, D., Ediger, V. Þ., Meriç, N. and Özdoðan M. I., 1991. Kuþdili, Kadýköy, Kuvaterner'inin sedimanter jeolojisi ve paleoekolojisi. C. Ü. Müh. Fak. Jour., Seri A - Yerbilimleri 81, pp.83-91.

Milliyet, 2009. En eski Ýstanbullu. Issue of Erbil, Ö., Güzelce, O., 11 Nisan 2009.

Müller-Wiener, W., 2001. Ýstanbul'un Tarihsel Topografyasý, Yapý Kredi Yayýnlarý, 1419, 534p., Ýstanbul, 2001.

NTV, 2009. Yenikapý gemileri neden battý? Fýrtýnamý, Tsunami mi? Issue of Yýldýz, S., 09 Kasým 2009, pp.66-69.

Perinçek, D., 2008. Yenikapý Antik Liman Kazýlarýnda Jeoarkeoloji Çalýþmalarý ve Doðal Afetlerin

Jeolojik Kesitteki Ýzleri. 1. Ulusal Doðal Afetler ve Yerbilimleri Sempozyumu, 19-22 Mart 2008, Adapazarý. Sakarya Üniversitesi, Doðal Afetler ve Yerbilimleri Kulübü (DAYK) (Editör: M. Dinçer Köksal), Proceedings, pp.31-49.

Perinçek, D., Meriç, E., Pulak, C., Körpe, R., Yalçýner, A. C., Gökçay, M., Kozanlý, C., Avþar, N., Nazik, A., Yeþilyurt, S. K. and Gökgöz, Z., 2007. Yenikapý Antik Liman Kazýlarýnda Jeoarkeoloji Çalýþmalarý ve Yeni Bulgular. Türkiye Jeoloji Kurultayý, Proceedings, 131, 135p., 16-22 Nisan 2007, Ankara.

Pulak, C., 2007. Yenikapý Bizans Batýklarý. Gün ýþýðýnda Ýstanbul'un 8000 yýlý. Marmaray, Metro, Sultanahmet Kazýlarý. Vehbi Koç Vakfý publication, pp.202-215.

Ryan, W. B. F., Pitmann, W. C., Major, C. O., Shimkus, K., Moskalenko, V., Jones, G. A., Dimitrov, P., Görür, N., Sakýnç, M. and Yüce, H. 1997. An abrupt drowning of the Black Sea shelf. Marine Geology, 138: pp.119-126.

Ryan, W. B. F., Major, C. O., Lericolais, G., and Goldstein, S. L. 2003. Catastrophic flooding of the Black Sea. Annu. Rev. Earth Planet. Sci., 31: pp.525-554.

Stanley, D.J. and Blanpied, C., 1980. Late Quaternary water exchange between the eastern Mediterranean and the Black Sea. Nature, 285, pp.537-541.

Yalçýner, A.C. Alpar, B., Altýnok, Y., Özbay, I. and Imamura F., 2002. "Tsunamis in the Sea of Marmara: Historical Documents for the past, Models for Future" Marine Geology, 190, pp. 445-463.

Wikimedia, 2008. http://commons.wikimedia.org/wiki/Hagia_Sophia

NOTES TO THE AUTHORS

The authors should consider the publication rules of MTA Bulletin about scope and format. Some of the rules are summarized below

SCOPE: The bulletin accepts original research papers and comprehensive reviews in the every fields of earth sciences. The articles qualified by the editorial board is printed in the English edition of the bulletin. The authors who are native in Turkish, are asked to supply their articles in Turkish as well.

GENERAL: The papers submitted to the bulletin should not be published previously in English or in any other language in the same form.

An article should include title, the name and address of the author (s), abstract, introduction, main body of the text, conclusion (s), discussion (if necessary), references and additional explanations (if necessary).

ABSTRACT: Should be clear, informative and include the purpose, gathered data and brief conclusions of the paper which can be used in an abstract periodical directly. The abstract should not exceed 200 words.

PREPARATION OF THE DRAFT TEXT (MANUSCRIPT): All articles with their illustrations are considered as 1Draft Text (Manuscript)".

The articles should be typed on one side of an A4 paper (297x210 mm) with double spacing, by leaving 2,5 cm margins on the sides.

In the manuscript words in bold should be double, italics single underlined.

The places of the figures, illustrations and tables should be indicated by the authors on the side margins of the manuscript.

Footnotes should be avoided unless it is necessary, but should not be more than 10 lines. If there are more than one footnote, should be numbered in order.

The manuscript submitted for the publication should not exceed 30 typed pages with all illustrations.

REFERENCES: references in the text consist of surname of the authur (s) followed by the year of publication such as: "Sirel and Gündüz (1976)....., "according to Altýnlý (1971)....., or .....(Altýnlý, 1971).

Only the references cited in the text should be given in the reference list or vice versa. The style of the references are exampled below:

Pamir, H. N., 1953, Türkiye'de kurulacak hidrojeoloji Enstitüsü hakkýnda rapor: Türkiye Jeol. Kur. Bült. 4, 63-68

Baykal, F. And Kaya, O., 1963, Ýstanbul Bölgesinde bulunan Karbonifer genel stratigrafisi: Maden Tetkik Arama Derg., 61, 1-9.

Ketin, Ý., 1977, Genel Jeoloji: Ýst. Tek. Univ., Ýstanbul, 308 p.

Anderson, D.L., 1967, Latest information from seismic observations: In: Gaskell, T.F. (ed), The Earth's Mantle: Academic Press, London, 355-420.

If the authors of the reference are more than two "..... et al." Abbreviation should be used after the first author. For instance "Unalan et al. (1974) described the Kartal Formation". To refer to an article which is published in another publication, firstly the original and secondly the publication in which the article has appeared should be mentioned. For instance: "It is known that Lebling mentioned about Lias around Çakraz (Lebling, 1932; from Charles, 1933)". Personal communications and correspondences should be in the same way, like: "Eroskay (1978, personal communication)" or "according to Tokgöz (1976, written communications)".

ACKNOWLEDGEMENT: The persons who contribute important inputs to the paper should be acknowledged. The contributions of the persons who provide them as normal function of their duty should not be acknowledged.

ILLUSTRATIONS: Drawings, figures, tables, plates, maps in the article should be carefully selected with regards totheir quality, necessity and availability. The used pictures should be proportional to the volume of the text.

The drawings should be prepared in black and white and drawn carefully and clearly. Lines and Letters when reduced should not loose their details, and not be smaller than 2 mm in size. Unstandardized symbols and letters utilized for drawings should be explained either in the drawings or within the explanation section of the text. Bar scale should be used in the drawings.

Photographs must be of high quality, glossy prints with sharp details and good contrasts.

Illustrations should be classified as "Figures", "Tables" and "Plates"; the individual pictures should be classifed in "Figures".

Figures, tables, and plates should be numbered independently from each other, numbering should be in accordance with the order of the citation in the text. The figures and tables should be numbered with Latin numbers and the plates with Romen Letters.

The numbers of the illutrations and the name of the authors should be written with a pencil behind the illustrations.

Figure captions must not be written on the illustrations. Captions for figures and tables should be listed seperately.

But plate explanations should be on an individual page for each plate.

SENDING THE MANUSCRIPT- For sets of the manuscripts are required, one should be the original, and three copies. Photocopies of the illustrations are not accepted as the first set.

Copies of the illustrations might be optained in blue prints, photocopy or in similar ways.

The unaccepted paper is not returned to the authors.

Photographs which are designed to be printed as plates should be arranged on a white cardboard in the required order and the second set of it should be sent without arrangement. The dimensions of the cardboard should be in the same size of the page of the Bulletin or reducible into that size. Respective numbers should be written on each photograph in the plates.

If the manuspcript does not meet the requirements of MTA publication standards, it is returned to the authors for correction. The revised manuscript is reconsidered by the Editorial Board of MTA for publication.

CRITISM-An article taken place in the last issue of the bulletin may be subjected to a critic either completely or partially. Such writings take place in the folowing first issue of this period. Before the criticism is submitted, it is sent to the author of the article. The article is sent to the first author, if the article has many authors. If the criticism is responded in the defined period, the criticism and the responding article are published together. If the respond becomes late, then the criticism is issued alone the responding articles are not issued if they are sent later. Possibility of new criticisms are not allowed again.

In the criticism and respondings, scientific discussion rules should be preferred and personel claims should be avoided. The whole documents of the criticism or responds even if with their illustrations should not be more than four printer pages (the critisism papers should obey the publication rules of the bulletin).

SHORT NOTES SECTION- The data and new findings obtained from scientific researches and applications can be published as scientific news in short note section of the bulletin as short and basic texts. Such ''Short Notes'' are published in either first or second issue without delay, in order to make fast scientific communication. Short Notes does not include abstract and should not exceed four pages including the illustrations.

REPRINTS-For each issued article, authors receive 5 reprints free of charge. More reprints (extra copies) are subject to charge.

- Authors are reguested to submit their reports to the editorial board, with a floppy disc along with the original text.

- In order to the authors are paid of copyright for their submitted paper, they are asked to indicate a bank account number with their paper.